

DEPARTMENT OF PHARMACOLOGY
Medical Sciences Division



Atrial Cardiomyocytes Development from Human Induced Pluripotent Stem Cells

A thesis submitted for the degree of Master of Science by Research

Word Count: 20515

Meng Yuan

Dr. Ming Lei's Group

Department of Pharmacology

St Cross College

Student no. 1033716

Hilary 2018

Acknowledgements *4*

List of abbreviations *6*

Presentations *10*

Abstract *11*

Chapter 1. Introduction *12*

1.1 Cardiovascular diseases **12**

1.2 Human induced pluripotent stem cells **13**

1.3 ESC- and iPSC-derived cardiomyocytes **15**

1.4 Limitations of human PSCs in modelling cardiovascular diseases . **18**

1.5 Cardiac development **19**

1.6 Signalling pathways controlling cardiac development **21**

1.6.1 Overview 21

1.6.2 BMP signalling pathway 22

1.6.3 JNK signalling pathway 24

1.6.4 RA signalling pathway 25

1.7 Gremlin 2 in cardiac development **26**

1.7.1 Structure and working mechanisms of Gremlin 26

1.7.2 Gremlin 2 is essential for cardiac development 27

1.7.3 Gremlin 2 strengthens atrial differentiation in mouse ESCs 28

1.8 RA in cardiac development **29**

1.8.1 RA in heart regeneration and cardiac development 29

1.8.2 RA drives atrial-like cardiomyocytes from human ESCs 30

1.9 Properties of atrial cardiomyocytes **32**

1.10 Maturation of cardiomyocytes **33**

Chapter 2. Methods *36*

2.1 Episomal Human iPSC Line **36**

2.2 Matrigel plate coating **36**

2.3 Human iPSCs maintenance and passaging **37**

2.4 Human iPSC stocks preservation **37**

2.5 Resuscitation of frozen human iPSC lines **38**

2.6 Purification of human iPSCs **38**

2.7 Differentiation from human iPSCs to cardiomyocytes **39**

2.8 RNA isolation **40**

2.9 Reverse transcription **41**

2.10 Quantitative PCR (qPCR) **41**

2.11 Cardiomyocytes dissociation **43**

2.12 Immunofluorescence analysis **44**

2.12.1 Protocol 1 44

2.12.2 Protocol 2 45

2.13 Optical mapping **46**

2.14 Electrophysiological analysis **47**

2.15 Statistical analysis **48**

Chapter 3. Results *49*

3.1 Immunofluorescence analysis **49**

3.1.1 Human iPSC-derived cardiomyocytes without Gremlin 2 and RA treatment exhibited immature morphological features 49

3.1.2 Gremlin 2 and RA treatment during cardiac differentiation changed the morphology of human iPSC-derived cardiomyocytes 51

3.2 Gene expression analysis **54**

3.2.1 Gene expression changes during cardiac differentiation in human iPSC-derived cardiomyocytes receiving Gremlin 2 and RA treatment 55

3.2.2 Comparison of gene expressions in undifferentiated human iPSCs and Gremlin 2- and RA-treated Day 15 derived cardiomyocytes 58

3.2.3 Comparison of gene expressions in human iPSC-derived cardiomyocytes differentiated with and without Gremlin 2 and RA treatment 60

3.3 Optical mappings 63

3.3.1 α1- and β- adrenergic stimulation increased the calcium transient amplitude in human iPSC-derived cardiomyocytes receiving Gremlin 2 and RA treatment 63

3.3.2 α1- and β1- adrenergic antagonists abolished the effects of adrenergic stimulation on Gremlin 2- and RA-treated human iPSC-derived cardiomyocytes 66

3.4 Electrophysiological analysis 69

3.4.1 Human iPSC-derived cardiomyocytes receiving Gremlin 2 and RA treatment recapitulated atrial-type action potential characteristics 69

3.4.2 Gremlin 2- and RA-treated human iPSC-derived cardiomyocytes displayed mature action potential features 70

Chapter 4. Discussion 72

4.1 Rationale of the study 72

4.2 Approaches and main results 74

4.3 Hypothesis of mechanisms 84

4.4 Limitations of the study and future perspectives 86

Reference 91

Acknowledgements

I joined Prof. Ming Lei's group at the Department of Pharmacology, Oxford in October 2016. Since then I have been working on cardiovascular research and stem cells under the supervision of Prof. Ming Lei. During the past one and a half years, I received comprehensive biomedical research training, and gained experience and confidence as a scientist in training. I would like to thank Prof. Ming Lei for inviting me to his group, providing me with this great opportunity to study with the world's top scientists, and helping me overcome all the obstacles in my study.

Here I summarized my learning process and research progress between October 2016 and early 2018. My experience at Oxford is invaluable to me. It is an excellent beginning of my professional career in science. There are a number of people from the Department of Pharmacology that I would like to offer my thanks to.

The experiments were designed and conducted with the assistance of Faizzan Ahmad. I would like to thank him for bringing me into this research project, teaching me how to design and make plans for my experiments, and helping me build my laboratory skills.

Razik Mu-u-min, James Bae, Kaizhong Duan are the excellent teachers and friends of mine. They have always been helpful and supportive for me both in work and life. Prof. Daniel Anthony's group, Prof. Paolo Tammaro's group and Prof. John Parrington's group offered me great support for the RT-qPCR experiments. Gokhan Yilmaz from Prof. Frances Platt's group generously helped me with the confocal microscopy.

I would like to give my special thanks to Jay Roodselaar and Yifan Zhou for being part of my life, accompanying me and guiding me through my difficult times.

Lastly, I would like to take the opportunity to thank my family for their support for the choices I make. They have always been standing by my side, trusting me, and offering me endless love.

List of abbreviations

ACTN2: actinin alpha 2

ActR: activing receptor

ADRA1A: adrenoceptor alpha 1A

ADRB1: adrenoceptor beta1

AF: atrial fibrillation

ALK: anaplastic lymphoma kinase

AMHC: atrial myosin heavy chain

APA: action potential amplitude

bFGF: basic fibroblast growth factor

BMP: bone morphogenetic protein

BMPR: bone morphogenic protein receptor

CACNA1: calcium voltage-gated channel alpha1 subunits

cDNA: complimentary DNA

CICR: calcium induced calcium release

CMM: Cardiac Maintenance Medium

COUPTF: chicken ovalbumin upstream promoter transcription factor

CRABP: cellular retinoic acid-binding protein

CVD: cardiovascular disease

Daam1: dishevelled-associated activator of morphogenesis 1

Dsh: dishevelled

ESC: embryonic stem cell

ExE: extra-embryonic ectoderm

FHF: first heart field

GATA4: GATA binding protein 4

GDF: growth and differentiation factor

GJA5: gap junction protein alpha 5

GREM2: gremlin 2

HAND1: heart and neural crest derivatives expressed 1

HCM: hypertrophic cardiomyopathy

HEY: hes related family BHLH transcription factor

iPSC: induced pluripotent stem cell

IRX4: iroquois homeobox 4

ISO: isoprenaline

JIP: JNK-interacting protein

JNK: Jun N-terminal kinase

KCNA: potassium voltage-gated channel superfamily A

KCNH: potassium voltage-gated channel superfamily H

KCNJ: potassium inwardly-rectifying channel, superfamily J

KCNQ: potassium voltage-gated channel superfamily Q

Klf4: Kruppel-like factor 4

MAPK: mitogen-activated protein kinase

MAPKKK: mitogen-activated protein kinase kinase kinase

MESP1: mesoderm posterior BHLH transcription factor 1

MKK: mitogen-activated protein kinase kinase

mRNA: messenger RNA

MYH7: myosin heavy chain 7

MYL7: myosin regulatory light chain 2a (atrial)

NCX: Na^{2+}/Ca^{2+} exchanger

NFAT: nuclear factor of activated T cells

NKX2-5: NK2 homeobox 5

NPPA: natriuretic peptide A

Oct3/4: octamer-binding transcription factor 3/4

PE: phenylephrine

PKA: protein kinase A

PSC: pluripotent stem cell

qPCR: quantitative polymerase chain reaction

RA: retinoic acid

Rac1: ras-related c3 botulinum toxin substrate 1

RALDH2: retinaldehyde dehydrogenase 2

RAR: RA receptor

RARE: RA-response element

RhoA: ras homolog gene family, member A

ROCK: rho-associated, coiled-coil-containing protein kinase

RP: resting potential

RXR: retinoid X receptor

RyR: ryanodine receptor

SERCA: sarco/endoplasmic reticulum Ca^{2+} ATPase

SHF: second heart field

SLN: sarcolipin

Sox2: sex determining regtion Y-box 2

SR: sarcoplasmic reticulum

TAB: TGF-beta activated kinase 1 binding protein

TAK1: TGF-β activated tyrosine kinanse 1

TGF-β: transforming growth factor β

TNNT2: troponin T type 2 (cardiac)

VMHC: ventricular myosin heavy chain

XIAP: X-linked inhibitors of apoptosis

Presentations

1. Oxford BHF CRE Annual Symposium, UK. (September 2017)

   Poster presentation "Modelling development of atrial cardiomyocytes from human iPSCs".

2. OXION Annual Symposium, UK. (September 2017)

   Poster presentation "Modelling development of atrial cardiomyocytes from human iPSCs".

Abstract

Cardiovascular diseases are the leading cause of death around the globe. Despite ongoing progress, a shortage in the primary source of human cardiac tissue still presents a major limiting factor in relevant research. Human induced pluripotent stem cells (iPSCs) hold great promise in cardiovascular disease mechanistic research and treatment as they can provide an unlimited supply of cardiomyocytes. Nevertheless, so far, the cardiomyocytes derived from human iPSCs disproportionately recapitulated immature ventricular characteristics, which has hindered the application of iPSC-based models in studying atrial-specific diseases and developing relevant therapies. In the current study, the effectiveness of a combined treatment of Gremlin 2 and retinoic acid (RA) in directing atrial cardiomyocyte differentiation from human iPSCs and driving the *in vitro* maturation of those derived cardiomyocytes was explored.

Morphologically, human iPSC-derived cardiomyocytes treated with Gremlin 2 and RA recapitulated human adult atrial cardiomyocyte features. The treated cardiomyocytes showed elevated expressions of cardiac genes, atrial-specific genes, inward rectifier potassium channel coding genes and the β1-adrenergic receptor coding gene. However, no significant differences in gene expressions were identified between the treated cells and untreated cells. In addition, the treated cells displayed increases in calcium transient amplitude after α1- and β- adrenergic stimulations and they showed atrial-type action potentials with mature cardiomyocyte features as well. In conclusion, the above results are insufficient to determine the effectiveness of the combined treatment of Gremlin 2 and RA in directing atrial specification and driving *in vitro* cell maturation, but evidence has been provided that this treatment combination has the potential to produce mature atrial-type cardiomyocytes from human iPSCs with further optimization.

Chapter 1. Introduction

1.1 Cardiovascular diseases

Cardiovascular diseases (CVDs) encompass a number of pathological conditions of the heart and blood vessels. CVDs are the leading cause of death around the globe, and approximately 80% of the CVD deaths are resulted from strokes and heart attacks. Despite the significant progress having been made in improving the primary prevention and treatment of CVDs, there are still 17.7 million people dying from CVDs each year, accounting for 31% of all deaths worldwide (World Health Organization, www.who.int/cardiovascular_diseases/en/). In Europe, 3.9 million deaths are caused by CVDs each year, accounting for 45% of all deaths (Wilkins et al., 2017).

Atrial fibrillation (AF) is characterized by the presence of rapid and irregular beatings and the fibrillating waves in the atrium (Falk, 2001). It is the most widespread cardiac arrhythmia (Pellman et al., 2015). 0.5% of the people in their 50s have AF, comparing to a 10% in the population of 80- to 90- year-olds (Nattel, 2002). AF has been known to be associated with increased risks for stroke (Gregory, 2010), myocardial infarction (Soliman et al., 2014) (Lee, Yang et al., 2017), heart failure (Miyasaka et al., 2006), and eventually the increased mortality (Benjamin et al., 1998; Miyasaka et al., 2007). AF is governed by both clinical and genetic factors, with an overall lifetime risk of 37% (Weng et al., 2017) (Pellman et al., 2015).

The development and maintenance of AF require pathophysiological remodelling of the atria either primarily or secondarily associated with other CVDs (Pellman et al., 2015). The improvement in our understanding of the mechanisms underlie AF has given

rise to the development of multiple therapeutic strategies with a major goal of controlling the symptoms. New areas of investigation have recently emerged aiming to control the adverse effects of existing antiarrhythmic drugs used in AF patients (Pellman et al., 2015). The current antiarrhythmic drug therapies designed for AF have aimed for decreasing the frequency and duration of the arrhythmic episodes. They usually involve the regulation of certain ion channels, and have a variety of cardiovascular side effects like bradycardia and congestive heart failure, as well as the non-cardiovascular ones such as diarrhea and cinchonism (Zimetbaum, 2012).

1.2 Human induced pluripotent stem cells

The Nobel Prize in Physiology or Medicine was rewarded to Dr. Shingya Yamanaka and Dr John B. Gurdon in 2012 for their discovery of reprogramming mature somatic cells to pluripotent stem cells (PSCs). It was traditionally believed that cellular differentiation was a one-direction process. In 1962, Dr John B. Gurdon challenged this traditional view by demonstrating that the transfer of frog intestinal epithelial cell nuclei to enucleated recipient eggs was able to generate genetically identical tadpoles (Gurdon, 1962). In 2006, Dr Shinya Yamanaka successfully reprogrammed mouse fibroblasts to pluripotent stem cells by inducing four transcriptional factors, Oct3/4, Sox2, c-Myc and Klf4 (Takahashi et al., 2006). Their findings brought about a shift in the understanding of cellular differentiation and marked an important step in permitting the control of the cell pluripotency.

Early human embryonic development begins with a transition from oocyte to embryo. The developmental processes of the embryo are accompanied by the cellular differentiation. At blastocyst stage, the embryo consists of a fluid-filled cavity and an inner

cell mass surrounded by a layer of trophoblasts. The inner cell mass will grow into embryo while the trophoblasts give rise to extraembryonic tissues (Niakan et al., 2012). Embryonic stem cells (ESCs) are pluripotent cells that are derived from inner cell mass of the blastocyst. ESCs have self-renewal ability and can differentiate into all cell types of the mesodermal, ectodermal and endodermal layers (Keller, 1995). Most of the cells in human body are terminally differentiated, although some cell types such as hematopoietic stem cells and intestinal stem cells retain limited potency to proliferate and differentiate (Smith, 2003; Umar, 2010).

Following the establishment of the first mouse iPSCs (Takahashi et al., 2006), the first human iPSC line was established in 2007 by transducing the same factors, Oct3/4, Sox2, c-Myc and Klf4 (Takahashi et al., 2007), or another set of factors Oct4, Sox2, Nanog and Lin28 (Yu et al., 2007). The established human iPSC lines demonstrated their pluripotency and self-renewal ability and were reported to share morphological, genetic and epigenetic characteristics with human ESCs (Takahashi et al., 2007; Yu et al., 2007; Mallon et al., 2014). Thereafter, Mallon and her colleagues at National Institutes of Health (NIH), USA thoroughly compared the genetic and epigenetic profiles of human ESCs and human iPSCs. Bioinformatics analysis offered evidence that there were no significant differences in global gene expression pattern between ESC and iPSC populations. In addition, the researchers also found that there were no significant epigenetic differences between those two populations either. The reprogrammed iPSCs demonstrated a methylation profile that was 98-99 percent consistent with that of undifferentiated H1 ESCs (Mallon et al., 2014). At the present time, human iPSCs have been reported to be successfully reprogrammed from a variety of cell sources such as fibroblasts (Takahashi et al., 2007; Yu et al., 2007), keratinocytes (Aasen et al., 2008) and T cells (Staerk et al., 2010; Loh et al., 2010; Seki et al., 2010).

The establishment of human iPSCs has attracted growing attention. The demonstrated ability to reprogram somatic cells to an ESC-like stage by manipulating gene expressions has completely changed our understanding of cellular differentiation. Human iPSCs have effectively provided an *in vitro* tool to study human cells. Also, they have opened a new avenue of using iPSC-based models including patient-derived iPSCs for human disease mechanistic research and relevant treatment.

1.3 ESC- and iPSC-derived cardiomyocytes

Cardiomyocytes account for 30% of the cell population within a mammalian heart (Freund et al., 2009). In mammals, cardiomyocytes proliferate rapidly during foetal development but they become quiescent soon after birth. After birth, the growth of the heart is mainly driven by the increase in the cell size instead of the cell number. In most species, mature cardiomyocytes are terminally differentiated cells and have highly organized structural patterns (Ahuja et al., 2007). Cardiac progenitor cells have been identified by many research groups in animal models (Dimmeler et al., 2005). For example, the multipotent resident cardiac progenitor cells with the ability to differentiate into cardiomyocytes, endothelial cells and smooth muscle cells were identified in murine animals (Beltrami et al., 2003). Nevertheless, it still remains questionable whether these progenitor cells exist in human hearts. Moreover, even though the cardiac progenitor cells are a promising source for cardiac regeneration, they have very limited self-renewal abilities which are compromised in cardiac pathological conditions (Freund et al., 2009).

Most preclinical cardiovascular disease studies and drug discoveries have been carried out using animal models. However, animal models may not be able to accurately represent the physiological conditions in humans due to the interspecies differences. For

example, a human heart is significantly larger than a mouse heart. Multiple other anatomical differences between human and mouse hearts have been reported as well such as the position of outflow aortic tract (Wessels et al., 2003). A human heart starts to contract approximately on the 22th day after fertilization, while it's the 9th day in a mouse heart (Wessels et al., 2003). More than 500 genes were identified to have distinct expression patterns during the process of cardiac maturation between mice and humans (Uosaki et al., 2016). Moreover, the action potential shapes as well as the Ca^{2+} dynamics are distinct in mouse and human hearts too (Knollmann et al., 2007). Because of the potential of animal models being unrepresentative as well as the infeasibility of using human cardiac samples for research and therapeutic purposes, major obstacles present in cardiovascular studies and regenerative medicine which call for a reliable and practical source of human cardiomyocytes.

It was first reported in 2002 the induction of cardiomyocytes from human ESCs by co-culturing human ESCs with mouse visceral endoderm-like cells (Mummery et al., 2003). In this co-culturing system, an out layer of endoderm was formed first to serve as an inductive signal for cardiac differentiation (Mummery et al., 2003). Alternatively, cardiomyocyte differentiation could also be initiated by applying a combination of different factors to induce cardiac mesoderm specification. Human ESCs, when treated with a set of factors including activin A, bone morphogenetic protein 4 (BMP4) and basic fibroblast growth factor (bFGF), generated embryoid bodies and subsequently differentiated into contracting cardiomyocytes (Yang et al., 2008).

However, using human ESCs for research and therapeutic purposes has raised ethical and political concerns. Particularly, using oocytes and embryos to generate pluripotent stem cells is controversial because some argue that this process will initiate embryonic development and human personhood. In addition, there are medical risks

arising from oocyte retrieval such as infection, bleeding and ovarian hyperstimulation syndrome. Moreover, somatic cell nuclear transfer is also fraught with ethical controversies. To generate embryos only for research use shows a disrespect of human life. Also, because of the potential errors during reprogramming processes, the new-born embryos were found to misexpress 4%-5% of the overall genome and 30%-50% of the imprinted genes (Lo et al., 2009; Jaenisch, 2004). Because of these concerns, there are strict regulations in using human ESC-based models for research and treatment. Those regulations contribute to a shortage in the source of human ESCs.

After Dr. Shinya Yamanaka's group established the first human iPSC line in 2007 (Takahashi et al., 2007), they tested its cardiac differentiation capability by subjecting the iPSCs to activin A and BMP4 treatment. The results showed that contracting cardiomyocytes were generated after 12 days from the induction of differentiation (Takahashi et al., 2007). In 2009, Zhang and colleagues further confirmed the cardiac differentiation potential of human iPSCs (Zhang et al., 2009). Subsequently, the researchers compared the properties of human iPSC-derived cardiomyocytes to human ESC-derived cardiomyocytes. The results showed that the derived cardiomyocytes from iPSCs have similar gene expression patterns as those differentiated from ESCs, and the time courses for the cardiac differentiation process from iPSCs and ESCs were comparable. In addition, both of the iPSC- and ESC-derived cardiomyocytes were able to respond to β -adrenergic stimulation, and the sarcomeric organizations of both cell populations were alike. Importantly, the electrophysiological studies indicated that human iPSCs were able to differentiate into ventricular- , atrial- , and nodal- cell types (Zhang et al., 2009).

Because of the pluripotency and self-renewal ability of human iPSCs, they hold great promise in human cardiac disease studies for they can provide an unlimited source

of cardiomyocytes. By utilizing human iPSCs, scientists have managed to build various cardiac disease models to study the underlying mechanisms of those diseases. For instance, the hypertrophic cardiomyopathy (HCM) model was established by Lan and colleagues using the iPSC lines generated from a family of 10 individuals carrying a hereditary HCM missense mutation (Arg663His) in their *MYH7* genes (Lan et al., 2013). Using this model, researchers were able to identify the irregular Ca^{2+} activity as the central mechanism of HCM pathogenesis.

Human iPSC-derived cardiomyocytes serve as an alternative to primary human cardiac tissue with less ethical and political concerns than human ESCs. They have substantially enriched the source of human cardiomyocytes that could be used for research and therapeutic purposes. Moreover, human iPSC-based cardiac models serve as a necessary and powerful supplement to animal models for they circumvent many limitations associated with using animal models to study human diseases such as the interspecies differences.

1.4 Limitations of human PSCs in modelling cardiovascular diseases

Even though human PSCs hold great promise in cardiovascular research, there remains three major obstacles. Firstly, the derived cardiomyocytes from human ESCs are heterogeneous pools of ventricular-, atrial-, and nodal-cardiomyocytes with a bias towards ventricular type (Blazeski et al., 2012). The similar heterogeneity was published with human iPSCs as well (Cao et al., 2008). This heterogeneity has hindered the application of ESC- and iPSC-based models in studying cell-type-specific diseases such as AF. Secondly, human PSC-derived cardiomyocytes display developmentally immature characteristics which more resemble foetal cardiomyocytes than adult ones. Structurally,

they have small cell sizes, an absence of transverse tubules and irregular sarcomeres. Furthermore, they show persistent automaticity and display foetal-stage action potential features as well as foetal-stage gene expression patterns (Mummery et al., 2003, Yang et al., 2014; Zhu et al., 2014). The immaturity of human PSC-derived cardiomyocytes makes them a less suitable model for studying age-related cardiac diseases which are more likely to occur to adult hearts. It also decreases the suitability of such models for drug screening. Third, the human PSC-derived cardiomyocytes are not capable of modelling the disease phenotypes at a tissue level. For example, they are not able to simulate the conditions of scar tissue formation.

1.5 Cardiac development

The heart is the first organ to develop in human embryos (Schleich et al., 2013). There are four steps leading to the formation of the heart: specification of cardiac mesoderm, determination of bilateral symmetry of cardiac fields, patterning of cardiac fields and terminal cardiac differentiation (Burridge et al., 2015). During gastrulation, the blastula is transformed to a three-layer organism that consists of ectoderm, mesoderm and endoderm (Keller, 2005). Multiple cellular changes occur in gastrulation process involving the morphology, mobility and adhesion of the cells. During this process, many cells that are originally located at or near the surface of the embryo migrate to an interior location through primitive streak (Mikawa et al., 2004). Mesodermal layer is established after the process of gastrulation and it eventually gives rise to the heart (Moorman et al., 2003).

After gastrulation, the mesodermal cells migrate and spread laterally and cranially within the embryonic disk to form a series of structures including lateral plate mesoderm which gives rise to the heart eventually (Moorman et al., 2003). In mammals, a structure

called cardiac crescent is developed before the formation of the heart tube by the cells in lateral plate mesoderm fusing at the midline. After this fusion, the primitive heart tube, which is comprised of an inner layer of endocardial cells and an outer layer of myocardial cells, is formed as the cells in the cardiac crescent coalesce (Srivastava, 2006). With the further folding of embryonic disk, the heart forming area gradually relocates to the neck of the embryo (Moorman et al., 2003).

The primitive tubular heart is then quickly divided into five regions- the truncus arteriosus that will undergo further division to form aorta and pulmonary artery, the bulbus cordis that is the origin of right ventricle and the outflow parts of both ventricles, the primitive ventricle that forms the trabeculated part of left ventricle, the primitive atrium that gives rise to the trabeculated parts of left and right atria, and the sinus venosus that will grow into the posterior part of right atrium, coronary sinus as well as sinoatrial node (Betts et al., 2013).

Two groups of cardiac progenitor cells are formed within splanchnic mesoderm, the inner layer of lateral plate mesoderm. The cell population arising from the lateral anterior splanchnic mesoderm is called first heart field (FHF) while the population coming from the splanchnic pharyngeal mesoderm is called second heart field (SHF) (Burridge et al., 2015). The FHF cells migrate out of anterior splanchnic mesoderm to form the cardiac crescent and the SHF cells come to join them at a later stage. Importantly, the SHF cells that express *Nkx2-5* gene are the progenitors of most cardiomyocytes (Prall et al., 2007). It is believed that the two heart fields contribute to the formation of different cardiac regions. The FHF forms the entire left ventricle and some of the right ventricle and atrium, while the SHF forms some of the right ventricle and atria along with the entire outflow tract (Abu-Issa et al., 2007).

As the heart tube grows and expands, it starts to undergo a series of folding within

the pericardial cavity. During this process, the developing heart tube extends and develops dilatations and constrictions, and the cranial part of the tubular heart bends ventrally and caudally and slightly to the right (Pansky, 1982). The looping of heart tube provides the first visualized evidence for the asymmetry of the embryo (Moorman et al., 2003).

The four chambers of the heart are divided by the formation of septal regions. During the process of a mammalian heart transforming from a tube to a four-chamber organ, two atria are separated by the formation of primary and secondary atrial septa (Webb et al., 1998; Franco et al., 2006; Kim et al., 2001) while the separation of two ventricles is completed by the development of interventricular septum. (Franco et al., 2006; De La Cruz, 1997; Kaufman, 1992)

1.6 Signalling pathways controlling cardiac development

1.6.1 Overview

Early cardiac progenitor cell populations are assigned to specific development paths around the time of gastrulation (Devine et al., 2014). In mouse models, the NODAL, a protein that belongs to the Transforming Growth Factor β (TGF-β) superfamily, is critical for the regulation of all cell lineages of early post-implantation conceptus. The initiation of mesoderm formation begins with a high expression level of NODAL in the proximal epiblast on mouse embryonic day (E)5.0 (Burridge et al., 2015). NODAL is necessary and sufficient to maintain the expression of the key patterning molecule BMP4 in extra-embryonic ectoderm (ExE) (Brennan et al., 2001). BMP4 belongs to BMP family which is also a member of TGF-β superfamily. It serves as a secondary signal for the induction of mesodermal layer. On E5.5, primitive streak is developed with the help of

NODAL, mesoendodermal transcriptional factors as well as the fibroblast growth factors (FGFs). On E6.25, cardiac progenitor cell populations expressing MESP1 leave the primitive streak, travel around in lateral plate mesoderm and converge at the midline of the embryo to form the heart (Burridge et al., 2015).

Cardiac development is tightly regulated by a series of signalling pathways such as TGF-β pathway, BMP pathway, JNK pathway, Wnt pathway and RA pathway. BMP pathway, JNK pathway and RA pathway that are relevant to this study will be discussed in detail in the following chapters.

1.6.2 BMP signalling pathway

BMPs are the largest sub-family of TGF-β superfamily. They are known to play vital roles in embryonic development and patterning by regulating cell proliferation, differentiation and apoptosis (Kirkbride et al., 2008).

The functionality of BMPs is achieved through receptor-mediated intracellular signalling. They signal through both canonical and non-canonical pathways. Type I and type II receptors are required in this process. Three type I receptors for BMP are ALK2, ALK3 and ALK6, and four type II receptors are BMPR-2, ActR-2A and ActR-2B (Wang et al., 2014).

The signalling begins with the binding of the BMP ligands to the transmembrane receptors. Different combinations of type II and type I receptors will lead to different subsequent events. When the heterotetrameric complex of a ligand and its receptors is formed, type I receptor will be phosphorylated by type II receptor, which will subsequently activate the downstream R-SMADs in canonical BMP signalling pathway (Wang et al., 2014). The specific R-SMADs in BMP signalling pathways are SMAD1, SMAD5 and SMAD8. The R-SMADs interact with SMAD4 to form a heterotrimeric

complex, and the R-SMAD/SMAD4 complexes translocate into the nucleus where they accumulate. By interacting with DNA, the complexes function as transcriptional factors to mediate the expressions of target genes by cooperating with other transcriptional factors (Rahman et al., 2015; Zhang, Li, 2005).

The parallel non-canonical pathways are mediated by the TGF-β activated tyrosine kinanse 1 (TAK1). X-linked inhibitors of apoptosis (XIAP) connects the BMP receptors to TAK1. TAB1/2/3 are required for the activation of TAK1. After the binding of TAB1/2/3 to TAK1, multiple signalling cascades are stimulated such as Jun N-terminal kinase (JNK) and NF-kB (Zhang, Li et al., 2005).

BMP signalling pathways are essential for cardiac development. Importantly, an NKX2-5/BMP2/SMAD1 negative feedback loop model was revealed by Prall and colleagues. The secreted BMP2 ligand induces the expression of NKX2-5 by stimulating canonical SMAD signalling. However, SMAD signalling represses the proliferation of those NKX2-5-positive cardiac progenitor cells. Thus, NKX2-5 in turn suppresses the expression of BMP2 to reduce the functionality of SMAD signalling. In this way, the cardiac progenitor cell populations are allowed to expand (Prall et al., 2007).

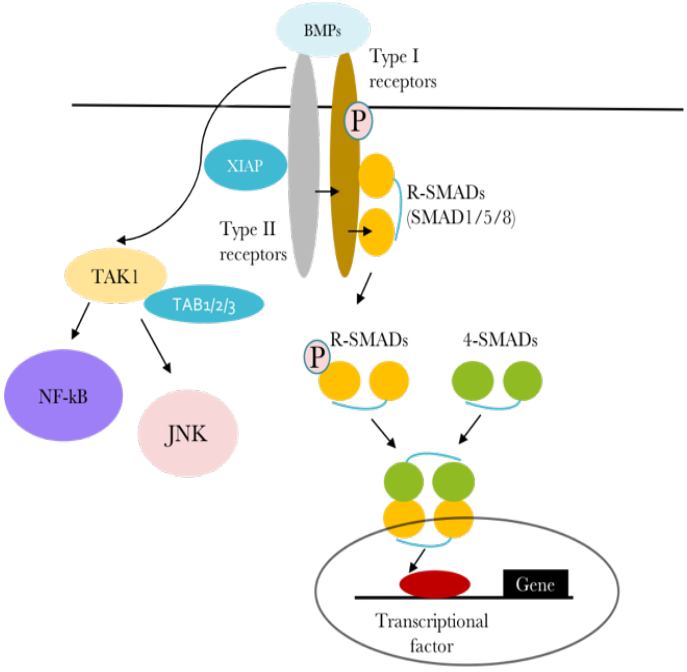


Figure 1.1 Overview of canonical and non-canonical BMP signalling pathways. In canonical BMP pathway, a BMP ligand binds to the transmembrane receptors to initiate the signalling. A type I receptor is phosphorylated by a type II receptor and subsequently it activates the R-SMADs (SMAD1/5/8). Then the R-SMAD/4-SMAD complexes are formed. As the complexes translocate into the nucleus, they work with other transcriptional factors to regulate the expression of target genes. In non-canonical pathways, BMP receptors are connected to TAK1 by XIAP. When TAK1 binds to TAB1/2/3, multiple signalling cascades are activated including JNK and NF-kB.

1.6.3 JNK signalling pathway

Mitogen-activated protein kinases (MAPKs) function to integrate the signals from multiple receptors and convey those signals from the activated receptors into the cells (Alam et al., 2011). JNKs (MAPK8-10) is one of the major groups of MAPKs that play essential roles in multiple biological processes including cardiac differentiation, neural development and cell apoptosis.

In JNK pathways, MAPKKKs are turned on by the Rho-family GTPases to subsequently phosphorylate the downstream MKK4/7. The phosphorylated MKK4/7 leads to the activation of JNKs. The MKKs and JNKs are modified by a group of scaffold proteins including JIP1/2/3 (Davis, 2000; Wang et al., 2007). Different factors and agents activate JNKs through different signalling pathways. The JNK signalling can also be stimulated through non-canonical TGF-β, BMP and Wnt signalling pathways.

The stimulated JNKs translocate into cell nucleus to phosphorylate and activate multiple transcriptional factors such as c-Jun, NF-kB, p53 and NFAT1 (Liu et al., 2016; Davis, 2000). Importantly, the JNKs have a regulatory effect on COUPTFII, an atrial cardiomyocyte-specific transcriptional factor (Tanwar et al., 2014). The relevant details will be discussed in Chapter 1.7.3.

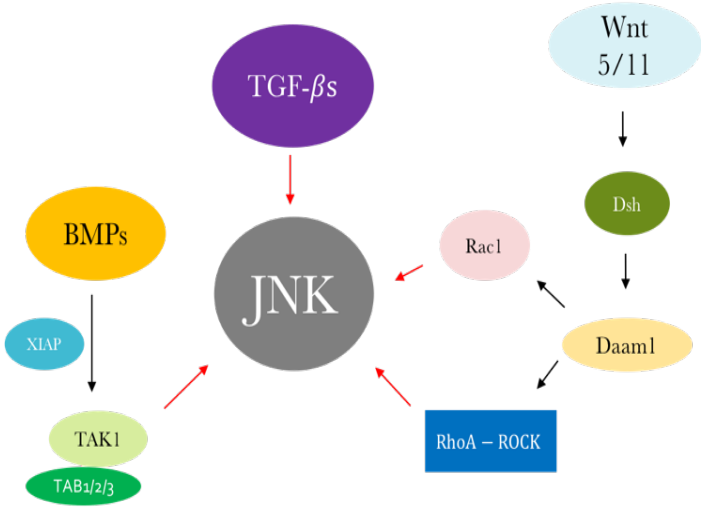


Figure 1.2 JNK signalling can be stimulated through non-canonical TGF-β, BMP and Wnt signalling pathways. Dsh, dishevelled; Daam1, dishevelled-associated activator of morphogenesis 1; Rac1, ras-related c3 botulinum toxin substrate 1; RhoA, ras homolog gene family, member A; ROCK, rho-associated, coiled-coil-containing protein kinase.

1.6.4 RA signalling pathway

RA is a non-peptidic small molecule generated from vitamin A (retinol) that is able to regulate Vitamin A during embryonic development processes. It works as ligand to bind the RA receptors (RARs) within cell nucleus (Rochette-Egly et al., 2009). Upon binding, the RARs function as transcriptional activators (Rhinn et al., 2012). RA has significant effects on cell growth and differentiation which are essential for the embryonic development (Di Masi et al., 2015).

RA originates from Vitamin A through a series of oxidative reactions (Parés et al., 2008). It is either synthesized within the cell from the circulating Vitamin A, or comes from the cells nearby. Within the cell, RA is transported to the nucleus by cellular retinoic acid-binding proteins (CRABPs). After entering cell nucleus, RA binds to the dimer formed by RARs and retinoid X receptors (RXRs). RA, together with the RAR/RXR dimer then binds to the DNA promoter regions, RA-response elements (RAREs), to initiate the expression of the target genes (Rhinn et al., 2012, Mangelsdorf et al., 1990).

Without RA binding to the receptors, the RAR/RXR dimer is also able to bind to RAREs, however, there is no transcription of the target genes because of the existence of a group of co-repressors. While with the presence of RA, the co-repressor group is replaced by a group of co-activator complexes which assist with the recruitment of transcription pre-initiation complex (Rhinn et al., 2012).

In cardiac development, the RA signalling is involved in many processes. For instance, the presence of RA signalling in the posterior region of cardiac field is believed to mediate the formation of SHF. Retinaldehyde dehydrogenase 2 (RALDH2) is an essential enzyme that catalyses RA synthesis (Duester, 2008). The lost in RALDH2 function and RA synthesis results in the malformation of heart tube and leads to severe cardiac defects (Duester, 2008).

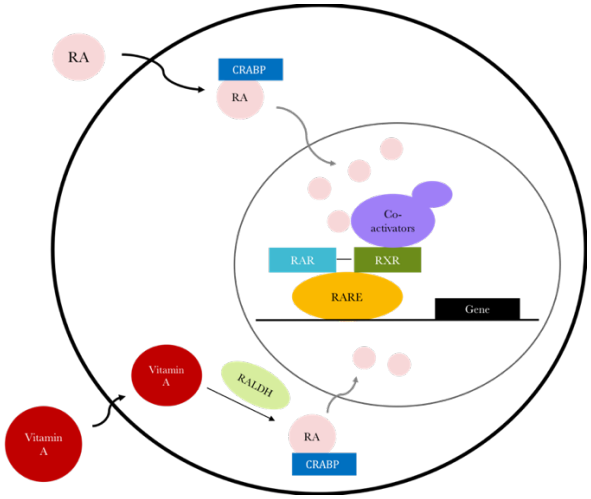


Figure 1.3 Overview of RA signalling pathway. RA is either synthesized within the cell from the circulating Vitamin A or comes directly from the cells nearby. Inside the cell, RA is transported to the nucleus by CRABPs. After entering cell nucleus, RA binds to RAR-RXR dimer to form a complex. Then the complex interacts with RAREs to initiate the expression of the target genes.

1.7 Gremlin 2 in cardiac development

1.7.1 Structure and working mechanisms of Gremlin

Gremlin has been identified as an antagonist for the BMP signalling pathway (Hsu et al., 1998). Its negatively regulating effect on BMP4 has been demonstrated in mouse model (Shi et al., 2001). Gremlin is classified into the DAN family (Nolan et al., 2014). A 30-amino acid peptide domain was identified in Gremlin which had a number of lysine and arginine residues that were positively charged. This provided a binding site for the negatively-charged patch on BMP ligands (Sun et al., 2006). This finding has helped explain the mechanism of Gremlin antagonizing BMP4. Gremlin functions by competitively binding to BMP ligands. They showed the most robust antagonizing effects on BMP2 and BMP4 (Sudo et al., 2004).

Gremlin proteins include Gremlin 1 and Gremlin 2. The analysis of the Gremlin 2 bound to the growth and differentiation factor (GDF) revealed the bindings of two

Gremlin 2 dimers to each GDF5 monomer. Importantly, a Gremlin 2 monomer is able to interact with both bone morphogenic protein receptor type I and II (BMPRI and BMPRII) binding domains of GDF5, leaving the nearby Gremlin 2 monomer free to bind another GDF5 (Nolan et al., 2016). This chain-like reaction can lead to a series of bindings to form a long protein chain. This binding mechanism makes Gremlin 2 distinct from other DAN family proteins like Noggin whose antagonistic effects are achieved through covering the binding sites of receptors to prevent BMP ligands from interacting with their receptors (Groppe et al., 2002). Importantly, Gremlin 2 was reported to have a combined effect of inhibiting canonical BMP signalling first and activating JNK signalling through non-canonical BMP pathway at a later stage (Tanwar et al., 2014). This multiplexed mechanism of Gremlin 2 is closely related to its role in directing atrial cardiomyocyte differentiation.

1.7.2 Gremlin 2 is essential for cardiac development

It was demonstrated in zebrafish that Gremlin 2 was essential for the development of the heart (Muller et al., 2013). Gremlin 2 was found to be highly expressed in the ventral portion of pharyngeal arch mesoderm, right near the cardiac field. It was the first factor reported to have effects on both cardiac laterality and contractility. In zebrafish, when Gremlin 2 was down-regulated, the asymmetric cardiac development was affected due to the reduced expressions of *atrial* and *ventricular myosin heavy chains* (*amhc* and *vmhc*), with *amhc* being more interfered (Bisgrove et al., 1999; Essner et al., 2000; Muller et al., 2013). Muller and colleagues also showed that the ventricular and atrial cardiomyocyte specification was affected by the expression of Gremlin 2 because of its role in mediating phosphorylated SMAD1/5/8 and BMP signalling. An up-regulated expression level of Gremlin 2 had a positive effect on atrial differentiation. However, the overexpression of

Gremlin 2 also led to a decreased cardiac contraction rate and a disruption in the propagation of contraction. In addition, the overactivity of Gremlin 2 turned on the AF candidate genes as well as the atrial natriuretic peptide during the cardiac differentiation of mouse ESCs (Muller et al., 2013).

In conclusion, Gremlin 2 is essential for cardiac development. It has multiple roles such as enhancing atrial differentiation, assisting with the asymmetric cardiac development and maintaining normal cardiac contracting rate and rhythm. The expression of Gremlin 2 during cardiac development is tightly regulated. An aberrant expression will result in cardiac defects and diseases.

1.7.3 Gremlin 2 strengthens atrial differentiation in mouse ESCs

Gremlin 2 was reported to enhance cardiac differentiation and increase atrial cell population in mouse ESC-derived cardiomyocytes (Tanwar et al., 2014). Without exogenous Gremlin 2 protein, gene expression analysis showed that *Grem2* gene was turned on on the 4th day after the initiation of differentiation and eventually reached a high level. This was concurrent with the expressions of mesoderm and endoderm progenitor cell markers as well as the early cardiac progenitor cell markers.

Tanwar and colleagues found that the Gremlin 2-treated cells began to contract at an earlier stage compared to the control cells and had a higher proportion of contracting cell pool. The flow cytometry results indicated sharp increases in the cells expressing cardiac-specific markers. Gene expression analysis revealed that Gremlin 2-treated cells had significantly higher expressions of the cardiac specific gene markers: *Nkx2-5*, *Gata 4*, *Tnnt2* and *Myh6* (Tanwar et al., 2014).

Electrophysiological studies illustrated that the untreated cells had a mixture of different types of action potentials- ventricular, atrial and nodal, while the Gremlin 2-

treated cells had a dominant atrial-type action potential. Gene expression analysis showed significantly higher expression of atrial-specific genes, *Myl7*, *Gja5*, *Kcnj5*, *Cacna1d*, *Sln* and *Nppa* in the cells receiving Gremlin 2 treatment (Tanwar et al., 2014).

The transcription factors COUPTFII and HEY1 were known to restrictedly express in the developing atria (Pereira et al., 1999), while IRX4 and HEY2 exclusively express in the developing ventricles. IRX4 and HEY2 also work to suppress atrial cardiomyocyte specification (Nakagawa et al., 1999; Bao et al., 1999; Koibuchi et al., 2007). Tanwar and colleagues demonstrated that Gremlin 2 treatment stimulated *CoupTFII* and *Hey1* genes while suppressing the expressions of *Irx4* and *Hey2*.

Importantly, the researchers have illustrated the potential mechanism underlying the atrial-specification effects of Gremlin 2 on mouse ESCs. Protein expression analysis showed that Gremlin 2 suppressed SMADs phosphorylation shortly after differentiation, but significantly activated SMADs and JNK at a later stage. The incubation of the JNK inhibitors completely blocked the expressions of COUPTFII and HEY1 (Tanwar et al., 2014).

1.8 RA in cardiac development

1.8.1 RA in heart regeneration and cardiac development

RA contributes significantly to the differentiation and specification of cardiomyocytes and plays a vital role in heart regeneration. It was illustrated in zebrafish that RA was up-regulated after ventricular trauma, subsequently inducing the expression of *raldh2* gene in endocardial cells. The *raldh2*-positive epicardial cells were abundant in the injured part of the heart. When RA was blocked, the cardiomyocyte regeneration was

inhibited (Kikuchi et al., 2011).

In cardiac differentiation, RA is essential for the development of SHF. The down-regulated level of RA resulted in the failure in heart looping and atrial sinus venosus development. RA also functions to restrict the SHF posteriorly. In addition, RA displayed the ability to stimulate BMP signalling, assisting with the normal organization of heart tube. In RA-deficient situations, this BMP stimulating effect was disturbed, affecting the contribution of SHF cells to the outflow and inflow poles (Ryckebusch et al., 2008).

Importantly, the role of RA in driving atrial cardiomyocyte specification has been demonstrated by a number of publications (Yutzey et al., 1994; Xavier-Neto et al., 1999; Devalla et al., 2015; Lee, Protze et al., 2017). Yutzey and colleagues reported that the expansion of atrial area was observed in chicken after RA treatment (Yutzey et al., 1994). In a recent study, Devalla and colleagues managed to generate atrial-type cardiomyocytes from human ESCs with the addition of RA (Devalla et al., 2015). Similarly, Lee and colleagues reported that the over-expression of RA led to enlarged atrial chambers and decreased-sized ventricular chambers in human PSCs while the application of RA inhibitor had the opposite effect (Lee, Protze et al., 2017). They concluded that the specification of atrial cardiomyocytes was achieved through autocrine RA signalling and that the generation of ventricular and atrial cells depended on different mesoderm cell populations. Mesodermal cells expressing RALDH2 eventually gave rise to atrial cardiomyocytes (Lee, Protze et al., 2017).

Apart from the impact of RA on cardiomyocyte subtype specification, the RA signals also induce ventricular cell maturation. Relevant mechanisms still remain largely unexplored, but a specific RA receptor, RARα, has been identified to play a leading role in this RA-directed maturation process (Hoover et al., 2008).

1.8.2 RA drives atrial-like cardiomyocytes from human ESCs

Enhancing RA signalling is able to improve the atrial cardiomyocyte differentiation from human ESCs (Devalla et al., 2015). The *in vitro* specification of atrial cardiomyocytes is initiated after the induction of mesoderm and before the appearance of cardiac progenitor cell populations. Thus, RA treatment was given to the differentiating ESCs within this time window by the researchers. While the RA-treated cells had a smaller contracting cell pool in general, they showed an increase in atrial populations.

Day 31 cardiomyocytes showed up-regulated expression levels of atrial-specific genes (*NPPA*, *SLN*, *HEY1* and *PITX2*) and down-regulated expression levels of ventricular-specific genes (*HEY2*, *MYL2, IRX4*, and *HAND1*). Notably, by comparing the gene expression patterns of RA-treated and untreated cells to the 15-week-old human foetal cardiomyocytes, the researchers found that of those 292 genes whose expressions were higher in RA-treated cells, 31 percent were more enriched in human atrial cardiomyocytes, while only 8 percent were more expressed in ventricular cells. Electrophysiological studies indicated that 85 percent of the RA-treated cells recapitulated atrial-type action potential features, while in the untreated cell group, 80 percent displayed ventricular-type action potentials.

Protein expression analysis suggested that COUPTFI and COUPTFII, the transcriptional factors that mediate atrial-specific ion channel coding genes were turned on after 24h of RA treatment, and their expression levels were significantly increased thereafter compared to the untreated cells. The knockdown of COUPTFs in human ESC-derived cardiomyocytes had no effect on the expressions of the cardiac gene *TNNT2*, however, it led to the decreased levels of the atrial-specific potassium channel coding genes, *KCNA5* and *KCNJ3*. The above results highlighted the potential mechanism underlying RA-induced atrial specification.

In addition, in a recently published paper aforementioned in Chapter 1.8.1, Lee

and colleagues reported that the specification of atrial cardiomyocytes was achieved through autocrine RA signalling. They found that ventricular and atrial cardiomyocytes were derived from different mesodermal cell populations expressing CD235a and RALDH2 respectively (Lee, Protze et al., 2017). As RALDH2 is a key RA-synthetic enzyme, these findings suggested that RA signalling during the development of mesoderm was required for atrial cardiomyocyte specification.

1.9 Properties of atrial cardiomyocytes

Atrial cardiomyocytes are distinct from ventricular cells structurally. In animal model, it was demonstrated that the atrial cells were smaller in size and had significantly fewer T tubules but abundant mitochondria. There are also prominent Golgi complexes connected to atrial granules. The small cell size and low density of T tubules in atrial cardiomyocytes allow for a quicker conduction of action potential (McNutt et al., 1969).

There are substantial differences in the expressions of transcriptional factors and functional genes between atrial and ventricular cardiomyocytes as well. For example, HEY1 is essential for the accurate development of atrial-ventricular border and it is highly expressed in atrial cardiomyocytes but not ventricular ones. Similarly, COUPTFII is also known to restrictedly express in developing atria (Pereira et al., 1999). *MYL7* that codes for myosin regulatory light chain 2, atrial isoform (Kubalak et al., 1994), *GJA5* that codes for connexin40 (Leaf et al., 2008), *CACNA1*, *KCNJ3*, *KCNJ5* and *KCNA5* that code for ion channels Cav1.3, Kir3.1, Kir3.4 and Kv1.5 (Zhang, He et al., 2005; Krapivinsky et al., 1995; Bettahi et al., 2002; Wang et al., 1993), *NPPA* that codes for atrial natriuretic peptide (Houweling et al., 2002) and *SLN* that codes for Sarcolipin (Minamisawa et al., 2003) are atrial-specific gene markers.

Human atrial cardiomyocytes are also distinct from ventricular cells in electrophysiological characteristics. The resting membrane potential for atrial and ventricular cardiomyocytes are -74mV and -81mV. Compared to the ventricular cells, atrial cells have less negative resting membrane potential. In addition, atrial cardiomyocytes exhibited a smaller upstroke amplitude as well as an absence in plateau phase during repolarization process (Grandi et al., 2011). In animal models, atrial cells also displayed lower and shorter action potentials (Giles et al., 1988).

The low density of T tubules and the small size of atrial cardiomyocytes also lead to a distinct calcium signalling pattern in response to electrical stimulations. Because of a lack in T tubules, the Ca^{2+} response to depolarization starts around the edges of atrial cells, without penetrating the cell centre in resting situations. Under positive inotropic stimulations, the ability of ryanodine receptors (RyRs) to recognize calcium transient signals and sarco/endoplasmic reticulum Ca^{2+} ATPase (SERCA) activity was strengthened, and the calcium induced calcium release (CICR) was enhanced. The centripetal propagation of calcium signalling was thus achieved to fulfil the important functions of the atria such as refilling blood for the ventricles (Bootman et al., 2011).

1.10 Maturation of cardiomyocytes

The maturity of cardiomyocytes can be determined by many aspects. Morphologically, cardiomyocyte maturation and cell subtype specification are accompanied by an increase in the cell size (Laflamme et al., 2011). Importantly, it was reported that the human ESC-derived cardiomyocytes were significantly smaller than human adult cardiomyocytes (Yang et al., 2014). Another important factor that assists with the determination of cell maturation stage is the shape of the cells. The mature

cardiomyocytes have a length/width ratio of 7-9.5 (Yang et al., 2014).

As the cardiac development progresses, the expression levels of cardiac genes undergo specific changes. For example, the sarcomere-related genes such as the α-myosin heavy chain (*MYH6*), α-actinin (*ACTN2*) and *TNNT2* were undetectable or at a very low expression level in the undifferentiated human PSCs but were found to be dramatically up-regulated at a later stage (Gupta et al., 2010).

Cardiomyocyte maturation is accompanied by ion channel remodelling as well (Laflamme et al., 2011). The expressions of the genes coding for a variety of ion channels experience certain changes during cardiac differentiation process. The L-type calcium channel coding genes *CACNA1C* and *CACNA1D*, potassium voltage-gated channel superfamily H (*KCNH*s), potassium voltage-gated channel superfamily Q (*KCNQ*s), inward rectifier potassium ion channel coding genes (*KCNJ*s) and many others were reported to increase during the maturation of the cardiomyocytes (Yang et al., 2014) . The expression changes of the genes related to calcium handling such as *RYR2* were also observed during the cardiomyocyte maturation (Yang et al., 2014).

As a consequence of the changes in ion channel coding genes, the density of ion currents is distinct in the cardiomyocytes of different developmental stages. In rat it was illustrated that from day 5 to day 15 of differentiation, the density of the transient outward potassium current (I_{to}) was doubled (Guo et al., 1996). Also, it was the rapidly activating delayed rectifier potassium current (I_{Kr}) but not the slowly activating component (I_{Ks}) that was observed in ventricles of the dogs younger than 30 days old whereas both of the currents were present in adult dogs. This finding suggested that the young dogs depended more on I_{Kr} rather than I_{Ks} for the repolarization process (Obreztchikova et al., 2003). The changes happening to ion currents and channels during cardiac development lead to different action potential characteristics of the mature and immature cardiomyocytes. In

human heart it was demonstrated that the resting membrane potential was less negative in immature cardiomyocytes (Yang et al., 2014). This is due to the lower membrane capacitance of immature cells (Kolanowski et al., 2017). Moreover, the increases in the upstroke velocity and the action potential duration were observed as the human ESC-derived cardiomyocytes matured, which was thought to be because of the elevated level of inward currents (Sartiani et al., 2007).

Furthermore, as the cardiomyocytes mature, their responsiveness to the adrenergic stimulation is eventually developed, demonstrated by the increases in beating rates and isometric force under β-adrenergic stimulation (Yang et al., 2014).

In order to optimize the PSC-derived cardiomyocytes, many attempts have been made and several methods of driving the *in vitro* maturation of the derived cardiomyocytes have been discovered such as increasing cell culture time (Kamakura et al., 2013) as well as the application of electrical, biochemical and physical stimulations (Radisic et al., 2004; Földes et al., 2011; Zimmermann et al., 2002; Ronaldson-Bouchard et al., 2018).

In the current study, we aim to examine the effectiveness of a combined treatment of Gremlin 2 and RA in directing atrial specification and driving the *in vitro* maturation of human iPSC-derived cardiomyocytes. By doing so, we hope to develop a novel protocol to produce atrial-type cardiomyocytes with adult cell characteristics from human iPSCs so as to create a model for human atrial-specific disease studies as well as the development of relevant therapies.

Chapter 2. Methods

2.1 Episomal Human iPSC Line

The human iPSCs used for the differentiation experiments were provided by Gibco® by Life Technologies, Carslbad, USA. The iPSC line was generated from cord blood-derived CD34+ progenitor cells using a three-plasmid and seven-factor (Oct4, Sox2, Klf4, Myc, Nanog, Lin28 and SV40L T antigen) episomal system.

2.2 Matrigel plate coating

Matrigel Matrix (Corning) was stored at -20℃. 5ml of Matrigel was allowed thawing at 4℃ overnight and 0.5ml Matrigel aliquots were prepared on ice. The ready-to-use Matrigel aliquots were stored at -20℃. To coat plates, each aliquot was thawed on ice or at 4℃ for 1 hour. While thawing Matrigel, the 4-, 6-, or 24-well culture plates as well as the pipettes were placed in -20℃ for pre-cooling. The mTeSR™1 (STEMCELL™ Technologies) culture medium was kept cold at 4℃. When Matrigel was fully thawed, it was 1:60 diluted in the cold mTeSR™1 medium to coat the pre-cooled plates. Matrigel diluted in mTeSR™1 medium was added to the wells using the pre-cooled pipettes. For 6-well culture plates, the coating medium was added 2ml per well and for the 4- and 24-well culture plates, the medium was added 0.5ml per well. Subsequently, the coated plates were stored at 4℃ overnight. Before use, they were incubated at 37℃ for 1h for the Matrigel layer to solidify.

2.3 Human iPSCs maintenance and passaging

Episomal Human iPSC Line was cultured on Matrigel-coated six-well culture plates with mTeSR™1 medium. Undifferentiated human iPSCs were maintained with daily medium change. The mTeSR™1 medium was pre-warmed under room temperature every time before medium change. The iPSCs were passaged every 4 to 5 days. An approximately 70% confluence was observed before passaging the cells. For passaging, human iPSCs were treated with 1U/ml Dispase (STEMCELL™ Technologies) at 37℃ for 5-7 min to detach the cells from the Matrigel layer. After three washes with fresh medium, the cells were collected and centrifuged at 800rpm for 4min using HERAEUS MEGAFUGE 8 centrifuge (Thermo Scientific). Then the cells were resuspended in fresh medium and plated in new Matrigel-coated culture plates. The cells were passaged at a 1:3 ratio.

2.4 Human iPSC stocks preservation

Cell stocks of each passage were prepared in the freezing medium consisting of 40% Knockout Serum Replacement (Gibco® Life Technologies), 50% mTeSR™1 medium and 10% DMSO, and were stored at -80℃. The ready-to-use freezing medium was stored at 4℃ before use. Cells were first treated with 1U/ml Dispase at 37℃ for 5-7 min. After three washes with fresh medium, they were collected and centrifuged at 800rpm for 4min. Then the cells were resuspended in the freezing medium described above and transferred into cryovials. One well (of a 6-well culture plate) of iPSCs were transferred into one cryovial. The cell stocks were preserved at -80℃.

2.5 Resuscitation of frozen human iPSC lines

When thawing the frozen human iPSC lines, a frozen cell stock was placed at 37℃ until it was fully thawed. Then the cells were carefully collected and transferred into a tube containing fresh mTeSR™1 medium drop by drop. Next, the cells were centrifuged at 800rpm for 4min and resuspended using fresh mTeSR™1 with 10μM Y-27632 (Cambridge Bioscience). One vial of frozen human iPSCs were plated in one well of a Matrigel-coated 6-well culture plate. After resuscitation, the iPSCs were maintained with daily medium change (fresh mTeSR™1 wi.th 10μM Y-27632) for three days. Afterwards, the cells were cultured with mTeSR™1 medium only.

2.6 Purification of human iPSCs

Human iPSCs were purified when spontaneous differentiation was observed. The iPSCs were treated with 1U/ml Dispase at 37℃ for 5-7 min. After three washes with fresh medium, each well of a 6-well culture plate was added with 1ml mTeSR™1 medium. Under the microscope, undifferentiated iPSC colonies were picked with a 200μl pipette tip and transferred into a tube for centrifugation. Then the cells were centrifuged at 800rpm for 4min, resuspended in fresh mTeSR™1 medium and plated in new Matrigel-coated culture plates. The purified iPSC colonies were passaged at a 1:1 ratio.

2.7 Differentiation from human iPSCs to cardiomyocytes

The human iPSCs were dissociated into single cells for differentiation experiments. Cells were given a 3-4 min treatment of 1U/ml Dispase at 37℃. After three washes with fresh medium, the cells were then treated with ACCUTASE™ (STEMCELL™ Technologies) at 37˚C for 5-8 min. After the addition of 2-3 volume of fresh mTeSR™1 medium to terminate the effect of ACCUTASE™, the cells were collected and centrifuged at 800rpm for 4min. Then the iPSCs were plated in Matrigel-coated 4- or 24-well culture plates and maintained daily using mTeSR™1 medium with 10μM Y-27632. Differentiation experiments were performed using PSC Cardiac Differentiation Kit (Gibco® Life Technologies) which contained Cardiac Differentiation Medium A, Cardiac Differentiation Medium B, and Cardiac Maintenance Medium (CMM). When the iPSCs reached an approximately 90% confluence, Medium A with 10μM Y-27632 was added to the plates, and the date of the addition of Medium A was labelled as Differentiation day 0 (Day 0). Medium B with 10μM Y-27632 was applied on Day 2. From Day 4, the cells were cultured with CMM and the medium was changed every other day. All the differentiation and culture media were pre-warmed under room temperature before applying to the cells. The undifferentiated cells were divided into experimental groups and control groups. For experimental groups, Gremlin 2 (R&D Systems; BioVision) was added to the culture medium at the concentration of 1-5μg/ml on Day 4, and RA (Sigma) was added at 0.5-1μM from Day 4 to Day 8. From passage 8, the cells were differentiated using the protocol described in Figure 2.1. Control groups were differentiated using the same protocol excluding the addition of Gremlin 2 and RA.

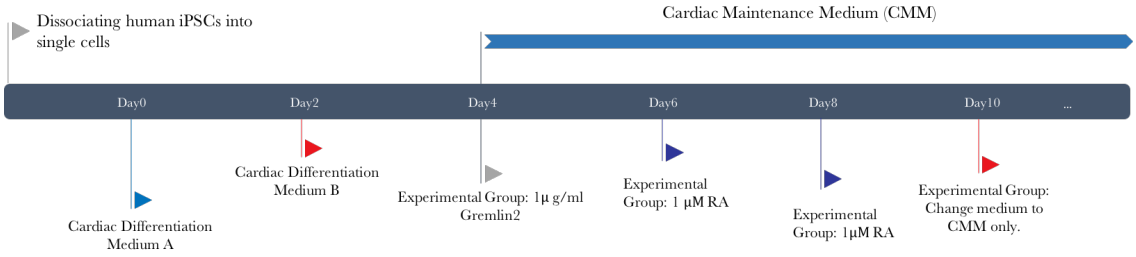


Figure 2.1 Gremlin 2- and RA-directed cardiac differentiation from human iPSCs (from passage 8). Human iPSCs were dissociated into single cardiomyocytes for the differentiation experiments. Cardiac Differentiation Medium A was added on Day 0 and Cardiac Differentiation Medium B was applied to the cells on Day 2. From Day 4 on, the cells were maintained with CMM. 1μg/ml of Gremlin 2 was added to the experimental group on Day 4 and 1μM of RA was applied to the experimental group on Day 6 and Day 8.

2.8 RNA isolation

RNA samples were harvested on Day 0, Day 1, Day 3, Day 5, up to Day 15 from both experimental groups and control groups using RLT buffer from RNeasy® Mini Kit (QIAGEN) with 10μl/ml β-mercaptoethanol. The samples were stored at -80℃ and before purification, they were allowed thawing on ice. To purify the samples, 350μl of RLT buffer was used for one well of a 4- or 24-well culture plate. Samples were purified with RNeasy® Mini Kit following the manuals from the manufacturer. In brief, the unpurified samples were mixed with 70% 200 proof ethanol at 1:1 volume ratio and transferred directly into the RNeasy spin columns placed in 2ml collection tubes. After the centrifugation at 10,000rpm for 15s using Centrifuge 5424R (Eppendorf), the flow-through was discarded. 700μl of Buffer RW1 was added into one column, and after the centrifugation at 10,000rpm for 15s, the flow-through was discarded. Buffer RPE were pre-mixed with 4 volumes of 96-100% ethanol to make working solution. 500μl of Buffer RPE working solution was applied to the samples for twice and the samples were centrifuged at 10,000rpm for 15s and 2min respectively after each RPE application. After disposing the flow-through, the RNeasy spin columns were placed into new 1.5ml

collection tubes. Subsequently, 40μl of nuclease free water was added directly to the membrane of each column for RNA elution. The columns were centrifuged again at 10,000rpm for 1min to collect RNA. The RNA concentration of each sample was measured using Nanodrop 2000c (Thermo Scientific).

2.9 Reverse transcription

Reverse transcription was carried out with High Capacity RNA-to-cDNA kit (Applied Biosystems by Thermo Fisher Scientific) according to the manufacturer's instructions. The kit was kept in -20℃ and before use, it was allowed thawing on ice. 1μg of RNA was used for a total reaction volume of 20μl. In brief, for each 20μl reaction volume, 10μl of Buffer Mix (containing MuLV and RNase inhibitor protein) and 1μl of Enzyme Mix (containing dNTPs, random octamers and oligo dT-16) were used. 1μg RNA was applied in each qPCR tube, with a maximal volume of 9μl. Nuclease free water was added to the reactions when needed. Then the reverse transcription was performed using the Mastercycler Gradient 5331 (Eppendorf). The reaction program was set to the following: 1h at 37℃, followed by 5min at 95℃ before returning to 4℃. After the reverse transcription, cDNA samples were stored at -20℃.

2.10 Quantitative PCR (qPCR)

Gene expressions were analyzed using qPCR. The analyses were carried out for Gremlin 2 protein coding gene (*GREM2*), cardiac progenitor cell marker (*NKX2-5*), cardiac troponin coding gene (*TNNT2*), atrial-specific genes (*NPPA*, *MYL7* and *KCNJ5*),

other inward rectifier potassium channel coding genes (*KCNJ4*, *KCNJ5* and *KCNJ12*), and adrenergic receptor coding genes (*ADRA1A* and *ADRB1*). The TaqMan® Gene Expression Assays were predesigned by Applied Biosystems by Thermo Fisher Scientific. The qPCR was performed with LightCycler®480 (Roche) using TaqMan® Gene Expression Master Mix (Applied Biosystems by Thermo Fisher Scientific) following the instructions from the manufacturer. The TaqMan® Gene Expression Assays and cDNA samples were stored at -20℃ and before qPCR experiments, they were allowed thawing on ice. A control for cDNA input was generated by amplifying human *HPRT1* gene (Applied Biosystems by Life Technologies). In brief, the total volume for each reaction was 20μl, consisting of 10μl of Gene Expression Master Mix, 1μl of Gene Expression Assays, 1μl of human *HPRT1* gene, 1μl of cDNA sample and 7μl of RNase-free water. Cycling parameters were set to 2 min at 50℃, followed by 10 minutes at 95℃, then followed by 40 cycles of 15 seconds at 95℃ and 60 seconds at 60℃. The relative expressions of target genes were determined by comparing the Ct values of target genes with those of the house-keeping gene using -ΔCt method (equation as below). The results from two or three technical replicates were averaged. Four experimental groups were differentiated independently for qPCR experiments (n=4), and parallel analyses were done in two sets of experimental and control groups differentiated simultaneously using the human iPSCs from the same passage. The information of the TaqMan® Gene Expression Assays used in this study is provided in Fig 2.2.

$$\text{Relative expression}(\%) = \frac{Expression\ of\ target\ gene}{Expression\ of\ house-keeping\ gene} = 2^{-\Delta Ct}$$

$$\Delta Ct = Ct_{\text{target}} - Ct_{\text{house-keeping}}$$

Table of TaqMan® Gene Expression Assays

Supplied by Applied Biosystems by Thermo Fisher Scientific

Gene	Assay no.	Target species
TNNT2	Hs00943911_m1	Human
NKX2-5	Hs00231763_m1	Human
GREM2	Hs03986140_s1	Human
NPPA	Hs00383231_m1	Human
MYL7	Hs01085598_g1	Human
KCNJ5	Hs00168476_m1	Human
KCNJ4	Hs00705379_s1	Human
KCNJ12	Hs00266926_s1	Human
ADRA1A	Hs00169124_m1	Human
ADRB1	Hs02330048_s1	Human

Figure 2.2 Information of TaqMan® Gene Expression Assays supplied by Applied Biosystems by Thermo Fisher Scientific. Sequences for the pre-designed TaqMan® Gene Expression Assays are confidential.

2.11 Cardiomyocytes dissociation

Cardiomyocyte aggregates were dissociated using 100units/ml Collagenase I (Gibco® by Life Technologies). Collagenase I treatment was given to the cardiomyocyte aggregates for 45min at 37℃. After fully pipetted with a 1000µl pipette tip, the cells from one culture well (of a 4- or 24-well culture plate) were transferred directly into a 1.5ml tube and centrifuged at 1200rpm for 2min at 20℃ using Centrifuge 5424R (Eppendorf). The supernatant was discarded and the cells were washed with PBS. 0.05% Trypsin-

EDTA (Gibco® by Life Technologies) treatment was applied to the cells for 2min at 37℃. CMM with 10% KnockOut™ Serum Replacement (Gibco® by Life Technologies) was subsequently added to the tube and the cells were centrifuged at 1200rpm for 2min at 20℃. In order to fully dissociate the aggregates, the cells were pipetted for 5-10 times with a 1000μl pipette tip before each centrifugation. Then the supernatant was discarded and the cells were resuspended in CMM with 10μM Y-27632 and plated in new Matrigel-coated 4-well culture plates with coverslips. The cardiomyocytes were split at a ratio of 1:4 (used for the immunofluorescence analysis Protocol 1) or 1:12 (used for the immunofluorescence analysis Protocol 2 and patch clamp experiments).

2.12 Immunofluorescence analysis

The dissociated cardiomyocytes were cultured in CMM with 10μM Y-27632 for 2 days at 37℃. Immunofluorescence analysis of the single cardiomyocytes grown on coverslips were performed using the following protocols.

2.12.1 Protocol 1

The dissociated cardiomyocytes cultured on the coverslips were fixed first with 2% paraformaldehyde (PFA) with 0.1% glutaraldehyde at room temperature for 20min, followed by 0.1% PFA at room temperature for 10min. The cells were then washed for 3 times using 0.3% Triton X-100 in PBS, and permeabilized and blocked from non-specific bindings with the incubation of 0.3% Triton X-100 and 0.1% Bovine Serum Albumin (BSA) (Sigma) in PBS for 20min at room temperature. Next, the cells were incubated overnight at 4℃ with α-actinin primary antibody produced in mouse (Sigma) 1:200 diluted in the solution consisting of 0.3% Triton X-100 and 0.1% BSA in PBS. After the

primary antibody incubation, the cells were washed with 0.1% Triton and 0.25% BSA in PBS for three times at room temperature, and incubated for 1h at room temperature with Alexa Fluor® 488 donkey anti mouse secondary antibody (Molecular Probes by Life Technologies) 1:1000 diluted in the solution consisting of 0.1% Triton and 0.25% BSA in PBS. After the secondary antibody incubation, the cells were washed for three times with 0.01% Tween-20 at room temperature. Finally, the coverslips were transferred onto the slides and the cardiomyocytes were mounted with Prolong™ Gold Antifade Reagent with DAPI (Molecular Probes by Life Technologies). The mounted slides were allowed drying at room temperature for 24h and examined using Leica SP8 Inverted scanning confocal microscope with oil immersion. The immunofluorescence images were analyzed using ImageJ.

2.12.2 Protocol 2

This protocol was applied by the collaborator group from Southwest Medical University in China using the experimental group cardiomyocytes differentiated by me.

The dissociated cardiomyocytes cultured on the coverslips were fixed with 4% PFA for 15 min at room temperature, and were then blocked with 5% BSA for 1h. 0.1% Triton-X100 was used for membrane permeabilization. Then the cardiomyocytes were incubated with 1:100 diluted primary mouse anti-actinin 2 antibody (Boster, Wuhan, China) at 4˚C overnight. After washed with cold PBS, the cardiomyocytes were incubated for 1h at room temperature with DyLight® 488-conjugated donkey anti-mouse secondary antibody at 1:200 dilution (Abcam, Cambridge, UK). Cardiomyocytes were then incubated with Rhodamine phalloidin (Cytoskeleton, USA), an F-actin probe conjugated with red-orange fluorescent dye for 30 min. 5 min incubation of DAPI was used for the

staining of cell nuclei. Immunofluorescence-labelled samples were examined using Nikon confocal laser scanning microscope (Tokyo, Japan).

2.13 Optical mapping

Optical mapping was carried out after the cells started to contract. The responsiveness of the derived cardiomyocytes in experimental groups to β- and α-adrenergic receptor agonists and antagonists was measured. Fluo4 was selected as a fluorescence-labelled Ca^{2+} indicator. LED lights were used to illuminate the indicator and the excitation wavelength was set to 488nm. Intracellular calcium transients were analyzed using a 128 x 128 EMCCD camera (Photometrics, Tucson, USA). In isoprenaline (ISO) experiment, the derived cardiomyocytes were pre-loaded with Fluo4 (Molecular Probes by Life Technologies) at a concentration of 1μM for 15min at 37˚C. Fluo4 was dissolved in DMSO and diluted with CMM. Calcium transients of the derived cardiomyocytes were first recorded without the addition of ISO as control. Recordings were then taken at 0min, 5min, 10min and 15min after 100nM ISO treatment. Using the same method, the responsiveness of the derived cardiomyocytes in the experimental group to 10μM phenylephrine (PE) treatment was tested. In adrenergic receptor antagonist tests, the cells were pre-treated with 600nM CGP20712A (CGP) (Sigma) dissolved in Fluo4 loading solution prior to 100nM ISO treatment. Recordings were taken in the same way as described above. Similarly, the cells were pre-treated with 1μM Prazosin dissolved in Fluo4 loading solution before the treatment of 10μM PE. Metamorph was used to take the recordings, and 4000 or 8000 frames were taken for each recording with a frame rate of 100Hz (for 4000 frames) or 333.33Hz (for 8000 frames). Regions of interest were selected using ImageJ. Raw traces were analyzed and

baseline corrections were conducted using Clampfit. Raw traces are displayed as F-F0/F0 where F refers to the peak fluorescence intensity and F0 is the baseline fluorescence intensity. Calcium transient amplitude change was calculated based on averaged trace using the equation below. Four independent experiments were conducted for each treatment condition (n=4).

$$\text{Amplitude change}(\%) = \frac{Amplitude(treatment) - Amplitude(control)}{Amplitude(control)}$$

2.14 Electrophysiological analysis

The electrophysiological studies were conducted by the collaborator group from Southwest Medical University in China using experimental group cells differentiated by me.

Action potential recordings of the experimental group cells which were differentiated with Gremlin 2 and RA treatment were obtained by patch clamp under whole-cell configuration using Axon 700B amplifier system (Molecular Devices, USA) in the pipette solution consisting of 136 mmol/L K-aspartate (K-Asp), 5.4mmol/L KCl, 5mmol/L NaCl, 1mmol/L MgCl2, 1mmol/L HEPES, 5mmol/L EGTA, MgATP 5mmol/L and 5mmol/L Phosphocreatine. The pH value of the pipette solution was adjusted to 7.2 with KOH. The bath solution was composed of 136mmol/L NaCl, 5.4mmol/L KCl, 1.0mmol/L MgCl2, 1.8mmol/L CaCl2, 0.33mmol/L NaH2PO4, 5mmol/L HEPES and 10mmol/L Glucose. The pH value of the bath solution was adjusted to 7.4 with NaOH.

2.15 Statistical analysis

Statistical analysis was done using Microsoft® Excel version 15.38 for mac and GraphPad Prism® Version 6.0c for Mac. Data are presented as Mean ± SEM. Unpaired parametric T tests were performed to test for significance. (*) indicates P value < 0.05, (**) indicates P value < 0.01, (***) indicates P value < 0.001 and (****) indicates P value < 0.0001.

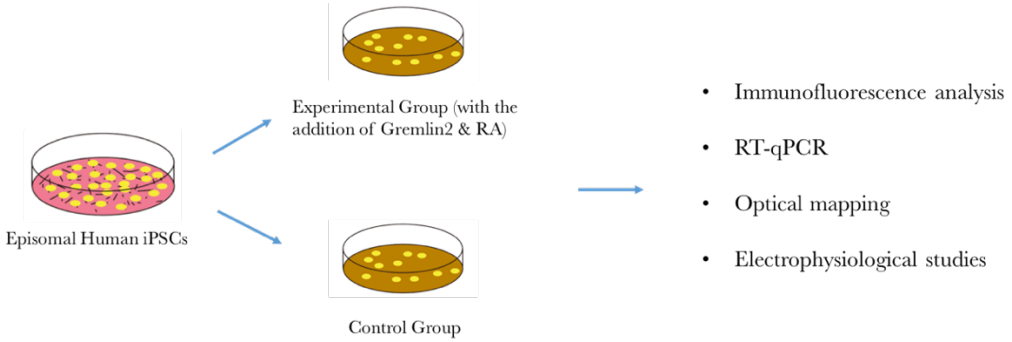


Figure 2.3 Outline of the project design. Human iPSCs were dissociated into single cells and differentiated into cardiomyocytes under controlled conditions. Experimental group cells were treated with Gremlin 2 and RA during cardiac development. Control group cells were differentiated following the same protocol excluding the addition of Gremlin 2 and RA. Cytoskeleton markers were visualized using immunofluorescence labelling to examine the morphology of the cells from both groups. The expressions of multiple genes were analyzed using RT-qPCR to test the properties of the derived cardiomyocytes including their cell subtypes. Optical mappings were carried out to test the responsiveness of the derived cardiomyocytes in experimental groups to adrenergic receptor agonists and antagonists. Electrophysiological studies were performed by the collaborator group in China to provide evidence for the cell subtype and maturation status of the human iPSC-derived cardiomyocytes receiving Gremlin 2 and RA treatment.

Chapter 3. Results

3.1 Immunofluorescence analysis

3.1.1 Human iPSC-derived cardiomyocytes without Gremlin 2 and RA treatment exhibited immature morphological features

In order to examine the morphology of control group cardiomyocytes which were differentiated without the addition of Gremlin 2 and RA, cytoskeleton marker, α-actinin was visualized with immunofluorescence labelling. The dissociated cardiomyocytes were stained following Protocol 1 described in Chapter 2.12.1.

Confocal microscopy revealed a mixture of different cell shapes in the control group, with the majority of the cells displaying irregular round shapes with edges (Fig 3.1). This cell shape resembles that of neonatal cardiomyocytes (Golden et al., 2012) and is consistent with the previously published literature on human iPSC-derived cardiomyocytes (Zhang et al., 2009). Moreover, the cells in the control group had relatively big nuclei (Fig 3.1), a characteristic which is observed in stem cells. In conclusion, the derived cardiomyocytes in control group exhibited immature morphological features. This cell morphology serves as an indication for the developmental stage of those cells.

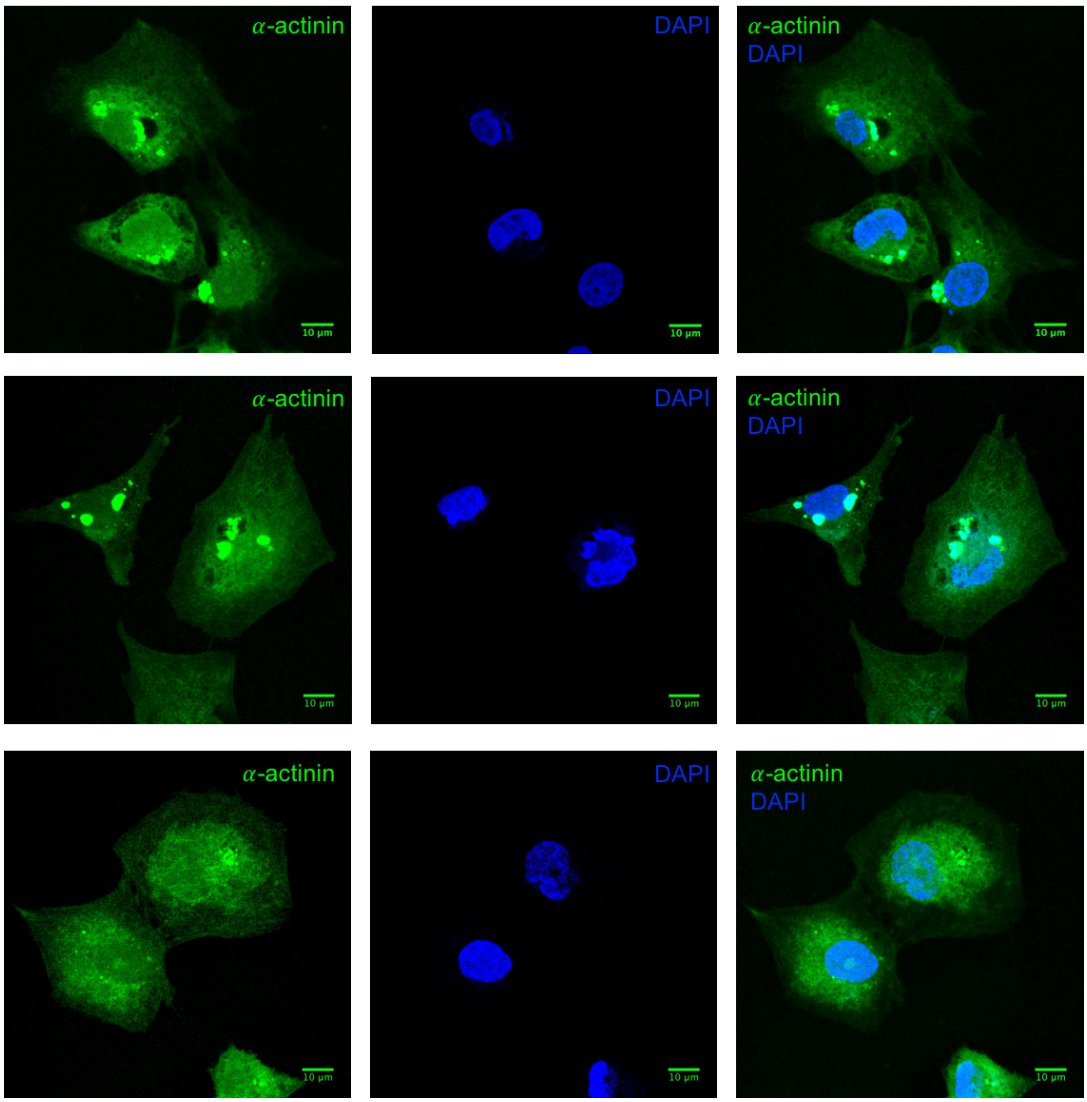


Figure 3.1 Cardiomyocytes derived from human iPSCs without the addition of Gremlin 2 and RA displayed immature morphological features. Cytoskeleton marker, α-actinin was visualized by immunofluorescence labelling. Primary antibody was applied at 1:200 dilution and secondary antibody was used at 1:1000 dilution. Labelled cells were examined with confocal microscopy. The results revealed a mixture of different cell shapes with the majority of the cells having irregular round shapes with big nuclei. The untreated cells recapitulated the morphological characteristics of immature cardiomyocytes.

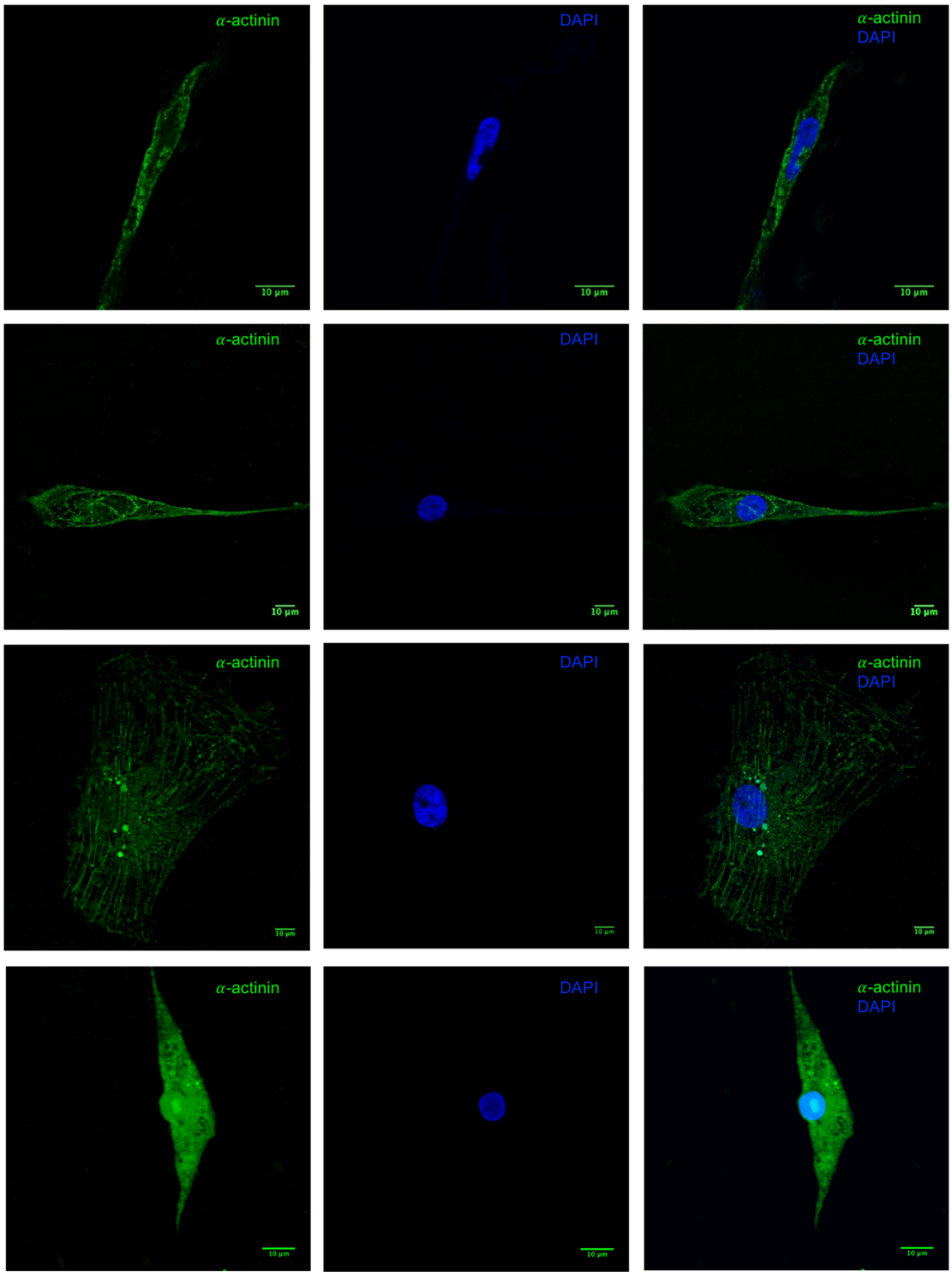
3.1.2 Gremlin 2 and RA treatment during cardiac differentiation changed the morphology of human iPSC-derived cardiomyocytes

In order to test the effects of the combined treatment of Gremlin 2 and RA on the morphology of human iPSC-derived cardiomyocytes, the treated cells in the experimental group were analyzed by immunofluorescence microscopy, and the morphological features of the cardiomyocytes in experimental group and control group were compared. The cytoskeleton marker, α-actinin was visualized. The dissociated cardiomyocytes in experimental group were stained using Protocol 1 described in Chapter 2.12.1. Part of the immunofluorescent staining experiments and analysis were done by the collaborator group from Southwest Medical University in China using Protocol 2 described in Chapter 2.12.2. α-actinin and F-actin were double-stained to visualize the cytoskeleton.

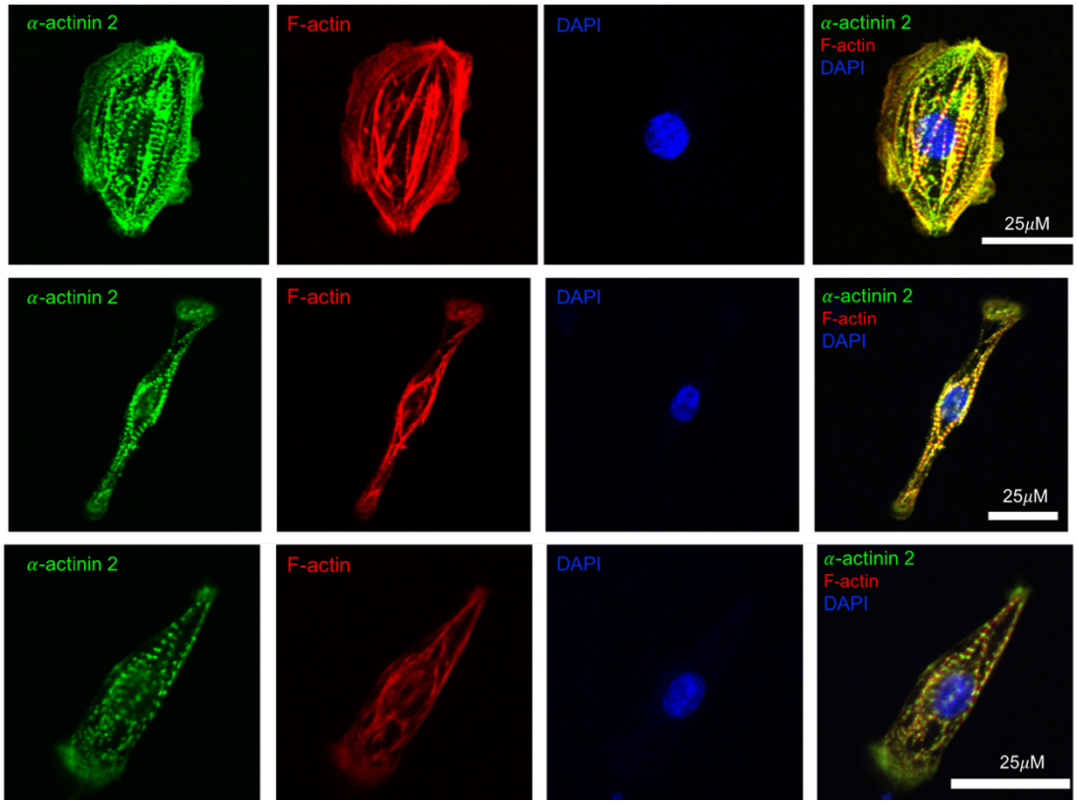
Confocal microscopy suggested that the derived cardiomyocytes in experimental group were a population of cells with heterogeneous shapes, and a substantial fraction of those cells showed elongated and rod-like shapes with a single nucleus situated in central cell (Fig 3.2A-B). This cell shape is similar to that of adult atrial cardiomyocytes observed in human and animal models (Bird et al., 2003; Smyrnias et al., 2010). The average length/width ratio calculated from 10 randomly selected rod-shaped cells in the experimental group was 6 ± 1. This number is comparable to that of mature mammalian cardiomyocytes (Yang et al., 2014). By contrast, the ratio of 10 control group cells was 1.4 ± 0.1 (Fig 3.2C). In addition, the cells receiving Gremlin 2 and RA treatment also showed organized sarcomere patterns with striation (Fig 3.2B), a feature which is broadly observed in adult cardiomyocytes (Smyrnias et al., 2010; Bootman et al., 2006). By comparing the morphological characteristics of experimental group cells and control group cells, it could be concluded that the application of the combined

treatment of Gremlin 2 and RA during cardiac differentiation changed the morphology of the derived cardiomyocytes and initiated the *in vitro* maturation in those cells.

A



B


α-actinin 2
F-actin
DAPI
α-actinin 2
F-actin
DAPI
25μM
α-actinin 2
F-actin
DAPI
α-actinin 2
F-actin
DAPI
25μM
α-actinin 2
F-actin
DAPI
α-actinin 2
F-actin
DAPI
25μM

C

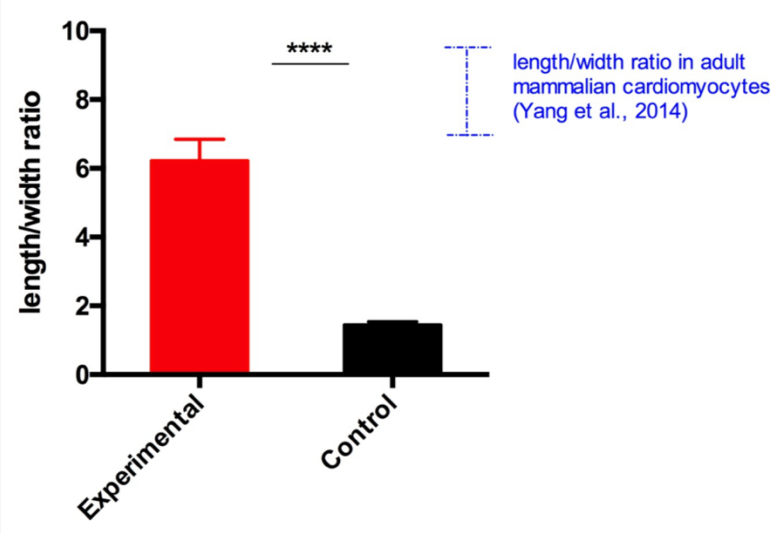


Figure 3.2 Human iPSC-derived cardiomyocytes receiving Gremlin 2 and RA treatment during cardiac differentiation displayed morphological features similar to adult cardiomyocytes. The derived cardiomyocytes in experimental group exhibited some of the morphological features of adult atrial cardiomyocytes. A. The experimental group cells were labelled for α-actinin and analyzed using Protocol 1 described in Chapter 2.12.1. Primary antibody was applied at 1:200 dilution and secondary antibody was used at 1:1000 dilution. Confocal microscopy revealed a population of cardiomyocytes with heterogeneous shapes. A substantial fraction of the those cells showed elongated and rod-like shapes with single nuclei situated in central cell. B. The derived cardiomyocytes from experimental group were double-stained for α-actinin and F-actin and analyzed using Protocol 2 in Chapter 2.12.2 by the collaborator group from Southwest Medical University in China. Primary antibody was applied at 1:100 dilution and secondary antibody was used at 1:200 dilution. The labelled cells showed organized sarcomere patterns with striation. C. The average length/width ratio calculated from ten randomly chosen rod-shaped cells in experimental group analyzed using Protocol 1 is 6 ± 1 (n=10). This number is significantly different from that of ten randomly selected control group cells which is 1.4 ± 0.1 (n=10). Blue line shows the length/width ratio obtained from adult mammalian cardiomyocytes. The length of an irregular-shaped cell is defined as the maximum distance between two points on the cell membrane. The width is defined as the maximum distance the direction of which is roughly vertical to the length measurement.

3.2 Gene expression analysis

Gene expressions were examined using RT-qPCR. *TNNT2*, which encodes troponin T type 2 (cardiac) was selected as a cardiac marker. *NKX2-5*, which encodes the homeobox protein NKX2-5, was selected as a cardiac progenitor cell marker (Kuhn et al., 2010). *NPPA* that codes for atrial natriuretic peptide, *MYL7* that codes for myosin regulatory light chain 2, atrial isoform and *KCNJ5* that codes for the inward rectifier

potassium channel component Kir 3.4, were chosen as atrial-specific gene markers (Houweling et al., 2002; Kubalak et al., 1994; Bettahi et al., 2002). In addition, *KCNJ4* and *KCNJ12* that encode the inward rectifier potassium channel components Kir 2.3 and Kir 2.2, were analysed to provide evidence for the development of relevant ion channels. The adrenergic receptor coding genes, *ADRA1A* and *ADRB1*, were tested to examine the development of α1a- and β1-adrenergic receptors in the derived cardiomyocytes. Changes in the expression levels of the Gremlin 2 protein coding gene *GREM2* were tracked during differentiation process.

3.2.1 Gene expression changes during cardiac differentiation in human iPSC-derived cardiomyocytes receiving Gremlin 2 and RA treatment

Four experimental groups were differentiated independently from human iPSCs for RT-qPCR analysis (n=4). Relative expression was defined as the ratio of the expression of target genes to that of the control gene. Calculations were conducted using the method described in Chapter 2.10.

Of all the ten genes examined, nine showed expressions in experimental group cells. The expression of *ADRA1A* was undetectable in all samples. Of the other nine genes, four displayed similar expression levels in four independent experiments *(KCNJ4*, *KCNJ12*, *ADRB1* and *GREM2*) while the other five genes exhibited variabilities in expression levels among different experiments (*TNNT2*, *NKX2-5*, *NPPA*, *MYL7* and *KCNJ5*). However, despite the existence of this variation, similar trends in gene expression changes could be observed (Fig 3.3).

GREM2 expressions increased steadily in all four groups. *TNNT2* and *NKX2-5* showed the most prominent increases in Group4. The expressions of both genes reached

peak values on Day 7 and remained stable afterwards. It is worth mentioning the *TNNT2* expressions in Group 1 and 2 were at high levels originally on Day 1, and no significant increases could be observed afterwards. The expression levels of *NKX2-5* in Group 2 and 3 showed slight increases on Day 5, and Group 2 continued to rise until Day 15. However, in Group1, *NKX2-5* did not show obvious increase from Day 1 to Day 15. *NPPA* expression was dramatically elevated from Day 1 to Day 15 in Group 4 whereas in other three groups it increased in the first two days and stayed relatively stable afterwards. Similar to *NPPA*, the other two atrial-specific genes, *MYL7* and *KCNJ5* displayed the most significant increases in Group 4 as well and similar patterns of expression changes were observed in all four groups. *MYL7* rose rapidly in the beginning, and then the increasing rate declined and the expression levels remained stable until Day15. The expression levels of *KNCJ5* were relatively stable from Day3 on in all groups. Notably, *KCNJ5* was at a high level originally on Day 1 in Group 1 (Fig 3.3).

KCNJ4, *KCNJ12*, *ADRB1* and *GREM2* showed comparable expression levels in all four groups. *KCNJ4* had sharp increases from Day 3 to Day 7 in four groups. Afterwards, they stayed at high levels until Day 15. *KCNJ12* rose steadily from Day 1 to Day 15 in all groups. *ADRB1* increased steadily in Group 1, 3 and 4. However, in Group 2, *ADRB1* started from a high level on Day 1 and a slight decrease could be observed from Day 1 to Day 15 (Fig 3.3).

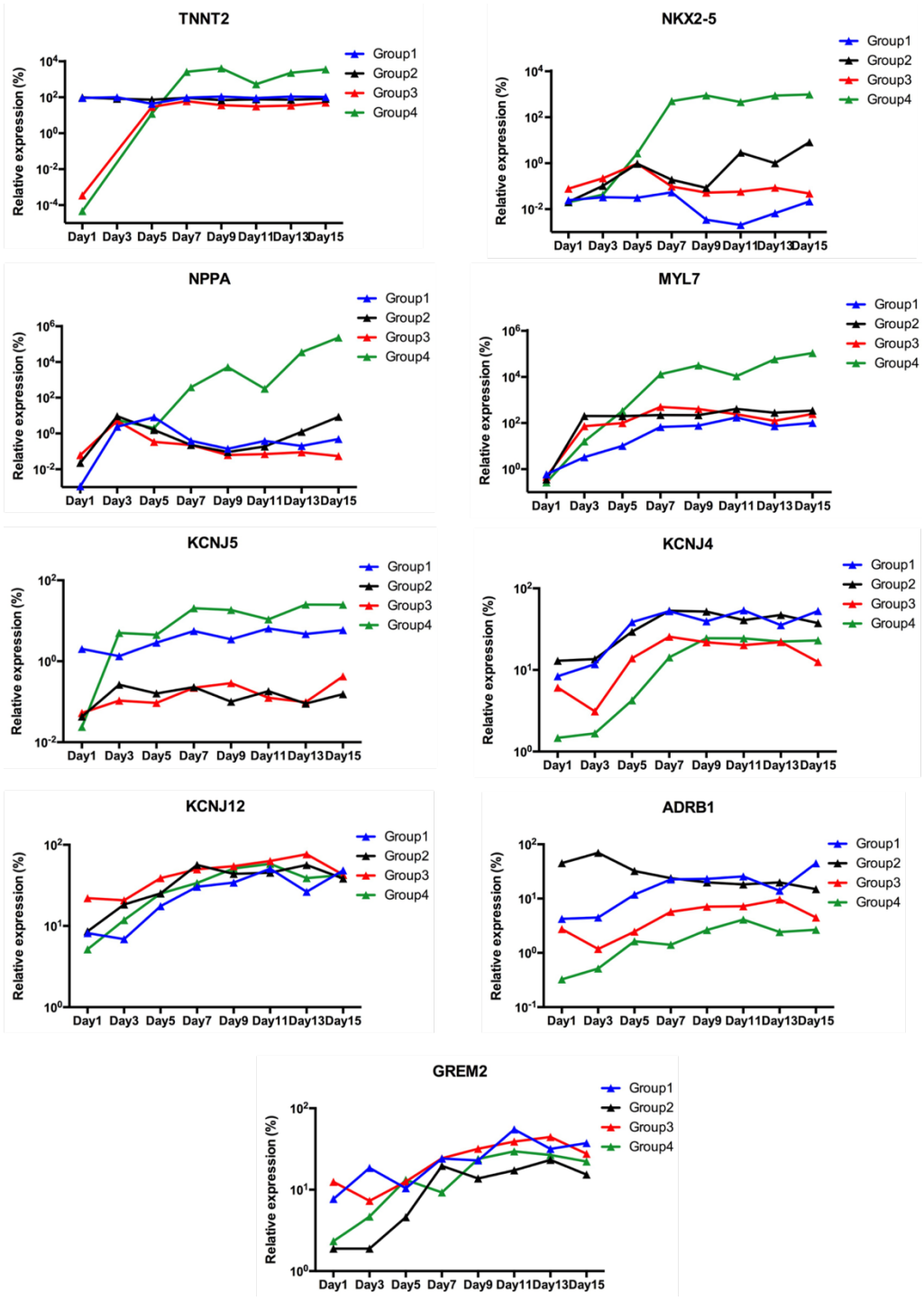


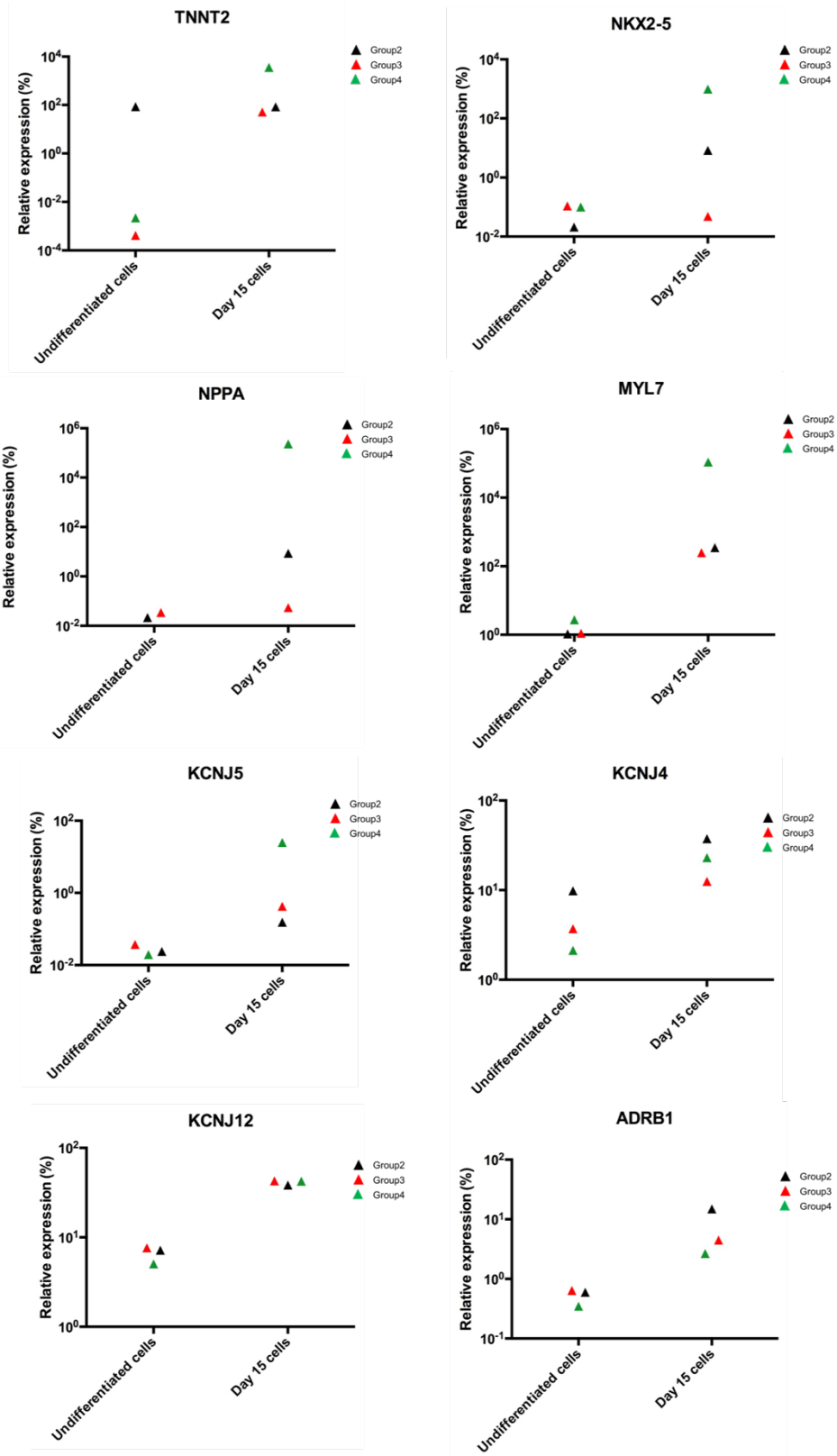
Figure 3.3 Gene expressions of human iPSC-derived cardiomyocytes receiving Gremlin 2 and RA treatment. Similar gene expression change trends were observed in four independent experiments (n=4). The expression levels of *TNNT2*, *NKX2-5*, *NPPA*, *MYL7* and *KCNJ5* displayed variabilities among different experiments with Group 4 having the most significant increases in these five genes. *KCNJ4*, *KCNJ12*, *ADRB1* and *GREM2* had comparable expression levels in all four groups. Abbreviations: *GREM2*, gremlin 2; *TNNT2*, troponin T2, cardiac type; *NKX2-5*, NK2 homeobox 5; *NPPA*, natriuretic peptide A; *MYL7*, myosin regulatory light chain 2a (atrial); *KCNJ5*, potassium inwardly-rectifying channel, superfamily J, member 5; *KCNJ4*, potassium inwardly-rectifying channel, superfamily J, member 4; *KCNJ12*, potassium inwardly-rectifying channel, superfamily J, member 12; *ADRB1*, adrenoceptor beta1. Group numbers were determined sequentially according to the passage numbers of iPSCs that were used for differentiation.

3.2.2 Comparison of gene expressions in undifferentiated human iPSCs and Gremlin 2- and RA-treated Day 15 derived cardiomyocytes

For experimental group 2, 3 and 4, Day 0 RNA samples were harvested before the initiation of cardiac differentiation. Gene expressions of undifferentiated iPSCs and Day 15 derived cardiomyocytes receiving Gremlin 2 and RA treatment were compared. *GREM2*, *TNNT2*, *NKX2-5*, *NPPA*, *MYL7*, *KCNJ5*, *KCNJ4*, *KCNJ12* and *ADRB1* all showed increased expression levels on Day 15 of differentiation, but the extent of the increases varied among different experiments (Fig 3.4).

Of the three groups, Group 4 had the most dramatic increases in *TNNT2*, *NKX2-5*, *NPPA*, *MYL7* and *KCNJ5* expression levels. The expressions of those genes were elevated from around 0 to 3,594%, 977%, 232,544%, 108,883% and 25% respectively. Notably, the *TNNT2* expression was at a high level in undifferentiated cells in Group2 and Day 15 cardiomyocytes showed similar expression level compared to the undifferentiated cells. For *NKX2-5*, Group 2 showed the second largest increase which was from around 0 to 8%. However, Group 3 did not show increase of *NKX2-5* expression in Day 15 cardiomyocytes compared to Day 0 cells. The *NPPA* expression in Group 2 was elevated from around 0 to 9% while Group 3 showed very small increase degree. Group 4 had no *NPPA* expression in undifferentiated cells. Group 2 and 3 had similar increases in *MYL7* expressions from around 1% to around 300%. The increases of *KCNJ5* expressions in Group 2 and 3 were slight, which were from around 0 to 0.2% in Group2 and to 0.4% in Group 3 (Fig 3.4).

The expression changes of *KCNJ4*, *KCNJ12*, *ADRB1* and *GREM2* were comparable in all three groups. An average increase from 5 ± 2% to 24 ± 7% for *KCNJ4*, 7 ± 1% to 41 ±1% for *KCNJ12*, 0.5 ± 0.1% to 7 ± 4% for *ADRB1*, and 2 ± 1% to 22 ± 4% for *GREM2* were observed (Fig 3.4).


TNNT2
NKX2-5
NPPA
MYL7
KCNJ5
KCNJ4
KCNJ12
ADRB1
Relative expression (%)
Group2
Group3
Group4
Undifferentiated cells
Day 15 cells

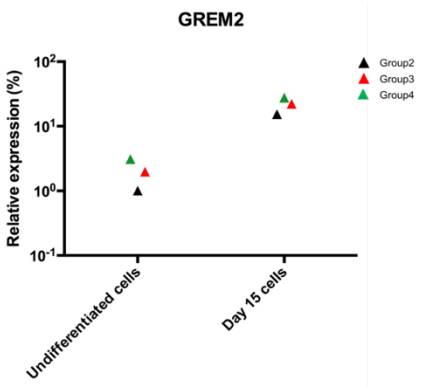


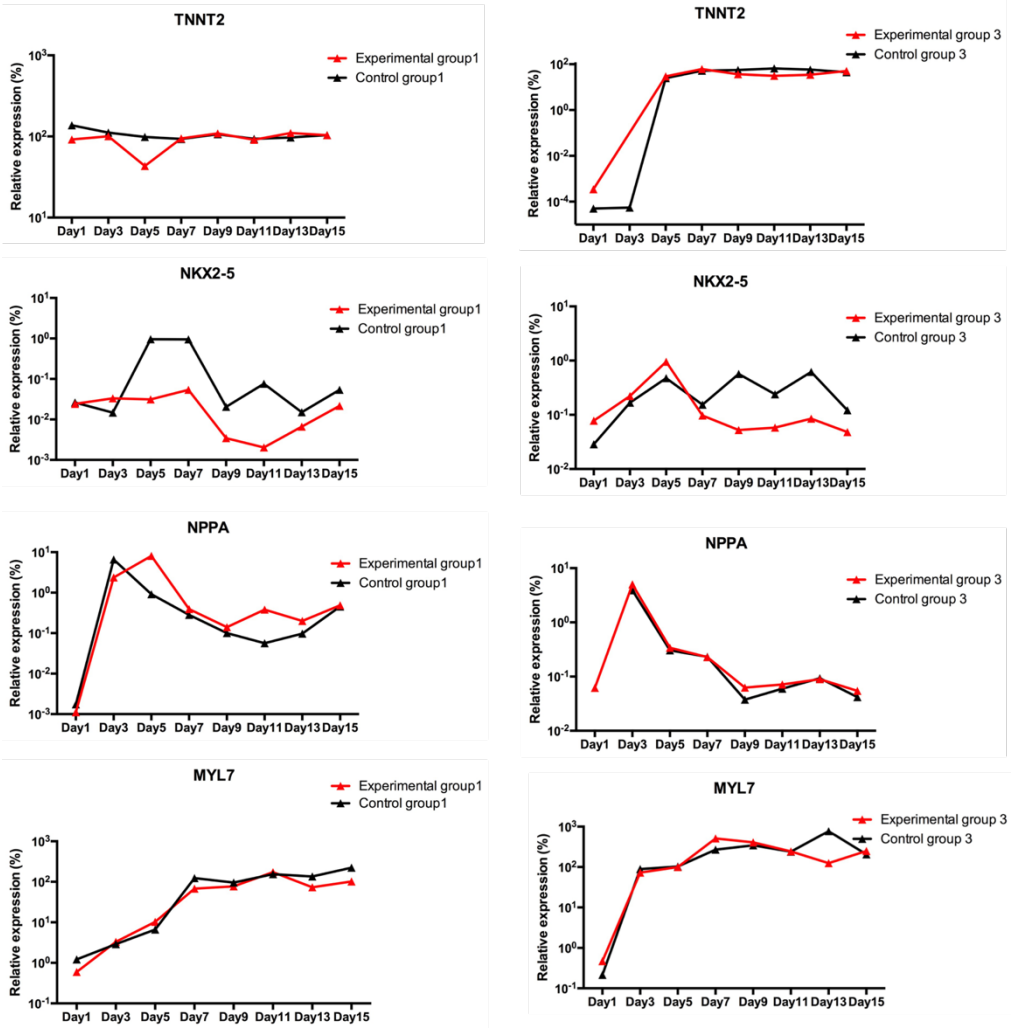
Figure 3.4 Comparison of gene expressions in undifferentiated human iPSCs and Day 15 derived cardiomyocytes receiving Gremlin 2 and RA treatment. Elevated levels of *GREM2*, *TNNT2*, *NKX2-5*, *NPPA*, *MYL7*, *KCNJ5*, *KCNJ4*, *KCNJ12* and *ADRB1* were observed on the Day 15 of differentiation in three independent experiments (n=3). The expressions of *TNNT2*, *NKX2-5*, *NPPA*, *MYL7* and *KCNJ5* displayed variabilities among different experiments, with Group 4 having the most dramatic increases in those five genes. The expression changes of *KCNJ4*, *KCNJ12*, *ADRB1* and *GREM2* were comparable in all three groups.

3.2.3 Comparison of gene expressions in human iPSC-derived cardiomyocytes differentiated with and without Gremlin 2 and RA treatment

In order to test the effect of Gremlin 2 and RA treatment on the gene expressions of iPSC-derived cardiomyocytes, parallel experiments were carried out in two sets of experimental and control groups differentiated simultaneously using the human iPSCs from the same passages. Experimental groups received Gremlin 2 and RA treatment during cardiac differentiation while control groups did not.

Notably, in the first set of experiments, *TNNT2* started from high levels on Day 1 in both experimental group cells and control group cells and did not show obvious increases afterwards. From Day 1 to Day 5, *TNNT2* expressions in experimental cells were lower in the first set of experiments, while in the other set they were higher. For other time points, its expressions were highly comparable in control and experimental groups in both sets. The biggest difference of *NKX2-5* expressions in two sets of comparison experiments was the Day 5 expression. In the first set, control cells had a

significantly higher expression on Day 5 while in the other set, the expression of experimental cells was slightly higher. From Day 7 on, control group cells were at higher levels constantly. For all three atrial-specific gene markers (*NPPA*, *MYL7*, *KCNJ5*), experimental group cells and control group cells had similar expression levels, with *NPPA* slightly more expressed in experimental groups and *KCNJ5* slightly more expressed in control groups at most time points. For *KCNJ4*, *KCNJ12* and *ADRB1*, two sets of comparison experiments showed variable results. In the first set, control groups constantly had higher expressions of those three genes while in the other set it was the opposite. For most time points, the expression levels of these three genes were similar in experimental and control cells (Fig 3.5).



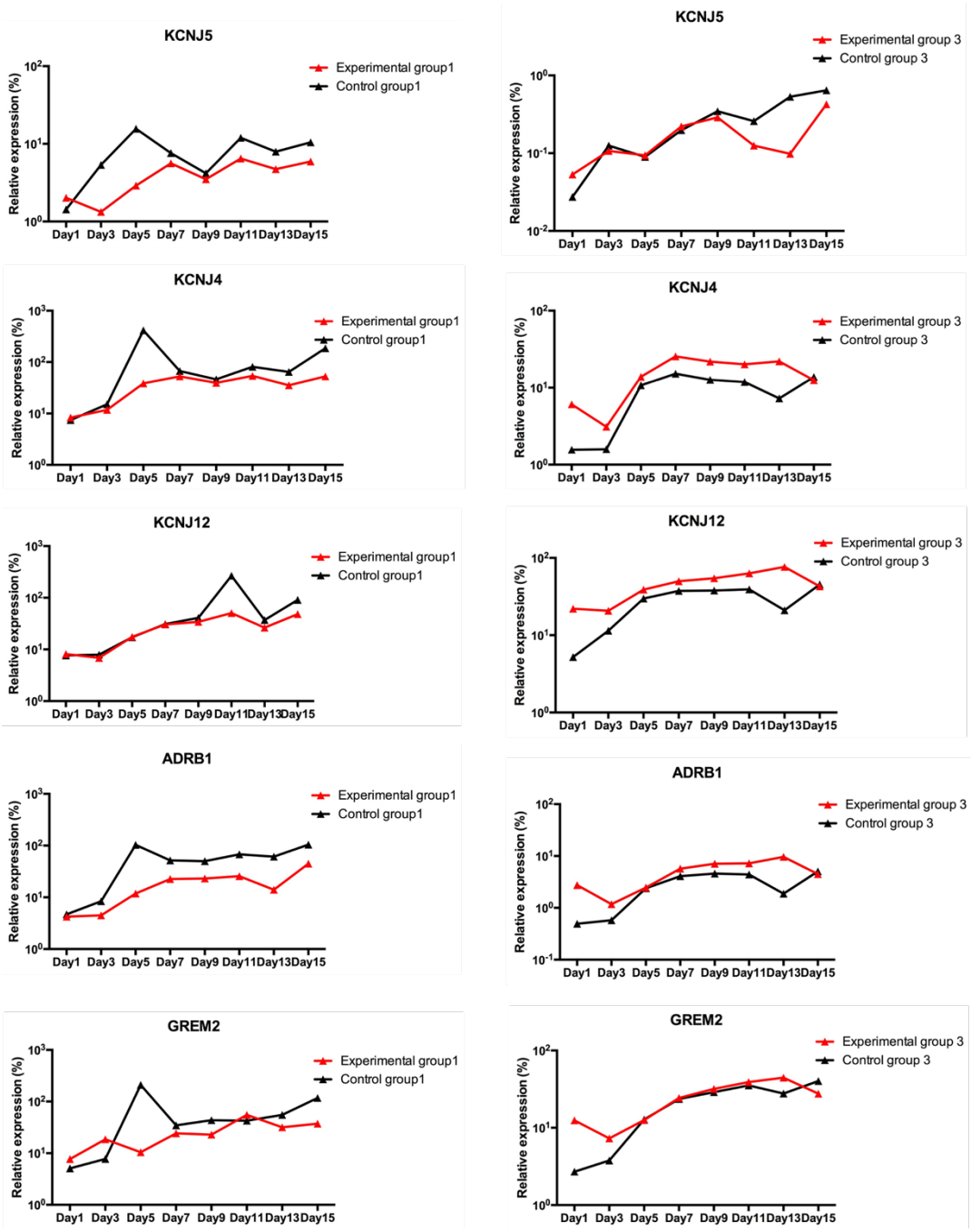


Figure 3.5 Comparison of gene expressions in human iPSC-derived cardiomyocytes with and without Gremlin 2 and RA treatment. Parallel experiments were carried out in two sets of experimental and control groups differentiated from the iPSCs of the same passages. Most genes showed comparable expression levels in experimental group cells and control group cells in both sets. No significant differences in the expressions of atrial-specific genes (*NPPA*, *MYL7* and *KCNJ5*) were observed between experimental groups and control groups.

3.3 Optical mappings

3.3.1 α1- and β- adrenergic stimulation increased the calcium transient amplitude in human iPSC-derived cardiomyocytes receiving Gremlin 2 and RA treatment

α- and β- adrenergic receptors are populated within human heart, with β-receptors more densely than α-receptors. The α1-adrenergic stimulation not only causes an increase in the Ca^{2+} released from sarcoplasmic reticulum (SR), but also enhances transsarcolemmal calcium transient and increases the sensitivity of myofilaments to Ca^{2+} signals (Brodde et al., 1999).The β- adrenergic stimulation activates PKA and subsequently phosphorylates L-type Ca^{2+} channels and phospholamban, leading to increased Ca^{2+} influx and Ca^{2+} uptake into SR (Brodde et al., 1999).

Intracellular calcium concentration is increased when calcium ions influx into the cells through L-type calcium channels and further activate RyRs, causing the release of additional calcium ions from SR (CICR). The calcium concentration then declines as calcium ions are retrieved into the SR by SERCA or pumped out of the cells through Na^{2+}/Ca^{2+} exchanger (NCX) (Guatimosim et al., 2002).

In order to test the responsiveness of experimental group cells to α1- and β-adrenergic stimulation, optical mappings were carried out on spontaneously contracting cardiomyocytes to examine the intracellular calcium transients. Fluo4 was used as a labelled Ca^{2+} indicator that would exhibit an increase in fluorescence upon binding to calcium ions. PE was selected as an α1-adrenergic receptor agonist, and the PE treatment was applied to the cells at a concentration of 10μM. Calcium transients of the cells were first recorded before the PE treatment as control. Recordings were then taken after the PE treatment. Similarly, ISO was selected as a non-selective β- adrenergic

receptor agonist, and the ISO treatment was given at a concentration of 100nM. Using the same method as described above, the calcium transient fluorescence analysis was carried out on the experimental group cells receiving ISO treatment. Four independent experiments were conducted for PE and ISO examinations respectively (n=4).

The recordings taken before and 10min after 10μM PE treatment were compared, and the relative calcium transient amplitude change was calculated based on the averaged traces (Fig 3.6). The result showed that 10μM PE treatment caused an average of 24 ± 6% increase of the calcium transient amplitude in experimental group cells (Fig 3.6C). Similarly, comparison of the recordings from before and 10min after 100nM ISO treatment revealed an average of 26 ± 5% increase in the calcium transient amplitude (Fig 3.7).

The responsiveness of myocytes to adrenergic stimulations has been demonstrated in animal models (Zeng et al., 2014; Yeoh et a., 2015; Shen, 2006). The increased intracellular calcium amplitude levels caused by PE and ISO suggested that the Gremlin 2- and RA-treated cardiomyocytes were able to respond to both α1- and β-adrenergic stimulations.

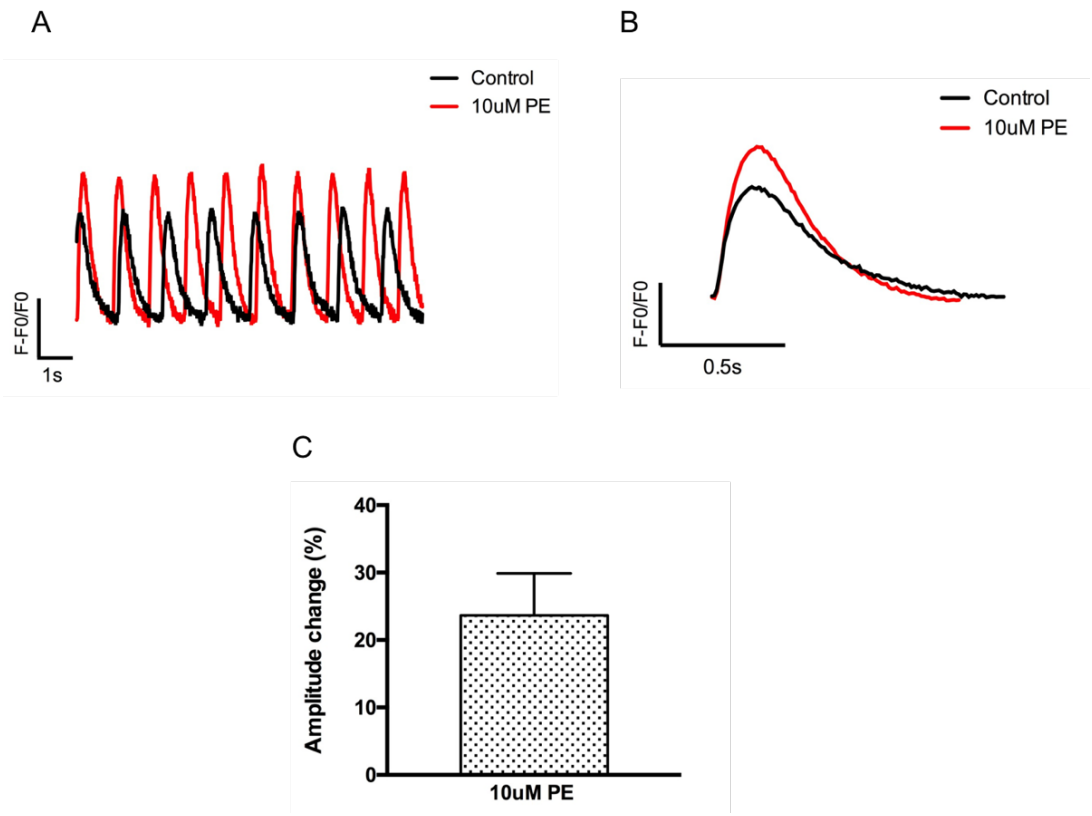


Figure 3.6 Ca^{2+} transient amplitude change caused by 10μM PE treatment in human iPSC-derived cardiomyocytes receiving Gremlin 2 and RA treatment. A. Calcium transient raw traces in one representative experiment before and 10min after PE treatment. B. Averaged calcium transient traces in one experiment before and 10min after PE treatment. Traces are displayed as F-F0/F0. F refers to the peak fluorescence intensity and F0 refers to the baseline fluorescence intensity. C. An average of 24 ± 6% increase in calcium transient amplitude caused by 10μM PE treatment was observed. Calculation was conducted using the equation described in Chapter 2.13. Four independent experiments were conducted (n=4). Data are presented as Mean ± SEM.

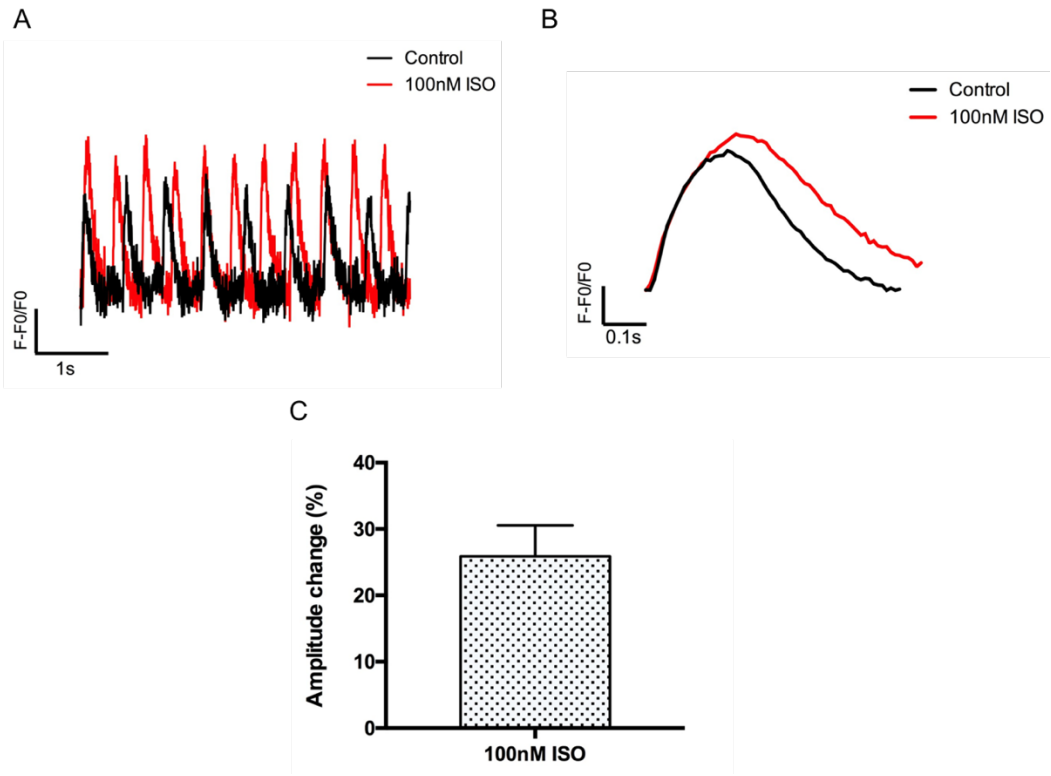


Figure 3.7 Ca^{2+} transient amplitude change caused by 100nM ISO treatment in human iPSC-derived cardiomyocytes receiving Gremlin 2 and RA treatment A. Calcium transient raw traces in one representative experiment before and 10min after ISO treatment. B. Averaged calcium transient traces in one experiment before and 10min after ISO treatment. C. An average of 26 ± 5% increase in calcium transient amplitude caused by 100nM ISO treatment was observed. Four independent experiments were conducted (n=4). Data are presented as Mean ± SEM.

3.3.2 α1- and β1- adrenergic antagonists abolished the effects of adrenergic stimulation on Gremlin 2- and RA-treated human iPSC-derived cardiomyocytes

The adrenergic receptor antagonist tests were conducted on spontaneously contracting cardiomyocytes. Prazosin was chosen as a selective α1-adrenergic antagonist for PE, and CGP20712A was chosen as a selective β1- adrenergic antagonist for ISO. The antagonists were added to the cells prior to the application of adrenergic stimulations. In PE experiments, the cells were first incubated with 1μM Prazosin dissolved in Fluo4 loading solution. After control recordings were taken, the cells were

given a 10μM PE treatment. Recordings were taken again after the PE treatment. Similarly, the derived cardiomyocytes in experimental group were incubated with 600nM CGP in Fluo4 loading solution prior to the 100nM ISO treatment. Recordings were taken in the same way as described above. Four independent experiments were conducted for PE and ISO examinations respectively (n=4).

The averaged calcium transient traces from the cells receiving 1μM Prazosin pre-treatment taken before and 10min after 10μM PE treatment were analyzed and the calculated amplitude change caused by α1-adrenergic stimulation was compared to the data obtained from cells without Prazosin pre-treatment. 10μM PE treatment led to an average of -14±13% calcium transient amplitude increase in the cardiomyocytes receiving 15min of 1μM Prazosin pre-treatment, which was significantly different from the 24 ± 6% obtained from the cardiomyocytes without Prazosin pre-treatment ($p<0.05$) (Fig 3.8C). In ISO experiment, an average of 12 ± 1% calcium transient amplitude change was observed in the cardiomyocytes receiving 15min of 600nM CGP pre-treatment, and it was significantly different from the 26 ± 5% observed in cells without CGP pre-treatment ($p<0.05$) (Fig 3.8C).

The results described above suggested that $\alpha 1$-adrenergic antagonist, Prazosin, inhibited the stimulating effect of PE on the experimental group cardiomyocytes, and the $\beta 1$- adrenergic antagonist, CGP, abolished part of the adrenergic stimulation caused by ISO in the same cell population.

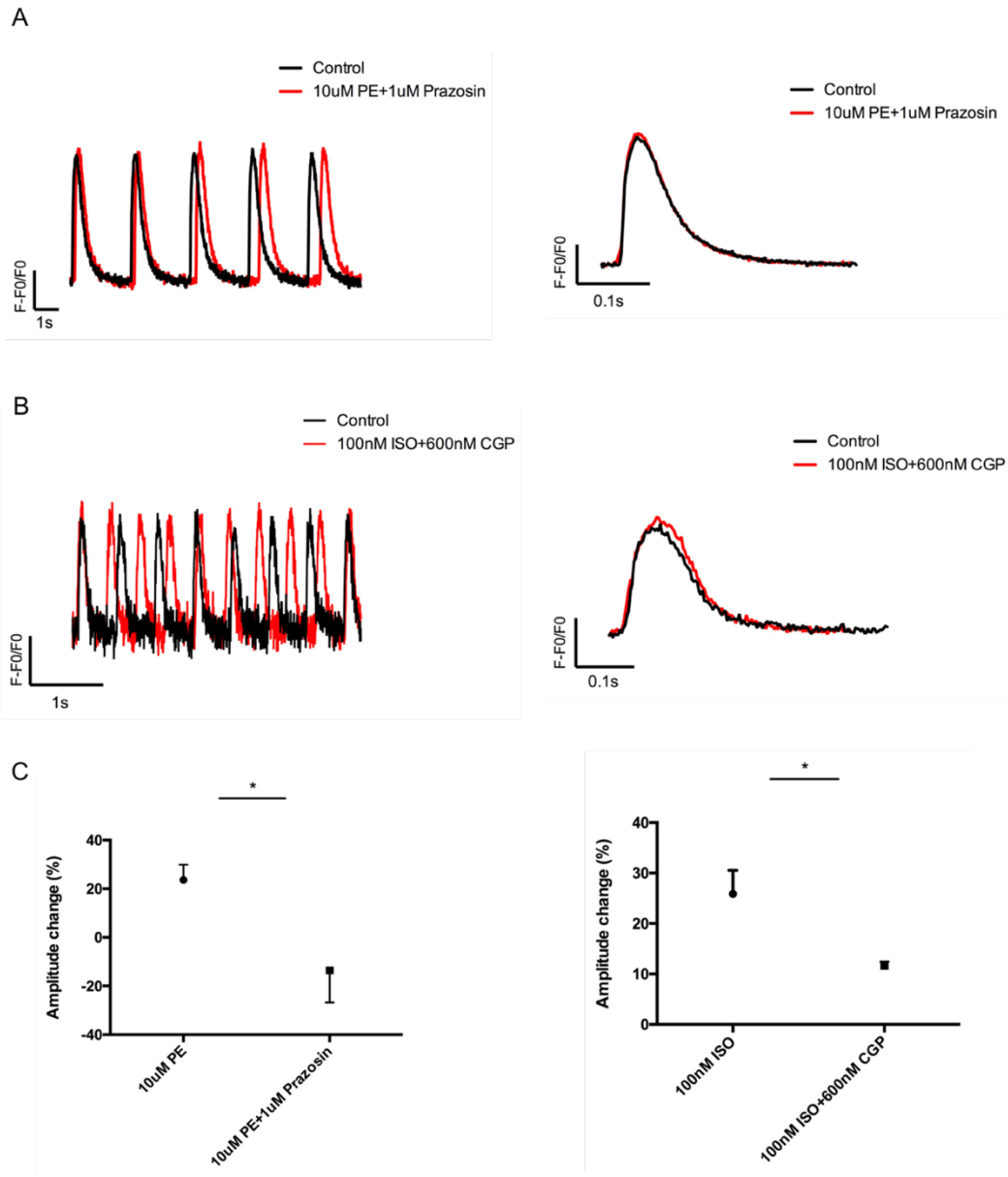


Figure 3.8 α1- and β1- adrenergic antagonists abolished the effects of adrenergic stimulation on human iPSC-derived cardiomyocytes receiving Gremlin 2 and RA treatment. A. Calcium transient raw traces and averaged traces obtained in the cells receiving 1μM Prazosin pre-treatment in one representative experiment before and 10min after 10μM PE treatment. B. Calcium transient raw traces and averaged traces obtained in cells receiving 600nM CGP pre-treatment in one experiment before and 10min after 100nM ISO treatment. C. Comparison of calcium transient amplitude changes caused by 10μM PE and 100nM ISO with and without the antagonist pre-treatments. Significant differences were observed in both PE and ISO experiments. Four independent experiments were conducted for PE and ISO examinations respectively (n=4). Data are presented as Mean ± SEM, * $p<0.05$.

3.4 Electrophysiological analysis

3.4.1 Human iPSC-derived cardiomyocytes receiving Gremlin 2 and RA treatment recapitulated atrial-type action potential characteristics

The electrophysiological properties of atrial cardiomyocytes are distinct from those of ventricular cells. The resting membrane potential for human atrial cells is -74mV, compared to the -81mV for ventricular cells. Also, the atrial cells have a smaller upstroke amplitude, an absence of a prominent plateau phase and a shorter action potential duration (Grandi et al., 2011; Giles et al., 1988).

In order to test the subtype of the derived cardiomyocytes differentiated with the combined treatment of Gremlin 2 and RA, electrophysiological studies were carried out on Day 20 of differentiation by the collaborator group from Southwest Medical University, China. Action potential recordings of the experimental group cells were obtained by patch clamp under whole-cell configuration.

Patch clamp results revealed an atrial-type action potential in experimental group cells. Fig 3.9A shows the action potential morphology of one single beat from a representative cell. Its atrial type was demonstrated by the absence of plateau phase during repolarization process (Fig 3.9A). The average resting membrane potential from 7 experimental group cells was -67 ± 6 mV (Fig 3.9B). This number is similar to that obtained from human atrial cardiomyocytes which is -74 ± 6 mV (Dawodu et al., 1996). In addition, the action potential amplitude (APA) observed in seven experimental group cells were 99 ± 3 mV (Fig 3.9C). This number is comparable to that of human adult atrial cardiomyocytes which is 89 ± 11mV (Dawodu et al., 1996).

In conclusion, the action potential features of the derived cardiomyocytes in experimental group revealed their atrial type. This result is consistent with the atrial-type

gene expression patterns observed in this cell population.

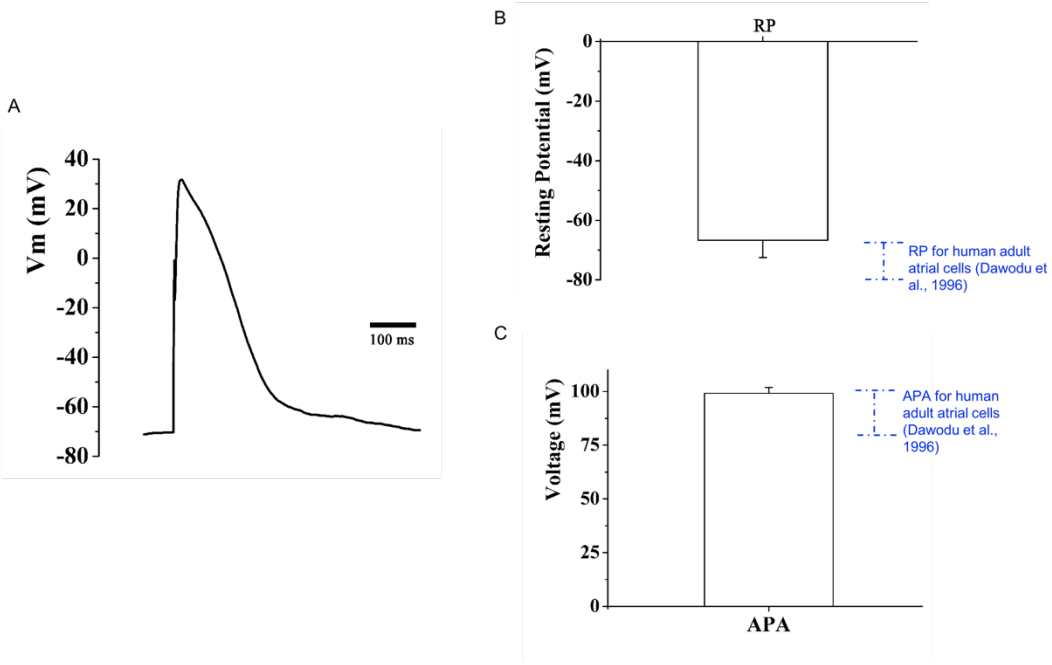


Figure 3.9. Action potential characteristics of Day 20 human iPSC-derived cardiomyocytes receiving Gremlin 2 and RA treatment. A. Action potential of one single beat from a representative cell. B. Average resting potential (RP) of seven cells from experimental group was -67 ± 6 mV (n=7). Blue line shows the RP for human atrial cells. C. Average APA of seven cells from experimental group was 99 ± 3 mV (n=7). Blue line shows the APA for human atrial cells. Data are presented as Mean ± SEM. (Figure produced by the collaborator group from Southwest Medical University, China)

3.4.2 Gremlin 2- and RA-treated human iPSC-derived cardiomyocytes displayed mature action potential features

Action potential characteristics serve as an indication for the maturation stage of cardiomyocytes. Due to the low level of I_{K1} channel, the immature cardiomyocytes have much higher resting membrane potential (≈-60mV) compared to the mature ones, and the lower density of sodium and calcium channels in immature cells leads to a slower upstroke (Yang et al., 2014). In addition, an increase in APA was observed as cardiomyocytes matured (Kato et al, 1996).

The patch clamp results of the derived cardiomyocytes in experimental group showed an average resting membrane potential of -67 ± 6 mV (Fig 3.9B), which is comparable to the -74 ± 6 mV observed in adult atrial cardiomyocytes (Dawodu et al., 1996). Most reported action potentials of the human PSC-derived cardiomyocytes in former publications did not reach a sufficiently negative resting membrane potential level compared to human adult cardiomyocytes (Robertson et al., 2014). Experimental group cells had an average APA of 99 ± 3 mV (Fig 3.9C), which was comparable to the 89 ± 11mV observed in human adult atrial cardiomyocytes (Dawodu et al., 1996).

In conclusion, the experimental group cells that received Gremlin 2 and RA treatment during their cardiac differentiation process recapitulated some of the mature action potential features, indicating the suitability of those cells as a tool for research purposes, especially for drug screening.

Chapter 4. Discussion

4.1 Rationale of the study

Human iPSCs hold great promise in cardiovascular disease mechanistic research and treatment as they can provide an unlimited supply of cardiomyocytes. However, there remains major obstacles in using human iPSC-based cardiac models to study atrial-specific diseases including the heterogeneous cardiomyocyte subtypes generated from iPSCs following established protocols (Cao et al., 2008) as well as the immature developmental stage displayed by the iPSC-derived cardiomyocytes (Mummery et al., 2003, Yang et al., 2014; Zhu et al., 2014). In order to address these issues, we aimed for developing a novel protocol to direct the differentiation of atrial-type cardiomyocytes with adult cell characteristics from human iPSCs.

Cardiac development is tightly regulated by a series of signalling pathways including BMP pathway and RA pathway. The NKX2-5-BMP2-SMAD negative feedback loop model described in Chapter 1.6.2 suggested that BMP signalling initiated the development of cardiac progenitor cells and assisted with the differentiation and specification of those progenitor cells. However, the inhibition of BMP signalling was required for the progenitor cell population to expand. Although it was reported that the suppression of BMP signalling had a negative effect on the differentiation and specification of cardiac progenitor cells (Prall et al., 2007), Gremlin 2, a unique BMP antagonist, is known to enhance atrial cardiomyocytes differentiation. It has been reported that Gremlin 2 is able to mediate the ventricular and atrial cardiomyocyte specification through regulating phosphorylated SMAD1/5/8 and BMP signalling. A low level of BMP signalling is preferred in atrial specification and an up-regulated expression

of Gremlin 2 has a positive effect on atrial cardiomyocytes differentiation (Muller et al., 2013). Importantly, in mouse ESCs it was demonstrated that Gremlin 2 treatment promoted atrial specification by stimulating JNK signalling which subsequently up-regulated the expressions of atrial-specific transcriptional factors, COUPTFII and HEY1 (Tanwar et al., 2014). This finding provided indications for the potential mechanisms underlying the effects of Gremlin 2 in directing atrial cardiomyocytes differentiation.

RA is known to promote the activity of BMP signalling (Ryckebusch et al., 2008) and RA signalling works to regulate cardiac development and direct atrial specification. In human ESCs it was demonstrated that enhancing RA signalling was able to increase the proportion of atrial cells in the derived cardiomyocyte populations (Devalla et al., 2015). Importantly, it was suggested that the effect of RA in directing atrial cardiomyocytes differentiation was achieved through the activation of COUPTFI and COUPTFII, two transcriptional factors that mediate atrial-specific genes (Devalla et al., 2015). Also, it was demonstrated that atrial specification was achieved through autocrine RA signalling, and the ventricular and atrial cardiomyocytes originated from different mesodermal cell populations. The population expressing RALDH2, a key RA-synthetic enzyme was the origin of atrial cardiomyocytes (Lee, Protze et al., 2017). These findings suggested that the RA signalling during mesoderm development was required for atrial cardiomyocytes specification. In addition, RA signals also induce ventricular cardiomyocytes maturation. A specific RA receptor, RARα, has been identified to play the central role in the mechanisms underlying the RA-directed cell maturation (Hoover et al., 2008).

4.2 Approaches and main results

In this study, the effectiveness of a combined use of Gremlin 2 and RA during cardiac differentiation in directing atrial cardiomyocyte differentiation and driving the *in vitro* maturation of those cells was tested. The undifferentiated human iPSCs were divided into experimental groups and control groups. Experimental group cells were treated with Gremlin 2 and RA during cardiac differentiation process. The control group cells were differentiated using the same protocol excluding the addition of Gremlin 2 and RA.

As aforementioned, BMP signalling serves as a secondary signal for the development of mesoderm and is required for cardiac progenitor cell induction and differentiation (Burridge et al., 2015; Prall et al., 2007). The *in vitro* specification of cardiomyocyte subtypes is initiated after the induction of mesoderm and before the appearance of cardiac progenitor cell populations (Devalla et al., 2015). Therefore, the Gremlin 2 and RA treatment has been designed to be applied to the differentiating iPSCs within this time window. 1μg/ml of Gremlin 2 was added to the experimental group cells on Day 4, followed by 1μM of RA on Day 6 and Day 8. Gremlin 2 was added prior to RA due to its function to first inhibit BMP signalling and subsequently promote it at a later stage. A series of examinations were carried out to test the properties of the derived cardiomyocytes including cell subtype, maturation status and physiological functionality.

Different batches of human iPSC-derived cardiomyocytes that were differentiated from the iPSCs of different passages (passage number ranging from 3 to 25) started to contract at different time points. The initial contracting point ranged from approximately Day 8 to Day 18 of differentiation. Generally, the cardiomyocytes differentiated from early passages of iPSCs required a longer period of time to start contracting. This phenomenon was observed in both experimental groups and control groups, regardless

of Gremlin 2 and RA treatment. Moreover, the parallel experimental and control groups which were derived simultaneously from the same passages of iPSCs started contracting at similar day points. The above observations have suggested the iPSC passage number as a potential contributing factor to the inconsistency among different batches of cells. Passage number has been reported as an important contributor to the genetic and epigenetic variations of iPSCs (Liang et al., 2013; Liu et al., 2014). Additionally, the differentiation potential of early passages of iPSCs was found to be affected by the transient transcriptional and epigenetic memory obtained from their somatic cell origins, which favoured their differentiation towards the donor cells while restricting other cell types. This impact could be attenuated by the continuous passaging of iPSCs (Polo et al., 2010; Kim et al., 2010). Therefore, it is not unreasonable to speculate that the variable initial contracting time points of the derived cardiomyocytes observed in this study could be due to the wide-ranging passage numbers of iPSCs used to differentiate them.

In addition, the iPSCs were observed to undergo spontaneous differentiation at early passages. The cells were purified by the continuous selections of undifferentiated iPSC colonies from each passage. Cardiac differentiation experiments were not initiated until no spontaneous differentiation could be observed. However, this selection process, as is described in Chapter 2.6, involved long time of exposing the iPSCs under room temperature as well as physical contact of the cells. Both of those factors could have changed the conditions of iPSCs and affected their differentiation abilities. Also, the early passages of iPSCs were differentiated using the Gremlin 2 provided by R&D Systems whereas the late passages were treated with the Gremlin 2 purchased from BioVision. The qualities of the products from different manufacturers may vary. Furthermore, the batch-to-batch differences of the cardiac differentiation kit and other reagents as well as the iPSC confluence prior to cardiac differentiation could have led to this variation too.

Mature cardiomyocytes have a length/width ratio of 7-9.5 (Yang et al., 2014). This elongated shape has been widely acknowledged. In this study, the immunofluorescence analysis of cytoskeleton markers revealed a mixed pool of differently shaped cells in both control group and experimental group. Control group cells displayed the characteristics of immature cardiomyocytes, with the majority of the cells exhibiting irregular round shapes with edges. This cell shape is similar to that of neonatal cardiomyocytes (Golden et al., 2012) and is consistent with the previously published results from human iPSC-derived cardiomyocytes (Zhang et al., 2009). The immaturity of control group cells was also demonstrated by their relatively large nuclei, which is a symbolic feature of stem cells. On the other hand, the derived cardiomyocytes receiving Gremlin 2 and RA treatment during cardiac differentiation recapitulated some of the mature cardiomyocyte morphological features. In experimental group, a substantial fraction of cells showed elongated and rod-like shapes with a single nucleus situated in central cell. This cell shape is comparable to that of adult atrial cardiomyocytes observed in human and animal models (Bird et al., 2003; Smyrnias et al., 2010). In addition, those cells had an average length/width ratio of 6 ± 1. This number is similar to that obtained from mature cardiomyocytes as mentioned above (Yang et al., 2014). Furthermore, the cells receiving Gremlin 2 and RA treatment also showed organized sarcomere patterns with striation, a feature that has been confirmed in adult cardiomyocytes (Smyrnias et al., 2010; Bootman et al., 2006). In conclusion, from the comparison of the morphological features of human iPSC-derived cardiomyocytes in control group and experimental group, it could be concluded that the addition of Gremlin 2 and RA during cardiac differentiation changed the morphology of the cells and initiated the *in vitro* maturation of those derived cardiomyocytes.

However, it is worth mentioning that the organized sarcomere patterns in

experimental group cells were only observed in the results produced by the collaborator group from Southwest Medical University in China following Protocol 2 in Chapter 2.12.2. Since there is no parallel analysis for the control group cells, no comparison could be made at the present time regarding the structural patterns in Gremlin 2- and RA-treated and untreated cells.

The expressions of ten genes were measured using RT-qPCR. Of all the ten genes, only the α1a-adrenoceptor coding gene (*ADRA1A*) was undetectable in all samples. However, in optical mappings, the responsiveness of experimental group cells to α1-adrenergic stimulation was demonstrated by the increased calcium transient amplitude after PE treatment, and this effect was also observed to be blocked by Prazosin, the α1-adrenergic antagonist. As α1a-adrenergic receptor is the most abundant α1-adrenergic receptor subtype in human heart (Brodde et al., 1999), this observation is difficult to explain. It could be because other subtypes of α1-adrenergic receptor dominated in the cardiomyocytes produced by our protocol, or the pre-designed primer for *ADRA1A* purchased from commercial manufacturer was poorly-designed.

Gene expression analyses on the experimental group cell samples harvested at different day points showed the elevated expressions of cardiac troponin coding gene (*TNNT2*) and early cardiac development marker (*NKX2-5*), which revealed a cardiomyocyte population in the derived cells in experimental groups. Importantly, *TNNT2* is expected to be turned on after the induction of *NKX2-5*. However, in Group 1 and 2, *TNNT2* were expressed at high levels originally on Day 1 and remained stable afterwards. Group 1 and 2 were differentiated from early passages of iPSCs. Apart from *TNNT2*, *KCNJ5* also showed a high level on Day 1 in Group1, and no obvious increase was observed afterwards. This phenomenon was also observed in the *ADRB1* expression in Group2. As mentioned before, the iPSCs of early passages were observed to

differentiate spontaneously. Although no differentiation experiments were initiated until no spontaneous differentiation could be observed in those iPSCs, it is possible that a number of differentiated cells expressing these three genes remained in cell culture until the day the differentiation experiments were conducted. Furthermore, both in Group 3 and 4, *NKX2-5* and *TNNT2* expressions were observed to reach high levels concurrently rather than sequentially. This could be because the gene expressions were examined every other day and thus, the subtle changes happening within 2 days could not be identified.

The increases in atrial-specific gene expressions (*NPPA*, *MYL7* and *KCNJ5*) in experimental group cells revealed an atrial-type cell population in the derived cardiomyocytes receiving Gremlin 2 and RA treatment. However, variabilities in the expressions of these genes were observed among different batches of cardiomyocytes differentiated from the iPSCs of different passage numbers, with Group4 having the most dramatic increases among four groups. Due to this variability, relative expression data were presented as raw traces rather than Mean ± SEM. As aforementioned, iPSCs of different passages displayed distinct genetic and epigenetic properties (Liang et al., 2013; Liu et al., 2014). Thus, the variable observations in four experimental groups could be because of the wide-ranging cell passages used to differentiate them. Also, early passages of iPSCs preferably differentiate towards their donor somatic cells and have restricted differentiation abilities for other cells types (Polo et al., 2010; Kim et al., 2010). This helps to explain the most significant increases observed in Group4, which was differentiated from the latest passage of iPSCs (passage 25). In addition, the Gremlin 2 purchased from different manufacturers, the batch-to-batch differences of differentiation medium and other reagents, as well as the iPSC confluence prior to cardiac differentiation might be contributing factors to this variation too. Furthermore, it is also worth mentioning that the different time point samples were collected from separate wells of cells. Even though

the cardiomyocytes within the same group were simultaneously differentiated from the iPSCs of the same passage number under the same experimental conditions, well-to-well differences still exist.

Four other genes, *KCNJ4*, *KCNJ12*, *ADRB1* and *GREM2*, showed elevated expression levels in four experimental groups as well. Moreover, they displayed comparable expression levels at most time points in the four groups. Together with *KCNJ5*, the expressions of *KCNJ4* and *KCNJ12* have demonstrated the development of inward rectifier potassium channels in the treated cells. The elevated expression level of *ADRB1* indicated the development of β1-adrenergic receptors in this cell population.

The comparison of the gene expressions in iPSC-derived cardiomyocytes with and without Gremlin 2 and RA treatment showed variable results. Most genes were similarly expressed in experimental group and control group cells. *NKX2-5*, as a cardiac progenitor cell marker, had higher expressions in untreated cells at most time points. This observation could be due to the inhibitory effect of RA on the formation of cardiac progenitor cell populations. As aforementioned, in an NKX2-5-BMP2-SMAD negative feedback loop, the secreted BMP2 induces the expression of NKX2-5 through canonical SMAD signalling and thus initiate the formation of cardiac progenitor cells. However, SMAD signalling represses the proliferation of those NKX2-5-positive cardiac progenitor cells. Therefore, NKX2-5 in turn suppresses BMP2 and SMAD signalling to enhance the expansion of cardiac progenitor cell populations (Prall et al., 2007). In conclusion, the inhibition of BMP signalling is required for the NKX2-5-positive cardiac progenitor cells to grow. Since RA is known to promote the activity of BMP signalling (Ryckebusch et al., 2008), it is reasonable to speculate that in this study, the *NKX2-5* expression of treated cells could have been inhibited by RA treatment. In fact, the effect of RA in decreasing NKX2-5-positive cell proportion has been reported in human ESCs (Devalla et al., 2015).

However, due to the combined treatment applied in this study, the effect of RA on restricting cardiac progenitor cell pool could have been attenuated by Gremlin 2, the BMP inhibitor.

In general, the three atrial markers, *NPPA*, *KCNJ5* and *MYL7* were expressed at similar levels in the treated and untreated iPSC-derived cardiomyocytes, with *NPPA* slightly more expressed in treated cells while *KCNJ5* was more expressed in untreated ones at most time points. This observation is important, however, hard to explain as Gremlin 2 and RA were both reported to enhance atrial cardiomyocytes differentiation in mouse and human embryonic stem cells. This observation could be due to:

1. Since the *in vitro* specification of atrial cardiomyocytes is initiated after the induction of mesoderm and before the advent of cardiac progenitor cells (Devalla et al., 2015), the Gremlin 2 and RA treatment should both be applied within this time window. However, as aforementioned, the derived cardiomyocytes differentiated from different passages of iPSCs required different time period to start contracting (ranging from 8 days to 18 days). Therefore, it could be speculated that the time point for the advent of cardiac progenitor cells varied among different batches of cells. Because in this study the Gremlin 2 and RA treatments were given to the cells at fixed time points, it is likely that those treatments missed the effective time window to direct atrial cardiomyocytes differentiation.
2. Although both Gremlin 2 and RA have been reported to direct atrial cardiomyocyte differentiation by promoting the expression of atrial-specific transcriptional factors such as COUPTFI (Tanwar et al., 2014; Devalla et al., 2015), they have distinct working mechanisms. RA increases BMP signalling while Gremlin 2 inhibits canonical BMP pathway first and promotes the

activities of both canonical and non-canonical pathways at a later stage (Tanwar et al., 2014). In this study, the Gremlin 2 treatment was given on Day 4, followed by RA treatments on Day 6 and 8. In this case, the effect of RA in promoting BMP signalling could have been diminished by the continued effect of Gremlin 2 if it persisted for a longer period of time than expected. This could also help explain the variabilities observed in different batches of cells. As the cells were observed to require different time period to differentiate and develop, to apply the treatments at fixed time points could have had distinct effects on different batches of cells. For example in Group 1 where cells started contracting at the latest time point, Gremlin 2 and RA might have functioned at an earlier stage than needed to promote BMP signalling and thus, the expansion of cardiac progenitor cells was affected and the effects on atrial cell specification could hardly been observed.

3. Although iPSCs share multiple characteristics with ESCs such as self-renewal ability and pluripotency, they are distinct from ESCs in many ways including their genetic and epigenetic features (Chin et al., 2009; Chin et al., 2010; Hussein et al., 2011; Lister et al., 2011). These studies also revealed the instability and variability of iPSC lines in multiple aspects such as their differentiation abilities. Gremlin 2 has only been reported to have a positive effect in directing atrial cardiomyocyte differentiation from ESCs. The dissimilarities between iPSCs and ESCs as well as the variable conditions of iPSCs could have hindered the effects of Gremlin 2 in driving atrial cell specification from iPSCs.

The elevated levels of atrial-specific genes in experimental group cells have provided evidence for the potential of this protocol to induce atrial cardiomyocyte

differentiation *in vitro*. However, as no significant differences in atrial gene expressions have been observed between treated and untreated cells, the roles of this combined treatment of Gremlin 2 and RA in promoting atrial cardiomyocyte differentiation are still unclear at present time.

α- and β- adrenergic receptors are populated within human heart and they have essential roles in regulating intracellular Ca^{2+} transients. Both α1- and β-adrenergic stimulations can cause up-regulated Ca^{2+} levels inside the cells. The responsiveness of myocytes to adrenergic stimulations has been demonstrated in animal models (Zeng et al., 2014; Yeoh et a., 2015; Shen, 2006).

In this study, the intracellular Ca^{2+} transient conditions in human iPSC-derived cardiomyocytes receiving Gremlin 2 and RA treatment were visualized with fluorescence-labelled Ca^{2+} indicator and examined under the optical mapping system. α1-adrenergic stimulation resulted in a 24 ± 6% increase in the calcium transient amplitude in the treated cardiomyocytes. Similarly, a 26 ± 5% amplitude increase was observed after the cells were provided with β- adrenergic stimulation. These calcium transient amplitude changes demonstrated that the cardiomyocytes differentiated with the addition of Gremlin 2 and RA were able to respond to both α1- and β- adrenergic stimulations. In addition, this study also provided evidence that the Ca^{2+} transient amplitude increases caused by adrenergic stimulations in experimental group cells could be abolished by α1- and β1- adrenergic antagonists.

Human atrial cardiomyocytes have distinct action potential features compared to ventricular cells. They have an approximately -74mV resting membrane potential which was slightly more depolarized than ventricular cells. They also have a smaller upstroke amplitude, a shorter action potential duration as well as an absence in the plateau phase during the repolarization process (Grandi et al., 2011; Giles et al., 1988).

Apart from the differences among cardiomyocyte subtypes, the mature and immature cardiomyocytes also exhibited distinct action potential features due to the remodelling of ion channels during cardiac differentiation process. The mature cardiomyocytes have a more negative resting membrane potential (Yang et al., 2014), an up-regulated upstroke velocity as well as a longer action potential duration (Sartiani et al., 2007).

In the current study, patch clamp results revealed an atrial-type action potential with multiple adult cardiomyocyte characteristics in Gremlin 2- and RA-treated cells. The single beat action potential showed an absence in plateau phase which was consistent with the observations from human atrial cardiomyocytes (Grandi et al., 2011). The average resting membrane potential of seven experimental group cells was -67 ± 6 mV, which was similar to that obtained from human adult atrial cardiomyocytes as mentioned above (Grandi et al., 2011; Dawodu et al., 1996). In addition, the APA observed in seven experimental group cells were 99 ± 3 mV. This number is comparable to the 89 ± 11mV which was obtained from human adult atrial cardiomyocytes (Dawodu et al., 1996). As is mentioned in Chapter 1.10, the difficulty in the *in vitro* maturation of the cardiomyocytes derived from PSCs presents a major obstacle in using the ESC- and iPSC-based models to study cardiovascular diseases and to develop relevant treatments. In fact, most previous publications on human PSC-derived cardiomyocytes suggested that those cells were at a relatively immature stage (Kolanowski et al., 2017) and that they were not able to reach a sufficiently negative resting membrane potential level as human adult cells (Robertson et al., 2014). Therefore, the current study has made an advancement in initiating the *in vitro* maturation in human iPSC-derived cardiomyocytes, and the mature electrophysiological characteristics observed in experimental group cells indicated the suitability of those treated cells to serve as a tool for drug discovery. However, since the

electrophysiological studies have not yet been carried out on untreated cells, no conclusions could be made at present time regarding the roles of Gremlin 2 and RA treatment in driving the *in vitro* cell maturation.

In conclusion, the results obtained in the current study suggested that the combined treatment of Gremlin 2 and RA produced cultures of human iPSC-derived cardiomyocytes with a substantial percentage of the cells displaying mature atrial-type morphology, whereas the cells differentiated without Gremlin 2 and RA treatment showed immature morphological characteristics. Patch clamps revealed atrial-type action potentials with adult cell features in this treated cell population. These electrophysiological features, together with the demonstrated ability of those treated cells to react to adrenergic stimulations have suggested the potential suitability of those cells as a tool for atrial cardiovascular disease studies and relevant drug development. Gene expression analysis revealed up-regulated levels of cardiac genes, atrial-specific genes, inward rectifier potassium channel coding genes as well as the β1 adrenergic receptor coding gene in treat cells. Nevertheless, no significant differences in atrial gene expressions have been observed between the treated cells and untreated cells. Taken together, in this study, the cardiomyocytes with multiple mature atrial-type features were generated from human iPSCs using a combined treatment of Gremlin 2 and RA. However, the evidence is still insufficient at present time to make conclusions about the effectiveness of this combined Gremlin 2 and RA treatment in directing atrial cardiomyocyte specification and driving the *in vitro* cell maturation.

4.3 Hypothesis of mechanisms

As is discussed in previous chapters, Gremlin 2 suppresses the canonical BMP

signalling first and significantly activates JNK at a later stage. The activation of JNK signalling leads to the up-regulation of atrial-specific transcriptional factors COUPTFII and HEY1 (Tanwar et al., 2014). RA can promote the activity of BMP signalling (Ryckebusch et al., 2008), and the effect of RA in inducing atrial cardiomyocyte differentiation is achieved through the activation of atrial transcriptional factors, COUPI and COUPII (Devalla et al., 2015). Although so far there are no publications referring the activation of JNK signalling as the mechanism underlying RA-directed atrial specification, the positive relationship between RA and JNK has been demonstrated in neuronal development (Yu et al., 2003). Therefore, it is not unreasonable to speculate the involvement of JNK signalling in activating atrial-specific transcriptional factors and promoting atrial cell differentiation under RA treatment.

To understand the molecular mechanisms underlying the atrial specification and *in vitro* cell maturation induced by the combined use of Gremlin 2 and RA is essential for the further optimization of this protocol. My hypothesis is that Gremlin 2 and RA cooperate to up-regulate JNK signalling through non-canonical BMP pathway and subsequently lead to the stimulation of the transcriptional factors mediating atrial-specific genes.

In addition, as is mentioned in Chapter 1.8.1, the effect of RA in inducing the *in vitro* ventricular cardiomyocyte maturation has been verified and RARα has been identified as the central factor in this maturation process (Hoover et al., 2008). Therefore, it could be hypothesized: 1. this specific receptor could have a role in atrial cell maturation too; 2. in this project, the ventricular maturation driven by RA in the mixed cell pool of the derived cardiomyocytes in experimental group induced signalling cascades and influenced atrial cell population. In order to test the first hypothesis, atrial cell population needs to be purified from the heterogenic pool and RARα expression should be measured

in the purified atrial cells. The result could be compared to the atrial cardiomyocytes differentiated following established protocols which produce immature cells. In this way, it could be determined whether RARα has a role in the atrial maturation driven by Gremlin 2 and RA treatment. To test the second hypothesis, atrial cell population should be purified as soon as different cell subtypes become identifiable in order to minimize the effects of the ventricular cells on the atrial population. The atrial cells which are grown independent of ventricular ones need to be measured for their maturation status and compared with those co-cultured with ventricular cells.

4.4 Limitations of the study and future perspectives

Substantial progresses have been made in the current study regarding the differentiation of mature atrial-type cardiomyocytes from human iPSCs. Despite these advancements, there are a number of aspects worth improving on.

1. Optical mappings and patch clamps have not been performed in control group cells which were differentiated without Gremlin 2 and RA treatment. In order to examine the effects of Gremlin 2 and RA treatment on the physiological functionality as well as the electrophysiological properties of the human iPSC-derived cardiomyocytes, parallel optical mapping and patch clamp experiments should be carried out on experimental groups and control groups differentiated using the iPSCs of the same passages.
2. The organized sarcomere patterns in experimental group cells were only observed in the immunofluorescence analysis conducted by the collaborator group from Southwest Medical University in China following Protocol 2 described in Chapter 2.12.2. Parallel analysis needs to be done on control group

cells using the same method to provide evidence for the sarcomere patterning in control cells.

3. In this study, human iPSCs displayed variable differentiation abilities which was demonstrated by the different time point at which the derived cardiomyocytes started contracting as well as the variations observed in gene expressions among four independent experimental groups. As is discussed in Chapter 4.2, the factors such as the iPSC passage number, donor cell source and the cell confluence before differentiation are the potential contributors to this variability. In order to accurately test the effectiveness of this protocol and to further improve the consistency and efficiency of this protocol in producing mature atrial-type cardiomyocytes from human iPSCs, those parameters mentioned above need to be examined and controlled. For example, the variations in stem cell conditions could be attenuated by longer passaging time or using the iPSC line reprogrammed from cardiac cell sources and with higher purity.
4. As aforementioned, RT-qPCR results showed variabilities in multiple genes among different experimental groups. In order to improve the reliability of the RT-qPCR results, more biological replicates should be generated using the same passage of iPSCs. Also, this protocol needs to be tested on the iPSCs with various conditions to examine its consistency and efficiency in generating mature atrial-type cardiomyocytes.
5. In this study, RNA samples were harvested every other day and as a consequence, subtle changes of gene expressions within two days could not be identified as is discussed in Chapter 4.2. To solve this problem, RNA samples should be collected and analysed on a daily basis.

6. There was no evidence provided so far in this study regarding protein expression levels. As the mRNA level of a gene does not accurately predict the protein level, to further confirm protein expressions is necessary and important.
7. No evidence regarding gene expressions and protein expressions has been provided so far to examine the maturation status of the derived cardiomyocytes. This part could be done as a powerful supplement to functional studies.
8. The electrophysiological studies were carried out on only seven single cells from experimental group. This number needs to be increased in order to improve the reliability of the results.
9. In optical mappings, ISO and PE treatment were only applied at one concentration. Different treatment concentrations could be applied to determine the minimal concentration that is sufficient to stimulate the cells in experimental group and control group. By doing so, the physiological functioning abilities of the treated cells and untreated ones could be compared. In addition, the cells differentiated following this protocol could be compared to the adult cardiomyocytes obtained from animal or human cardiac tissues as well.
10. The proportion of the mature atrial-type cell population in treated and untreated groups have not been accurately measured. This needs to be done to provide evidence for the efficiency of the combined treatment of Gremlin 2 and RA in directing mature atrial-type cardiomyocytes differentiation. For example, ventricular- and atrial-specific markers could be visualized by immunofluorescence labelling and the cells expressing those markers can be counted.
11. The Gremlin 2 and RA treatments were applied to the differentiating human iPSCs at fixed time points. As the cells were observed to have dissimilar

differentiation potentials, to apply the treatments at fixed points could have had distinct effects on different batches of cells. To improve the effectiveness of this combined treatment, the cardiac differentiation processes should be tracked (for example by regularly testing the gene and protein markers representing different developmental stages), and the Gremlin 2 and RA treatment should be given to the cells at flexible points as needed.

12. Gremlin 2 and RA could be studied separately and compared to the combined treatment. This helps understand the working mechanisms of those two factors and also determine the contributions made by this combined treatment in improving the efficiency of producing mature atrial-type cells from human iPSCs.
13. The α1a-adrenergic receptor coding gene (*ADRA1A)* showed no expression in all the samples but an increase in the calcium transient amplitude caused by α1-adrenergic stimulation was observed in optical mappings. The reasons for this inconsistency need to be determined. Different gene expression assay products should be tested and the relevant protein expression levels need to be measured.
14. Importantly, in this project no evidence has been provided regarding the potential molecular mechanisms underlying the effects of this combined treatment of Gremlin 2 and RA in inducing atrial differentiation from human iPSC and driving the *in vitro* maturation of those cells. To understand the mechanisms is essential for the further optimization of this protocol.
15. The efficiency of this protocol in producing mature atrial-type cardiomyocytes from human iPSCs needs to be further improved. For example, as is mentioned in Chapter 1.8, the specification of ventricular and atrial cells depends on different types of mesodermal cell populations and those expressing RALDH2 eventually give rise to atrial cells (Lee, Protze et al., 2017). Therefore, the

efficiency of this protocol may be improved by purifying the RALDH2-positive mesodermal cell populations prior to the application of Gremlin 2 and RA treatment.

Reference

Aasen, Trond Raya, Angel Barrero, Maria J Garreta, Elena Consiglio, Antonella Gonzalez, Federico Vassena, Rita Bilić, Josipa Pekarik, Vladimir Tiscornia, G., Edel, Michael Boué, S., & Izpisúa Belmonte, J. C. (2008). Efficient and rapid generation of induced pluripotent stem cells from human keratinocytes. *Nature Biotechnology*, *26*(11), 1276–1284. https://doi.org/10.1038/nbt.1503

Abu-Issa, R., & Kirby, M. L. (2007). Heart Field: From Mesoderm to Heart Tube. *Annual Review of Cell and Developmental Biology*, *23*(1), 45–68. https://doi.org/10.1146/annurev.cellbio.23.090506.123331

Ahuja, P., Sdek, P., & Maclellan, W. R. (2007). Cardiac Myocyte Cell Cycle Control in Development, Disease , and Regeneration. *Physiol Rev*, *87*, 521–544. https://doi.org/10.1152/physrev.00032.2006.

Alam, R., & Gorska, M. M. (2011). MAPK Signaling and ERK1/2 bistability in Asthma. Clinical and Experimental Allergy : Journal of the British Society for Allergy and Clinical Immunology, 41(2), 149–159. http://doi.org/10.1111/j.1365-2222.2010.03658.x

Bao, Z. Z., Bruneau, B. G., Seidman, J. G., Seidman, C. E., & Cepko, C. L. (1999). Regulation of chamber-specific gene expression in the developing heart by Irx4. *Science*, *283*(5405), 1161–1164. https://doi.org/10.1126/science.283.5405.1161

Beltrami, A. P., Barlucchi, L., Torella, D., Baker, M., Limana, F., Chimenti, S., … Anversa, P. (2003). Adult cardiac stem cells are multipotent and support myocardial regeneration. *Cell*, *114*(6), 763–776. https://doi.org/10.1016/S0092-8674(03)00687-1

Benjamin, E. J., Wolf, P. A., D'Agostino, R. B., Silbershatz, H., Kannel, W. B., & Levy, D. (1998). Impact of Atrial Fibrillation on the Risk of Death : The Framingham Heart Study. *Circulation*, *98*(10), 946–952. https://doi.org/10.1161/01.CIR.98.10.946

Bettahi, I., Marker, C. L., Roman, M. I., & Wickman, K. (2002). Contribution of the Kir3.1 subunit to the muscarinic-gated atrial potassium channel IKACh. *Journal of Biological Chemistry*, *277*(50), 48282–48288. https://doi.org/10.1074/jbc.M209599200

Betts, J. G., College, O., & University, R. (2013). Anatomy & physiology. *OpenStax College*, 1355. Retrieved from https://openstax.org/subjects

Bird, S. D., Doevendans, P. A., Van Rooijen, M. A., Brutel De La Riviere, A., Hassink, R. J., Passier, R., & Mummery, C. L. (2003). The human adult cardiomyocyte phenotype. Cardiovascular Research, 58(2), 423–434. https://doi.org/10.1016/S0008-6363(03)00253-0

Bisgrove, B. W., Essner, J. J., & Yost, J. H. (1999). Regulation of midline development by antagonism of lefty and nodal signaling. Development, 126(14), 3253–3262.

Blazeski, A., Zhu, R., Hunter, D. W., Weinberg, S. H., Boheler, K. R., Zambidis, E. T., & Tung, L. (2012). Electrophysiological and contractile function of cardiomyocytes derived from human embryonic stem cells. *Progress in Biophysics and Molecular Biology*. https://doi.org/10.1016/j.pbiomolbio.2012.07.012

Bootman, M. D., Higazi, D. R., Coombes, S., Roderick, H. L. (2006). Calcium signalling during excitation-contraction coupling in mammalian atrial myocytes. Journal of Cell Science, 119(19), 3915–3925. https://doi.org/10.1242/jcs.03223

Bootman, M. D., Smyrnias, I., Thul, R., Coombes, S., & Roderick, H. L. (2011). Atrial cardiomyocyte calcium signalling. *Biochimica et Biophysica Acta - Molecular Cell Research*. https://doi.org/10.1016/j.bbamcr.2011.01.030

Breckenridge, R. A., Mohun, T. J., & Amaya, E. (2001). A role for BMP signalling in heart looping morphogenesis in Xenopus. Developmental Biology, 232(1), 191–203. https://doi.org/10.1006/dbio.2001.0164

Brennan, J., Lu, C. C., Norris, D. P., Rodriguez, T. A., Beddington, R. S. P., & Robertson, E. J. (2001). Nodal signalling in the epiblast patterns the early mouse embryo. *Nature*, *411*(6840), 965–969. https://doi.org/10.1038/35082103

Brodde, O.-E., & Michel, M. C. (1999). Adrenergic and Muscarinic Receptors in the Human Heart. Pharmacol Rev, 51, 651–690. Retrieved from http://pharmrev.aspetjournals.org/cgi/content/abstract/51/4/651

Burridge, P. W., Sharma, A., & Wu, J. C. (2015). Genetic and Epigenetic Regulation of Human Cardiac Reprogramming and Differentiation in Regenerative Medicine. *Annual Review of Genetics*, *49*(1), 461–484. https://doi.org/10.1146/annurev-genet-112414-054911

Cao, F., Wagner, R. A., Wilson, K. D., Xie, X., Fu, J.-D., Drukker, M., … Wu, J. C. (2008). Transcriptional and Functional Profiling of Human Embryonic Stem Cell-Derived Cardiomyocytes. *PLoS ONE*, *3*(10), e3474. https://doi.org/10.1371/journal.pone.0003474

Chin, M. H., Mason, M. J., Xie, W., Volinia, S., Singer, M., Peterson, C., … Lowry, W. E. (2009). Induced Pluripotent Stem Cells and Embryonic Stem Cells Are Distinguished by Gene Expression Signatures. *Cell Stem Cell*, *5*(1), 111–123. https://doi.org/10.1016/j.stem.2009.06.008

Chin, M. H., Pellegrini, M., Plath, K., & Lowry, W. E. (2010). Molecular analyses of human induced pluripotent stem cells and embryonic stem cells. *Cell Stem Cell*, *7*(2), 263–269. https://doi.org/10.1016/j.stem.2010.06.019

Davis, R. J. (2000). Signal transduction by the JNK group of MAP kinases. Cell. https://doi.org/10.1016/S0092-8674(00)00116-1

Dawodu, A. A., Monti, F., Iwashiro, K., Schiariti, M., Chiavarelli, R., & Puddu, P. E. (1996). The shape of human atrial action potential accounts for different frequency-

related changes in vitro. International Journal of Cardiology, 54(3), 237–249. https://doi.org/10.1016/0167-5273(96)02605-8

De La Cruz, M. V., Castillo, M. M., Villavicencio, G. L., Valencia, A., & Moreno-Rodriguez, R. A. (1997). Primitive interventricular septum, its primordium, and its contribution in the definitive interventricular septum: In vivo labelling study in the chick embryo heart. *Anatomical Record*, *247*(4), 512–520. https://doi.org/10.1002/(SICI)1097-0185(199704)247:4<512::AID-AR10>3.0.CO;2-S

Devalla, H. D., Schwach, V., Ford, J. W., Milnes, J. T., El-Haou, S., Jackson, C., … Passier, R. (2015). Atrial-like cardiomyocytes from human pluripotent stem cells are a robust preclinical model for assessing atrial-selective pharmacology. *EMBO Molecular Medicine*, *7*(4), 394–410. https://doi.org/10.15252/emmm.201404757

Devine, W. P., Wythe, J. D., George, M., Koshiba-Takeuchi, K., & Bruneau, B. G. (2014). Early patterning and specification of cardiac progenitors in gastrulating mesoderm. *eLife*, *3*. https://doi.org/10.7554/eLife.03848

Di Masi, A., Leboffe, L., De Marinis, E., Pagano, F., Cicconi, L., Rochette-Egly, C., … Nervi, C. (2015). Retinoic acid receptors: From molecular mechanisms to cancer therapy. *Molecular Aspects of Medicine*. https://doi.org/10.1016/j.mam.2014.12.003

Dimmeler, S., Zeiher, A. M., & Schneider, M. D. (2005). Unchain my heart: The scientific foundations of cardiac repair. *Journal of Clinical Investigation*. https://doi.org/10.1172/JCI200524283

Duester, G. (2008). Retinoic Acid Synthesis and Signaling during Early Organogenesis. Cell. https://doi.org/10.1016/j.cell.2008.09.002

Duque, P., Díez, C., Royo, L., Lorenzo, P. L., Carneiro, G., Hidalgo, C. O., … Gómez, E. (2002). Enhancement of developmental capacity of meiotically inhibited bovine oocytes by retinoic acid. Human Reproduction (Oxford, England), 17(10), 2706–2714. Retrieved from http://www.ncbi.nlm.nih.gov/pubmed/12351552

Essner, J. J., Branford, W. W., Zhang, J., & Yost, H. J. (2000). Mesendoderm and left-right brain, heart and gut development are differentially regulated by pitx2 isoforms. Development (Cambridge, England), 127(5), 1081–1093. Retrieved from http://dev.biologists.org/content/127/5/1081.abstract

Falk, R. H. (2001). Atrial Fibrillation. *New England Journal of Medicine*, *344*(14), 1067–1078. https://doi.org/10.1056/NEJM200104053441407

Földes, G., Mioulane, M., Wright, J. S., Liu, A. Q., Novak, P., Merkely, B., … Harding, S. E. (2011). Modulation of human embryonic stem cell-derived cardiomyocyte growth: A testbed for studying human cardiac hypertrophy? *Journal of Molecular and Cellular Cardiology*, *50*(2), 367–376. https://doi.org/10.1016/j.yjmcc.2010.10.029

Franco, D., Meilhac, S. M., Christoffels, V. M., Kispert, A., Buckingham, M., & Kelly, R. G. (2006). Left and right ventricular contributions to the formation of the

interventricular septum in the mouse heart. *Developmental Biology*, *294*(2), 366–375. https://doi.org/10.1016/j.ydbio.2006.02.045

Freund, C., & Mummery, C. L. (2009). Prospects for pluripotent stem cell-derived cardiomyocytes in cardiac cell therapy and as disease models. *Journal of Cellular Biochemistry*. https://doi.org/10.1002/jcb.22164

Freund, C., & Mummery, C. L. (2009). Prospects for pluripotent stem cell-derived cardiomyocytes in cardiac cell therapy and as disease models. *Journal of Cellular Biochemistry*. https://doi.org/10.1002/jcb.22164

Freund, C., Ward-van Oostwaard, D., Monshouwer-Kloots, J., van den Brink, S., van Rooijen, M., Xu, X., … Passier, R. (2008). Insulin Redirects Differentiation from Cardiogenic Mesoderm and Endoderm to Neuroectoderm in Differentiating Human Embryonic Stem Cells. *Stem Cells*, *26*(3), 724–733. https://doi.org/10.1634/stemcells.2007-0617

Gazzerro, E., Pereira, R. C., Jorgetti, V., Olson, S., Economides, a N., & Canalis, E. (2005). Skeletal overexpression of gremlin impairs bone formation and causes osteopenia. *Endocrinology*, *146*(2), 655–665. https://doi.org/en.2004-0766 [pii]\r10.1210/en.2004-0766

Giles, W. R., & Imaizumi, Y. (1988). Comparison of potassium currents in rabbit atrial and ventricular cells. *The Journal of Physiology*, *405*(1), 123–145. https://doi.org/10.1113/jphysiol.1988.sp017325

Golden, H. B., Gollapudi, D., Gerilechaogetu, F., Li, J., Cristales, R. J., Peng, X., & Dostal, D. E. (2012). Isolation of cardiac myocytes and fibroblasts from neonatal rat pups. Methods in Molecular Biology, 843, 205–214. https://doi.org/10.1007/978-1-61779-523-7_20

Grandi, E., Pandit, S. V., Voigt, N., Workman, A. J., Dobrev, D., Jalife, J., & Bers, D. M. (2011). Human Atrial Action Potential and Ca2+ Model: Sinus Rhythm and Chronic Atrial Fibrillation. *Circulation Research*, *109*(9), 1055–1066. https://doi.org/10.1161/CIRCRESAHA.111.253955

Gregory Y. H. Lip, M. (2010). Refi ning Clinical Risk Stratifi cation for Predicting Stroke and Thromboembolism in Atrial Fibrillation Using a Novel Risk The Euro Heart Survey on Atrial Fibrillation. *CHEST*, *137*(2), 263–272. https://doi.org/10.1378/chest.09-1584

Groppe, J., Greenwald, J., Wiater, E., Rodriguez-Leon, J., Economides, A. N., Kwiatkowski, W., … Choe, S. (2002). Structural basis of BMP signalling inhibition by the cystine knot protein Noggin. Nature, 420(6916), 636–642. https://doi.org/10.1038/nature01245

Guatimosim, S., Dilly, K., Santana, L. F., Saleet Jafri, M., Sobie, E. a, & Lederer, W. J. (2002). Local Ca(2+) signaling and EC coupling in heart: Ca(2+) sparks and the regulation of the [Ca(2+)](i) transient. *Journal of Molecular and Cellular Cardiology*, *34*(8), 941–950. https://doi.org/10.1006/jmcc.2002.2032

Guo, W., Kamiya, K., & Toyama, J. (1996). Modulated expression of transient outward current in cultured neonatal rat ventricular myocytes: comparison with development in situ. *Cardiovascular Research*, *32*(3), 524–533. https://doi.org/10.1016/S0008-6363(96)00107-1

Gupta, M. K., Illich, D. J., Gaarz, A., Matzkies, M., Nguemo, F., Pfannkuche, K., … Ari, T. (2010). Global transcriptional profiles of beating clusters derived from human induced pluripotent stem cells and embryonic stem cells are highly similar. *BMC Developmental Biology*, *10*. https://doi.org/10.1186/1471-213X-10-98

Gurdon, J. B. (1962). Adult frogs derived from the nuclei of single somatic cells. *Developmental Biology*, *4*(2), 256–273. https://doi.org/10.1016/0012-1606(62)90043-X

Hikasa, H., Shibata, M., Hiratani, I., & Taira, M. (2002). The Xenopus receptor tyrosine kinase Xror2 modulates morphogenetic movements of the axial mesoderm and neuroectoderm via Wnt signaling. *Development (Cambridge, England)*, *129*(22), 5227–5239. https://doi.org/10.1016/s0925-4773(00)00392-0

Hoover, L. L., Burton, E. G., Brooks, B. A., & Kubalak, S. W. (2008). The Expanding Role for Retinoid Signaling in Heart Development. The Scientific World JOURNAL, 8, 194–211. https://doi.org/10.1100/tsw.2008.39

Houweling, A. C., Somi, S., Van Den Hoff, M. J. B., Moorman, A. F. M., & Christoffels, V. M. (2002). Developmental pattern of ANF gene expression reveals a strict localization of cardiac chamber formation in chicken. *Anatomical Record*, *266*(2), 93–102. https://doi.org/10.1002/ar.10042

Hsu, D. R., Economides, A. N., Wang, X., Eimon, P. M., & Harland, R. M. (1998). The Xenopus dorsalizing factor Gremlin identifies a novel family of secreted proteins that antagonize BMP activities. *Molecular Cell*, *1*(5), 673–683. https://doi.org/10.1016/S1097-2765(00)80067-2

Hussein, S. M., Batada, N. N., Vuoristo, S., Ching, R. W., Autio, R., Narvä, E., … Otonkoski, T. (2011). Copy number variation and selection during reprogramming to pluripotency. *Nature*, *471*(7336), 58–62. https://doi.org/10.1038/nature09871

Iwamoto, M., Yagami, K., Shapiro, I. M., Leboy, P. S., Adams, S. L., & Pacifici, M. (1994). Retinoic acid is a major regulator of chondrocyte maturation and matrix mineralization. Microscopy Research and Technique, 28(6), 483–491. https://doi.org/10.1002/jemt.1070280604

Jaenisch, R. (2004). Human cloning - the science and ethics of nuclear transplantation. *The New England Journal of Medicine*, *351*(27), 2787–2791. https://doi.org/10.1056/NEJMp048304

Kamakura, T., Makiyama, T., Sasaki, K., Yoshida, Y., Wuriyanghai, Y., Chen, J., … Kimura, T. (2013). Ultrastructural Maturation of Human-Induced Pluripotent Stem Cell-Derived Cardiomyocytes in a Long-Term Culture. *Circulation Journal*, *77*(5), 1307–1314. https://doi.org/10.1253/circj.CJ-12-0987

Kato, Y., Masumiya, H., Agata, N., Tanaka, H., & Shigenobu, K. (1996). Developmental changes in action potential and membrane currents in fetal, neonatal and adult guinea-pig ventricular myocytes. Journal of Molecular and Cellular Cardiology, 28(7), 1515–1522. https://doi.org/10.1006/jmcc.1996.0141

Kaufman, M. H. (1992). *The atlas of mouse development.* San Diego: Academic Press.

Keller, G. M. (1995). In vitro differentiation of embryonic stem cells. *Current Opinion in Cell Biology*, *7*(6), 862–869. https://doi.org/10.1016/0955-0674(95)80071-9

Keller, R. (2005). Cell migration during gastrulation. Current Opinion in Cell Biology. https://doi.org/10.1016/j.ceb.2005.08.006

Kikuchi, K., Holdway, J. E., Major, R. J., Blum, N., Dahn, R. D., Begemann, G., & Poss, K. D. (2011). Retinoic Acid Production by Endocardium and Epicardium Is an Injury Response Essential for Zebrafish Heart Regeneration. *Developmental Cell*, *20*(3), 397–404. https://doi.org/10.1016/j.devcel.2011.01.010

Kim, J. S., Virágh, S., Moorman, A. F. M., Anderson, R. H., & Lamers, W. H. (2001). Development of the myocardium of the atrioventricular canal and the vestibular spine in the human heart. *Circulation Research*, *88*(4), 395–402. https://doi.org/10.1161/01.RES.88.4.395

Kim, K., Doi, A., Wen, B., Ng, K., Zhao, R., Cahan, P., … Daley, G. Q. (2010). Epigenetic memory in induced pluripotent stem cells. *Nature*, *467*(7313), 285–290. https://doi.org/10.1038/nature09342

Kirkbride, K. C., Townsend, T. a, Bruinsma, M. W., Barnett, J. V, & Blobe, G. C. (2008). Bone morphogenetic proteins signal through the transforming growth factor-beta type III receptor. *The Journal of Biological Chemistry*, *283*(12), 7628–7637. https://doi.org/10.1074/jbc.M704883200

Knollmann, B. C., Schober, T., Petersen, A. O., Sirenko, S. G., & Franz, M. R. (2007). Action potential characterization in intact mouse heart: steady-state cycle length dependence and electrical restitution. *American Journal of Physiology-Heart and Circulatory Physiology*, *292*(1), H614–H621. https://doi.org/10.1152/ajpheart.01085.2005

Koibuchi, N., & Chin, M. T. (2007). CHF1/Hey2 plays a pivotal role in left ventricular maturation through suppression of ectopic atrial gene expression. *Circulation Research*, *100*(6), 850–855. https://doi.org/10.1161/01.RES.0000261693.13269.bf

Kolanowski, T. J., Antos, C. L., & Guan, K. (2017). Making human cardiomyocytes up to date: Derivation, maturation state and perspectives. *International Journal of Cardiology*, *241*, 379–386. https://doi.org/10.1016/j.ijcard.2017.03.099

Krapivinsky, G., Gordon, E. a, Wickman, K., Velimirović, B., Krapivinsky, L., & Clapham, D. E. (1995). The G-protein-gated atrial K+ channel IKACh is a heteromultimer of two inwardly rectifying K(+)-channel proteins. *Nature*. https://doi.org/10.1038/374135a0

Kruithof, B. P. T., van Wijk, B., Somi, S., Kruithof-de Julio, M., Pérez Pomares, J. M., Weesie, F., … van den Hoff, M. J. B. (2006). BMP and FGF regulate the differentiation of multipotential pericardial mesoderm into the myocardial or epicardial lineage. Developmental Biology, 295(2), 507–522. https://doi.org/10.1016/j.ydbio.2006.03.033

Kubalak, S. W., Miller-Hance, W. C., O'Brien, T. X., Dyson, E., & Chien, K. R. (1994). Chamber specification of atrial myosin light chain-2 expression precedes septation during murine cardiogenesis. *Journal of Biological Chemistry*, *269*(24), 16961–16970.

Kühl, M., Sheldahl, L. C., Malbon, C. C., & Moon, R. T. (2000). Ca2+/calmodulin-dependent protein kinase II is stimulated by Wnt and Frizzled homologs and promotes ventral cell fates in Xenopus. *Journal of Biological Chemistry*, *275*(17), 12701–12711. https://doi.org/10.1074/jbc.275.17.12701

Kuhn, E. N., & Wu, S. M. (2010). Origin of cardiac progenitor cells in the developing and postnatal heart. *Journal of Cellular Physiology*. https://doi.org/10.1002/jcp.22281

Laflamme, M. A., & Murry, C. E. (2011). Heart regeneration. *Nature*. https://doi.org/10.1038/nature10147

Lan, F., Lee, A. S., Liang, P., Sanchez-Freire, V., Nguyen, P. K., Wang, L., … Wu, J. C. (2013). Abnormal calcium handling properties underlie familial hypertrophic cardiomyopathy pathology in patient-specific induced pluripotent stem cells. *Cell Stem Cell*, *12*(1), 101–113. https://doi.org/10.1016/j.stem.2012.10.010

Lawson, N. D., & Berliner, N. (1999). Neutrophil maturation and the role of retinoic acid. Experimental Hematology. https://doi.org/10.1016/S0301-472X(99)00085-5

Leaf, D. E., Feig, J. E., Vasquez, C., Riva, P. L., Yu, C., Lader, J. M., … Morley, G. E. (2008). Connexin40 imparts conduction heterogeneity to atrial tissue. *Circulation Research*, *103*(9), 1001–1008. https://doi.org/10.1161/CIRCRESAHA.107.168997

Lee, H. Y., Yang, P.-S., Kim, T.-H., Uhm, J.-S., Pak, H.-N., Lee, M.-H., & Joung, B. (2017). Atrial fibrillation and the risk of myocardial infarction: a nation-wide propensity-matched study. *Scientific Reports*, *7*(1), 12716. https://doi.org/10.1038/s41598-017-13061-4

Lee, J. H., Protze, S. I., Laksman, Z., Backx, P. H., & Keller, G. M. (2017). Human Pluripotent Stem Cell-Derived Atrial and Ventricular Cardiomyocytes Develop from Distinct Mesoderm Populations. Cell Stem Cell, 21(2), 179–194.e4. https://doi.org/10.1016/j.stem.2017.07.003

Liang, G., & Zhang, Y. (2013). Genetic and epigenetic variations in iPSCs: Potential causes and implications for application. *Cell Stem Cell*. https://doi.org/10.1016/j.stem.2013.07.001

Lister, R., Pelizzola, M., Kida, Y. S., Hawkins, R. D., Nery, J. R., Hon, G., … Ecker, J. R. (2011). Hotspots of aberrant epigenomic reprogramming in human induced pluripotent stem cells. *Nature*, *471*(7336), 68–73. https://doi.org/10.1038/nature09798

Liu, P., Kaplan, A., Yuan, B., Hanna, J. H., Lupski, J. R., & Reiner, O. (2014). Passage number is a major contributor to genomic structural variations in mouse iPSCs. *Stem Cells*, *32*(10), 2657–2667. https://doi.org/10.1002/stem.1779

Liu, X., Sun, Y., Yue, L., Li, S., Qi, X., Zhao, H., … Yu, H. (2016). JNK pathway and relative transcriptional factor were involved in ginsenoside Rh2- mediated G1 growth arrest and apoptosis in human lung adenocarcinoma A549 cells. Genetics and Molecular Research Mol. Res, 15(3). https://doi.org/10.4238/gmr.15039003

Lo, B., & Parham, L. (2009). Ethical issues in stem cell research. *Endocrine Reviews*. https://doi.org/10.1210/er.2008-0031

Loh, Y.-H., Hartung, O., Li, H., Guo, C., Sahalie, J. M., Manos, P. D., … Daley, G. Q. (2010). Reprogramming of T Cells from Human Peripheral Blood. *Cell Stem Cell*, *7*(1), 15–19. https://doi.org/10.1016/j.stem.2010.06.004

Mallon, B. S., Hamilton, R. S., Kozhich, O. A., Johnson, K. R., Fann, Y. C., Rao, M. S., & Robey, P. G. (2014). Comparison of the molecular profiles of human embryonic and induced pluripotent stem cells of isogenic origin. *Stem Cell Research*, *12*(2), 376–386. https://doi.org/10.1016/j.scr.2013.11.010

Mangelsdorf, D. J., Ong, E. S., Dyck, J. A., & Evans, R. M. (1990). Nuclear receptor that identifies a novel retinoic acid response pathway. *Nature*, *345*(6272), 224–229. https://doi.org/10.1038/345224a0

McNutt, N. S., & Fawcett, D. W. (1969). The ultrastructure of the cat myocardium. II. Atrial muscle. *Journal of Cell Biology*, *42*(1), 46–67. https://doi.org/10.1083/jcb.42.1.46

Mikawa, T., Poh, A. M., Kelly, K. A., Ishii, Y., & Reese, D. E. (2004). Induction and Patterning of the Primitive Streak, an Organizing Center of Glastrulation in the Amniote. *Developmental Dynamics*. https://doi.org/10.1002/dvdy.10458

Minamisawa, S., Wang, Y., Chen, J., Ishikawa, Y., Chien, K. R., & Matsuoka, R. (2003). Atrial chamber-specific expression of sarcolipin is regulated during development and hypertrophic remodeling. *Journal of Biological Chemistry*, *278*(11), 9570–9575. https://doi.org/10.1074/jbc.M213132200

Miyasaka, Y., Barnes, M. E., Bailey, K. R., Cha, S. S., Gersh, B. J., Seward, J. B., & Tsang, T. S. M. (2007). Mortality Trends in Patients Diagnosed With First Atrial Fibrillation. A 21-Year Community-Based Study. *Journal of the American College of Cardiology*, *49*(9), 986–992. https://doi.org/10.1016/j.jacc.2006.10.062

Miyasaka, Y., Barnes, M. E., Gersh, B. J., Cha, S. S., Bailey, K. R., Abhayaratna, W., … Tsang, T. S. M. (2006). Incidence and mortality risk of congestive heart failure in atrial fibrillation patients: A community-based study over two decades. *European Heart Journal*, *27*(8), 936–941. https://doi.org/10.1093/eurheartj/ehi694

Moorman et al. (2003). Development of the heart (1) formation of the cardiac chambers and arterial trunks. *Heart (British Cardiac Society)*, *89*(1), 806–814. https://doi.org/10.1136/heart.89.7.806

Muller, I. I., Melville, D. B., Tanwar, V., Rybski, W. M., Mukherjee, A., Shoemaker, M. B., … Hatzopoulos, A. K. (2013). Functional modeling in zebrafish demonstrates that the atrial-fibrillation-associated gene GREM2 regulates cardiac laterality, cardiomyocyte differentiation and atrial rhythm. *Disease Models & Mechanisms*, *6*(2), 332–341. https://doi.org/10.1242/dmm.010488

Mummery, C. (2003). Differentiation of Human Embryonic Stem Cells to Cardiomyocytes: Role of Coculture With Visceral Endoderm-Like Cells. *Circulation*, *107*(>21), 2733–2740. https://doi.org/10.1161/01.CIR.0000068356.38592.68

Nakagawa, O., Nakagawa, M., Richardson, J. A., Olson, E. N., & Srivastava, D. (1999). HRT1, HRT2, and HRT3: A new subclass of bHLH transcription factors marking specific cardiac, somitic, and pharyngeal arch segments. *Developmental Biology*, *216*(1), 72–84. https://doi.org/10.1006/dbio.1999.9454

Nattel, S. (2002). New ideas about atrial fibrillation 50 years on. Nature. https://doi.org/10.1038/415219a

Niakan, K. K., Han, J., Pedersen, R. A., Simon, C., & Pera, R. A. R. (2012). Human pre-implantation embryo development. *Development (Cambridge, England)*, *139*(5), 829–841. https://doi.org/10.1242/dev.060426

Nolan, K., & Thompson, T. B. (2014). The DAN family: Modulators of TGF-β signaling and beyond. *Protein Science*. https://doi.org/10.1002/pro.2485

Nolan, K., Kattamuri, C., Rankin, S. A., Read, R. J., Zorn, A. M., & Thompson, T. B. (2016). Structure of Gremlin-2 in Complex with GDF5 Gives Insight into DAN-Family-Mediated BMP Antagonism. *Cell Reports*, *16*(8), 2077–2086. https://doi.org/10.1016/j.celrep.2016.07.046

Obreztchikova, M. N., Sosunov, E. A., Plotnikov, A., Anyukhovsky, E. P., Gainullin, R. Z., Danilo, P., … Rosen, M. R. (2003). Developmental changes in IKrand IKscontribute to age-related expression of dofetilide effects on repolarization and proarrhythmia. *Cardiovascular Research*, *59*(2), 339–350. https://doi.org/10.1016/S0008-6363(03)00360-2

Orford, K., Crockett, C., Jensen, J. P., Weissman, A. M., & Byers, S. W. (1997). Serine phosphorylation-regulated ubiquitination and degradation of β- catenin. *Journal of Biological Chemistry*, *272*(40), 24735–24738. https://doi.org/10.1074/jbc.272.40.24735

Pansky, B. (1982). *Review of MEDICAL EMBRYOLOGY. McGraw-Hill,*. Retrieved from file:///Users/maryam/Desktop/litrature review for research/development/Chapter 77. Development of The Teeth - Review of Medical Embryology Book - LifeMap Discovery.webarchive

Parés, X., Farrés, J., Kedishvili, N., & Duester, G. (2008). Medium- and short-chain dehydrogenase/reductase gene and protein families: Medium-chain and short-chain dehydrogenases/reductases in retinoid metabolism. *Cellular and Molecular Life Sciences*. https://doi.org/10.1007/s00018-008-8591-3

Pellman, J., & Sheikh, F. (2015). Atrial fibrillation: Mechanisms, therapeutics, and future directions. *Comprehensive Physiology*, *5*(2), 649–665. https://doi.org/10.1002/cphy.c140047

Pereira, F. A., Yuhong, Q., Zhou, G., Tsai, M. J., & Tsai, S. Y. (1999). The orphan nuclear receptor COUP-TFII is required for angiogenesis and heart development. *Genes and Development*, *13*(8), 1037–1049. https://doi.org/10.1101/gad.13.8.1037

Polo, J. M., Liu, S., Figueroa, M. E., Kulalert, W., Eminli, S., Tan, K. Y., … Hochedlinger, K. (2010). Cell type of origin influences the molecular and functional properties of mouse induced pluripotent stem cells. *Nature Biotechnology*, *28*(8), 848–855. https://doi.org/10.1038/nbt.1667

Prall, O. W. J., Menon, M. K., Solloway, M. J., Watanabe, Y., Zaffran, S., Bajolle, F., … Harvey, R. P. (2007). An Nkx2-5/Bmp2/Smad1 Negative Feedback Loop Controls Heart Progenitor Specification and Proliferation. Cell, 128(5), 947–959. https://doi.org/10.1016/j.cell.2007.01.042

Radisic, M., Park, H., Shing, H., Consi, T., Schoen, F. J., Langer, R., … Vunjak-Novakovic, G. (2004). Functional assembly of engineered myocardium by electrical stimulation of cardiac myocytes cultured on scaffolds. *Proceedings of the National Academy of Sciences*, *101*(52), 18129–18134. https://doi.org/10.1073/pnas.0407817101

Rahman, M. S., Akhtar, N., Jamil, H. M., Banik, R. S., & Asaduzzaman, S. M. (2015). TGF-β/BMP signaling and other molecular events: Regulation of osteoblastogenesis and bone formation. *Bone Research*. https://doi.org/10.1038/boneres.2015.5

Rhinn, M., & Dolle, P. (2012). Retinoic acid signalling during development. *Development*, *139*(5), 843–858. https://doi.org/10.1242/dev.065938

Robertson, C., Tran, D. D., & George, S. C. (2013). Concise review: Maturation phases of human pluripotent stem cell-derived cardiomyocytes. Stem Cells. https://doi.org/10.1002/stem.1331

Rochette-Egly, C., & Germain, P. (2009). Dynamic and combinatorial control of gene expression by nuclear retinoic acid receptors (RARs). *Nucl. Recept. Signal.*, *7*(D), 1–18. https://doi.org/10.1621/nrs.07005

Ronaldson-Bouchard, K., Ma, S. P., Yeager, K., Chen, T., Song, L., Sirabella, D., … Vunjak-Novakovic, G. (2018). Advanced maturation of human cardiac tissue grown from pluripotent stem cells. Nature. https://doi.org/10.1038/s41586-018-0016-3

Ryckebusch, L., Wang, Z., Bertrand, N., Lin, S.-C., Chi, X., Schwartz, R., … Niederreither, K. (2008). Retinoic acid deficiency alters second heart field formation. *Proceedings of the National Academy of Sciences of the United States of America*, *105*(8), 2913–2918. https://doi.org/10.1073/pnas.0712344105

Sartiani, L., Bettiol, E., Stillitano, F., Mugelli, A., Cerbai, E., & Jaconi, M. E. (2007). Developmental changes in cardiomyocytes differentiated from human embryonic stem

cells: a molecular and electrophysiological approach. *Stem Cells (Dayton, Ohio)*, *25*(5), 1136–1144. https://doi.org/10.1634/stemcells.2006-0466

Schleich, J. M., Abdulla, T., Summers, R., & Houyel, L. (2013). An overview of cardiac morphogenesis. *Archives of Cardiovascular Diseases*, *106*(11), 612–623. https://doi.org/10.1016/j.acvd.2013.07.001

Seki, T., Yuasa, S., Oda, M., Egashira, T., Yae, K., Kusumoto, D., … Fukuda, K. (2010). Generation of induced pluripotent stem cells from human terminally differentiated circulating t cells. *Cell Stem Cell*, *7*(1), 11–13. https://doi.org/10.1016/j.stem.2010.06.003

Shen, J. X. (2006). Isoprenaline enhances local Ca2+ release in cardiac myocytes. Acta Pharmacologica Sinica, 27(7), 927–932. https://doi.org/10.1111/j.1745-7254.2006.00383.x

Smith, C. (2003). Hematopoietic stem cells and hematopoiesis. *Cancer Control : Journal of the Moffitt Cancer Center*, *10*(1), 9–16. https://doi.org/10.1177/107327480301000103

Smyrnias, I., Mair, W., Harzheim, D., Walker, S. A., Roderick, H. L., & Bootman, M. D. (2010). Comparison of the T-tubule system in adult rat ventricular and atrial myocytes, and its role in excitation-contraction coupling and inotropic stimulation. Cell Calcium, 47(3), 210–223. https://doi.org/10.1016/j.ceca.2009.10.001

Soliman, E. Z., Safford, M. M., Muntner, P., Khodneva, Y., Dawood, F. Z., Zakai, N. A., … Cushman, M. (2014). Atrial fibrillation and the risk of myocardial infarction. *JAMA Internal Medicine*, *174*(1). https://doi.org/10.1001/jamainternmed.2013.11912

Srivastava, D. (2006). Making or Breaking the Heart: From Lineage Determination to Morphogenesis. *Cell*. https://doi.org/10.1016/j.cell.2006.09.003

Staerk, J., Dawlaty, M. M., Gao, Q., Maetzel, D., Hanna, J., Sommer, C. A., … Jaenisch, R. (2010). Reprogramming of human peripheral blood cells to induced pluripotent stem cells. *Cell Stem Cell*, *7*(1), 20–24. https://doi.org/10.1016/j.stem.2010.06.002

Sudo, S., Avsian-Kretchmer, O., Wang, L. S., & Hsueh, A. J. W. (2004). Protein related to DAN and cerberus is a bone morphogenetic protein antagonist that participates in ovarian paracrine regulation. *Journal of Biological Chemistry*, *279*(22), 23134–23141. https://doi.org/10.1074/jbc.M402376200

Sun, J., Zhuang, F. F., Mullersman, J. E., Chen, H., Robertson, E. J., Warburton, D., … Shi, W. (2006). BMP4 activation and secretion are negatively regulated by an intracellular Gremlin-BMP4 interaction. *Journal of Biological Chemistry*, *281*(39), 29349–29356. https://doi.org/10.1074/jbc.M603833200

Takahashi, K., & Yamanaka, S. (2006). Induction of Pluripotent Stem Cells from Mouse Embryonic and Adult Fibroblast Cultures by Defined Factors. *Cell*, *126*(4), 663–676. https://doi.org/10.1016/j.cell.2006.07.024

Takahashi, K., Tanabe, K., Ohnuki, M., Narita, M., Ichisaka, T., Tomoda, K., & Yamanaka, S. (2007). Induction of Pluripotent Stem Cells from Adult Human Fibroblasts by Defined Factors. *Cell*, *107*(5), 861–872. https://doi.org/10.1016/j.cell.2007.11.019

Tanwar, V., Bylund, J. B., Hu, J., Yan, J., Walthall, J. M., Mukherjee, A., … Hatzopoulos, A. K. (2014). Gremlin 2 promotes differentiation of embryonic stem cells to atrial fate by activation of the JNK signaling pathway. *Stem Cells (Dayton, Ohio)*, *32*(7), 1774–1788. https://doi.org/10.1002/stem.1703

Umar, S. (2010). Intestinal stem cells. *Current Gastroenterology Reports*. https://doi.org/10.1007/s11894-010-0130-3

Uosaki, H., & Taguchi, Y. (2016). Comparative Gene Expression Analysis of Mouse and Human Cardiac Maturation. *Genomics, Proteomics & Bioinformatics*, *14*(4), 207–215. https://doi.org/10.1016/j.gpb.2016.04.004

Wang, R. N., Green, J., Wang, Z., Deng, Y., Qiao, M., Peabody, M., … Shi, L. L. (2014). Bone Morphogenetic Protein (BMP) signaling in development and human diseases. *Genes & Diseases*, *1*(1), 87–105. https://doi.org/10.1016/j.gendis.2014.07.005

Wang, R. N., Green, J., Wang, Z., Deng, Y., Qiao, M., Peabody, M., … Shi, L. L. (2014). Bone Morphogenetic Protein (BMP) signaling in development and human diseases. Genes & Diseases, 1(1), 87–105. https://doi.org/10.1016/j.gendis.2014.07.005

Wang, X., Destrument, A., & Tournier, C. (2007). Physiological roles of MKK4 and MKK7: Insights from animal models. Biochimica et Biophysica Acta - Molecular Cell Research. https://doi.org/10.1016/j.bbamcr.2006.10.016

Wang, Z., Fermini, B., & Nattel, S. (1993). Sustained depolarization-induced outward current in human atrial myocytes. Evidence for a novel delayed rectifier K+ current similar to Kv1.5 cloned channel currents. *Circulation Research*, *73*(6), 1061–1076. https://doi.org/10.1161/01.RES.73.6.1061

Webb, S., Brown, N. A., & Andersen, R. H. (1998). Formation of the atrioventricular septal structures in the normal mouse. *Circulation Research*, *82*(6), 645–656. https://doi.org/10.1161/01.RES.82.6.645

Weng, L.-C., Preis, S. R., Hulme, O. L., Larson, M. G., Choi, S. H., Wang, B., … Lubitz, S. A. (2017). Genetic Predisposition, Clinical Risk Factor Burden, and Lifetime Risk of Atrial Fibrillation. *Circulation*, CIRCULATIONAHA.117.031431. https://doi.org/10.1161/CIRCULATIONAHA.117.031431

Wessels, A., & Sedmera, D. (2003). Developmental anatomy of the heart: a tale of mice and man. *Physiological Genomics*, *15*(3), 165–176. https://doi.org/10.1152/physiolgenomics.00033.2003

Wilkins, E., Wilson, L., Wickramasinghe, K., Bhatnagar, P., Leal, J., Luengo-Fernandez, R., … Townsend, N. (2017). *European Cardiovascular Disease Statistics 2017 edition*. *European Heart Network, Brussels*. https://doi.org/978-2-9537898-1-2

Xavier-Neto, J., Neville, C. M., Shapiro, M. D., Houghton, L., Wang, G. F., Nikovits, W., … Rosenthal, N. (1999). A retinoic acid-inducible transgenic marker of sino-atrial development in the mouse heart. Development (Cambridge, England), 126(12), 2677–2687. Retrieved from http://www.ncbi.nlm.nih.gov/pubmed/10331979

Yang, L., Soonpaa, M. H., Adler, E. D., Roepke, T. K., Kattman, S. J., Kennedy, M., … Keller, G. M. (2008). Human cardiovascular progenitor cells develop from a KDR+ embryonic-stem-cell-derived population. *Nature*, *453*(7194). https://doi.org/10.1038/nature06894

Yang, X., Pabon, L., & Murry, C. E. (2014). Engineering adolescence: Maturation of human pluripotent stem cell-derived cardiomyocytes. *Circulation Research*. https://doi.org/10.1161/CIRCRESAHA.114.300558

Yeoh A, Finlay M, Anderson N, et al. (2015). Simultaneous measurement of calcium transients and electrical activity in murine cardiac tissue – a novel system for the study of cardiac arrhythmia. Heart; 101:A92-A93.

Yu, J., Vodyanik, M. A., Smuga-Otto, K., Antosiewicz-Bourget, J., Frane, J. L., Tian, S., … Thomson, J. A. (2007). Induced pluripotent stem cell lines derived from human somatic cells. *Science (New York, N.Y.)*, *318*(5858), 1917–1920. https://doi.org/10.1126/science.1151526

Yu, Y.-M., Han, P.-L., & Lee, J.-K. (2003). JNK pathway is required for retinoic acid-induced neurite outgrowth of human neuroblastoma, SH-SY5Y. NeuroReport, 14(7), 941–945. https://doi.org/10.1097/01.wnr.0000074341.81633.b8

Yutzey, K. E., Rhee, J. T., & Bader, D. (1994). Expression of the atrial-specific myosin heavy chain AMHC1 and the establishment of anteroposterior polarity in the developing chicken heart. Development (Cambridge, England), 120(4), 871–883.

Zeng, Z., Zhang, H., Lin, N., Kang, M., Zheng, Y., Li, C., … Luo, D. (2014). Role of Inositol-1,4,5-Trisphosphate Receptor in the Regulation of Calcium Transients in Neonatal Rat Ventricular Myocytes. Journal of Pharmacological Sciences, 126(1), 37–46. https://doi.org/10.1254/jphs.14029FP

Zhang, J., & Li, L. (2005). BMP signaling and stem cell regulation. *Developmental Biology*. https://doi.org/10.1016/j.ydbio.2005.05.009

Zhang, J., Wilson, G. F., Soerens, A. G., Koonce, C. H., Yu, J., Palecek, S. P., … Kamp, T. J. (2009). Functional cardiomyocytes derived from human induced pluripotent stem cells. *Circulation Research*, *104*(4). https://doi.org/10.1161/CIRCRESAHA.108.192237

Zhang, Z., He, Y., Tuteja, D., Xu, D., Timofeyev, V., Zhang, Q., … Chiamvimonvat, N. (2005). Functional roles of Cav1.3(alpha1D) calcium channels in atria: insights gained from gene-targeted null mutant mice. *Circulation*, *112*(13), 1936–1944. https://doi.org/10.1161/CIRCULATIONAHA.105.540070

Zhu, R., Blazeski, A., Poon, E., Costa, K. D., Tung, L., & Boheler, K. R. (2014). Physical developmental cues for the maturation of human pluripotent stem cell-derived cardiomyocytes. *Stem Cell Research & Therapy*, *5*, 117. https://doi.org/10.1186/scrt507

Zimetbaum, P. (2012). Antiarrhythmic drug therapy for atrial fibrillation. *Circulation*, *125*(2), 381–389. https://doi.org/10.1161/CIRCULATIONAHA.111.019927

Zimmermann, W. H., Schneiderbanger, K., Schubert, P., Didi??, M., M??nzel, F., Heubach, J. F., … Eschenhagen, T. (2002). Tissue engineering of a differentiated cardiac muscle construct. Circulation Research, 90(2), 223–230. https://doi.org/10.1161/hh0202.103644

Zuniga, E., Rippen, M., Alexander, C., Schilling, T. F., & Crump, J. G. (2011). Gremlin 2 regulates distinct roles of BMP and Endothelin 1 signaling in dorsoventral patterning of the facial skeleton. Development, 138(23), 5147–5156. https://doi.org/10.1242/dev.067785